UNCLASSIFIED

| AD NUMBER |
| --- |
| AD483929 |
| CLASSIFICATION CHANGES |
| TO: UNCLASSIFIED |
| FROM: CONFIDENTIAL |
| AUTHORITY |
| 28 Feb 1965, DoDD 5200.10 |

THIS PAGE IS UNCLASSIFIED

UNCLASSIFIED

Operation

# TUMBLER

NEVADA PROVING GROUNDS

April–June 1952

... VS TIME AND DISTANCE

AD 483929

CONFIDENTIAL
Security Information

This document consists of 113 pages

No. 318 of 329 copies, Series A

2

Report on OPERATION TUMBLER, Nevada Proving Grounds, April-June, 1952,

Project 1.7,

6

# EARTH ACCELERATION VS. TIME AND DISTANCE.

9 *REPORT TO THE TEST DIRECTOR*,

by

10 V. Salmon and S. R. Hornig,

18 AEC

19 WT-517

11 February 1953, 12 113p.

EACH TRANSMITTAL OF THIS DOCUMENT OUTSIDE THE AGENCIES OF THE U.S. GOVERNMENT MUST HAVE PRIOR APPROVAL OF THE DIRECTOR, DEFENSE ATOMIC SUPPORT AGENCY, WASHINGTON, D.C. 20301.

Stanford Research Institute
Stanford, California

CANCELLED
CONFIDENTIAL
Security Information

CANCELLED
RESTRICTED DATA
ATOMIC ENERGY ACT 1946

Reproduced Direct from Manuscript Copy by
AEC Technical Information Service
Oak Ridge, Tennessee

Inquiries relative to this report may be made to

Chief, Armed Forces Special Weapons Project
P. O. Box 2610
Washington, D. C.

If this report is no longer needed, return to

AEC Technical Information Service
P. O. Box 401
Oak Ridge, Tennessee

# ABSTRACT

The four air-dropped, air-burst nuclear explosions of the TUMBLER tests during the spring of 1952 were conducted primarily to obtain definitive air pressure information. The earth acceleration measurements were designed to study the interaction between phenomena in the air and phenomena in the earth. The main objective was to estimate the magnitudes of the energy absorbed by the ground and the energy fed back into the air by the ground. Subsidiary objectives included a study of the effects of gage depth and the relative importance of the three acceleration components. This report is concerned with these objectives as obtained from many acceleration-time records of the vertical component, 5 feet deep; a few records of the vertical component, 1 and 50 feet deep; and a few records of the horizontal radial and horizontal tangential components, 5 and 50 feet deep.

The performance was in general satisfactory. However, on quite a few gages the frequency of the important slap oscillation (occurring as the air blast passes over the gage) was close to the frequency of the gage, causing the amplitude to be in error. Corrections were made for this effect on Shot 2, in which more records required correction than in the other shots.

The important portion of each gage record is reproduced (in reduced form) in the Appendix. Data from the records have been tabulated and appear in numerous graphs.

In terms of the objectives of the test, the following statements can be made. For convenience, the statements are rather positive; the qualifications and assumptions which accompany them are detailed in the text.

1. The proportion of blast energy absorbed from the air by the earth was for Shot 1, 0.3 per cent; Shot 2, 0.06 per cent; Shot 3, 0.03 per cent; Shot 4, 0.18 per cent. The absorption of such small fractions of the total energy would probably not affect the blast wave.

2. Outrunning by the direct earth wave in front of the main slap took place at an average velocity of 2000 feet per second.

3. Peak slap acceleration as a function of maximum surface level air pressure for Shots 2, 3, and 4 could be approximated by

$$A = 0.32\, p^{0.89} \quad ,$$

where A is in g, and p is in psi.

For Shot 1 the accelerations were 60 per cent or more higher than for Shots 2, 3, and 4. Some of this difference is due to the differing character of the soil at the sites for the two groups of shots.

4. It is very unlikely that the precursor on Shot 4 is formed by energy transfer from air to earth to air again. Acoustic considerations give a "round-trip" pressure ratio of 1/1400.

5. Curves of peak particle slap velocity vs. maximum surface level air pressure for all four shots could be approximated by

$$v = 0.06\ p^{0.89} \quad ,$$

where v is in fps and p is in psi.

6. No firm quantitative conclusions could be drawn as to the effect of depth on acceleration and velocity. A reasonable assumption (which was used in the calculation of energy absorption) is that peak vertical particle velocity at the surface is four times the peak vertical velocity at a depth of 5 feet.

7. The magnitude of the horizontal radial component of acceleration is comparable with that of the vertical component. The horizontal tangential component is in general small enough to be neglected.

## ACKNOWLEDGMENTS

The planning and execution of Project 1.7 of Operation TUMBLER were under the direction of Dr. E. B. Doll. Some details of the instrument pattern were specified by the Test Command, in accordance with suggestions of Professor Maurice Ewing of Columbia University, and others. Dr. Doll supervised the activities of Project 1.7 at the Nevada Proving Grounds, with Mr. L. M. Swift serving as Field Party Chief. Mr. S. C. Ashton handled all logistics and supply problems, in addition to his normal duties as a member of the field party. Other members of the field party were: L. H. Inman, V. E. Krakow, C. C. Hughes, J. S. Thompson, G. Pippin, A. G. Green, and G. Luke. Data reduction and presentation were handled by Mrs. Jane C. Simons and Mrs. Joan Gates. This report was written by Dr. V. Salmon and Mrs. Sarah R. Hornig, with the editorial assistance of Dr. Doll. Mr. B. Sussholz of the Armed Forces Special Weapons Project supplied valuable detailed discussions and guided the presentation and inter-comparison of data. Mr. A. A. Thompson, formerly of AFSWP, prepared the material from which was written Section 5.8 on Energy Absorption. The invaluable assistance of CDR D. C. Campbell, USN, Director of Program One, is gratefully acknowledged.

CONTENTS

# ILLUSTRATIONS

# TABLES

# CHAPTER 1

# INTRODUCTION

## 1.1 HISTORY AND OBJECTIVES

The four air-dropped, air-burst nuclear explosion shots of Operation TUMBLER were conducted primarily to obtain definitive air-pressure information for constructing an empirical height of burst chart. The events leading to the selections of yields, burst heights, and sites have been covered in other reports,[1,2]* and will not be detailed here.

The principal objective of the earth acceleration measurements was to obtain information on the interaction between phenomena in the air and in the ground. More specifically, it was desired to estimate the magnitude of possible changes in the surface level air-blast pressures owing to absorption by the ground. Conversely, it was suspected that energy could be fed back into the air by the motion of the earth initially caused by air blast; an estimate of this effect was desired also. Subsidiary objectives included a study of the effects of gage depth and the relative importance of the three acceleration components.

This report is primarily concerned with the presentation and interpretation of Project 1.7 data and its correlation with Project 1.2[2] information from the point of view of the above objectives. No extensive comparison of these data with results from other test groups is attempted.

## 1.2 THEORETICAL CONSIDERATIONS

Four topics are considered briefly here: the process of transmitting information between air and earth, and vice versa; the effect of air-blast duration on the response of the earth; correction of gage records for limitations imposed by the gage response; and calculation of maximum particle velocity.

### 1.2.1 Transmission Process

The manner in which the air blast excites the earth may be

* Superscript numbers refer to references listed in the Bibliography at the end of this report.

discussed with reference to the wave front picture of Figure 1.1 and the time of arrival diagram of Figure 1.2. The refracted wave front of the earth wave in Figure 1.1 corresponds to those observed by Schmidt[3] and treated analytically by Ott.[4] If its seismic velocity increases with depth, as it does at the Nevada Proving Grounds,[2] then one would expect that the apparent source for the distant wave fronts would be lowered. However, this would not appreciably alter the nature of the information received in near-surface earth.

As the incident air blast sweeps along, its apparent horizontal velocity, $c'$, of contact with the earth is given by

$$c' = U/\sin\theta \quad , \tag{1.1}$$

where U is the shock velocity and $\theta$ is the angle of incidence. However, the information given the earth will eventually outrun this apparent velocity, $c'$. This may happen either by a near-surface seismic velocity that is greater than $c'$ or by earth transmission along a curved path which dips into the higher velocity lower earth strata. In the two diagrams this outrunning is shown as occurring at ground range $R_2$. Beyond $R_2$, the first information received by a near-surface earth-motion gage will be that from the earth wave running ahead. Its spectral composition will be altered by transmission in the earth, so that the information initiated by a pulse will, in general, appear as an oscillatory wave train.

Now, with reference to Figure 1.2, consider what happens in an amplitude sense at ground range $R_3$, beyond the outrunning distance. Information received at some time intermediate between earth and air arrivals will have suffered attenuation in both earth and air paths. Because of the much smaller attenuation in the air path, the largest amplitudes will occur when the earth path is a minimum. This, of course, corresponds to the air blast passing over the gages. Hence it may be expected that for gages beyond the outrunning limit $R_2$, the envelope of the received wave train should tend to increase and reach a maximum when the air blast passes over the gage. This direct local effect of the air blast is termed the "slap," because of the sudden increase in earth motion actually observed.

If the seismic velocity does increase with depth, then the time of arrival curve for the earth wave should be slightly concave downward. If this is the case, then the shapes of the more distant refracted wave fronts (shown in the lower part of Figure 1.1) will change so as to correspond to a lower position of apparent source.

When the earth wave outruns the air blast, it might be expected that information would be fed back into the air to form a

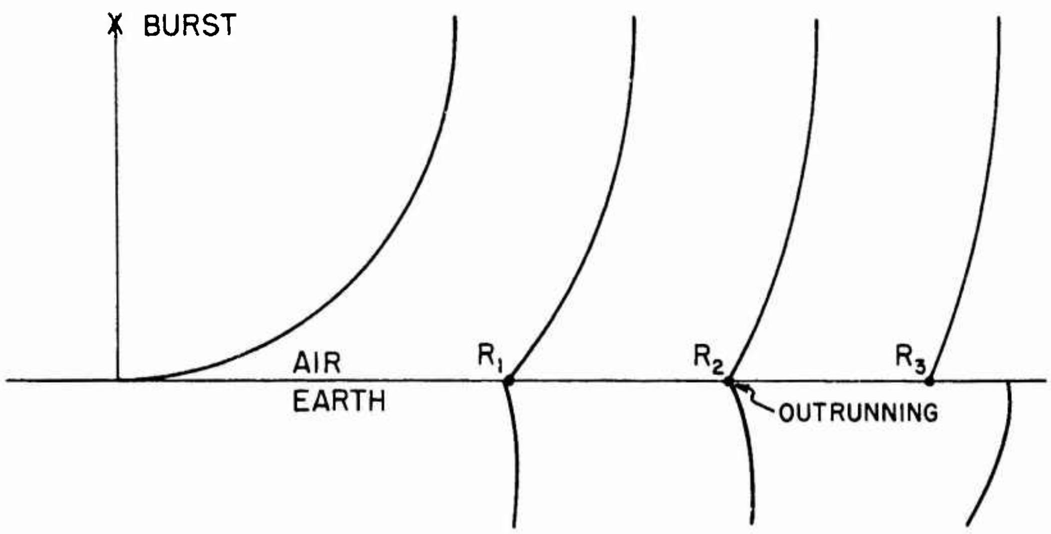


Fig. 1.1 Incident ar^ Refracted Wave Fronts for Air Burst. Earth wave outruns air blast beyond $R_2$

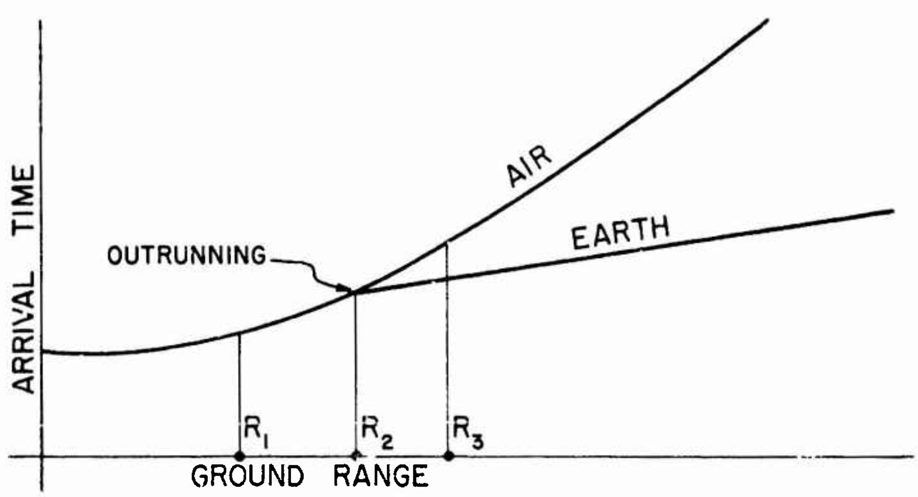


Fig. 1.2 Time of Arrival Diagram for Information Received by Surface Gage. Earth wave outruns air blast beyond $R_2$

"Kopfwelle,"[3] or precursor. To estimate the order of this effect, make the most optimistic assumption that the air blast produces an earth particle velocity which in turn reacts with undiminished amplitude upon the air. What is the "round trip" air pressure thus produced? Take air and earth as equivalent to loss-free fluids (1 and 2) having characteristic compressional wave impedances $z_1$ and $z_2$. Then, in transmission from air to earth, because the earth is relatively so much more rigid than the air, the motion of the earth affects to a negligible extent the air pressure $p_1$ existing at the surface. Thus the vertical earth particle velocity is given by

$$v_2 = \frac{p_2}{z_2} = \frac{p_1}{z_2} \quad , \tag{1.2}$$

because of the continuity of pressure. This earth velocity is then allowed to react with the air. Again, because the earth is so rigid, the actual surface velocity is practically doubled. The resulting round-trip air pressure is then

$$p_1' = z_1 v_1' = z_1 2v_2 = p_1 (2z_1/z_2) \tag{1.3}$$

The round-trip pressure ratio is

$$\frac{p_1'}{p_1} = \frac{2z_1}{z_2} = \frac{2\rho_1 c_1}{\rho_2 c_2} \quad , \tag{1.4}$$

where $\rho$ and c are respectively the density and sonic velocity in the two media.

In Section 5.5 this result will be used in the discussion of TUMBLER Shot 4 precursor.

### 1.2.2 Effect of Air-Blast Duration on Earth Response

It is known from electric circuit theory that if a step function is applied to an oscillatory circuit, the response of the circuit will contain frequencies characteristic of the circuit alone, and not the step function. If the step function is replaced by a decaying blast wave and the circuit by the earth, then the statement remains substantially true as long as the duration of the blast wave is much greater than the natural period of the earth it excites. Thus it should be expected that the frequencies of earth motion observed from the slap of the air blast passing over should be independent of the air blast duration and hence the yield, provided the yield is sufficiently large. Whether or not this situation obtains is easily determined by the relative durations of the air blast and of the earth slap.

Several side effects may be expected to alter the consistency of the observed effects: inhomogeneity of the earth, gage ringing, and system response limitations are among the more important. The last is considered in the next section.

### 1.2.3 Correction of Gage Records for System Response

When the mechanical input to the gage contains frequency components approaching the limit of flat frequency response of the gage-galvanometer system used, the input will not be correctly recorded. The following procedure may be used for making the correction. First, assume that the correction is that for a system with a single degree-of-freedom. In most recording channels, the gage was the limiting factor, so the assumption will be useful as long as the recording galvanometer does not further limit the system response. This leads to the further assumption that for the instrumentation system used, the displacement on the gage record is proportional to the deflection, x, of the gage armature (see Chapter 2). Then the idealized equation of motion may be written

$$m x'' + r x' + s x = s f(t) \quad , \tag{1.5}$$

where m, r, and s are the equivalent mass, resistance, and stiffness of the gage armature. The term f(t) corresponds to the input function (earth acceleration) to which the gage output is proportional at frequencies low compared with the undamped resonant frequency of the gage, which is given by

$$f_0 = \frac{\omega_0}{2\pi} = \frac{1}{2\pi}\sqrt{\frac{s}{m}} \quad . \tag{1.6}$$

Now divide Equation 1.5 by the stiffness, s, so that the desired proportionality of x and f(t) may be seen. Then, after simplification, there results

$$\frac{x''}{\omega_0^2} + \frac{2\beta}{\omega_0} x' + x = f(t) \quad , \tag{1.7}$$

where $\beta$ is the ratio of the resistance r to the critical damping resistance

$$r_c = 2\sqrt{sm} = 2\omega_0 m = 2s/\omega_0 \quad . \tag{1.8}$$

The damped resonant frequency is given by

$$\omega_d = \omega_0 \sqrt{1 - \beta^2} \tag{1.9}$$

Returning to the procedure for gage correction, Equation 1.7 says that for a sufficiently high gage frequency, $\omega_0$, the first two terms are negligible. The relation between x and f(t) is then given satisfactorily by a static calibration. Thus these first two terms are corrections which, when added to x, result in the correct value of f(t). To obtain them, the derivatives $\dot{x}$ and $\ddot{x}$ are calculated from the gage record supplied. Values of $\omega_0$ and $\beta$ are determined experimentally.

Workers at the National Bureau of Standards have calculated and plotted the gage response for a variety of transient inputs, relative gage frequencies, and dampings.[6] For values of $\beta$ below unity, a general result for a steeply rising input is that the recorded peak value is lower than the actual one, and occurs later. The difference in the peaks becomes significant for ratios of equivalent input frequency to damped gage resonance frequency greater than 0.3. Since $\beta$ is ordinarily between 0.6 and 0.7, this same behavior should be observed in the actual calculation, and constitutes a gross check on the correctness of the calculations.

The corrections found by this process are in themselves subject to considerable error, since differentiation is a divergent process, with small errors in the ordinates becoming magnified. At best we may expect corrections reliable to order of magnitude only. Figure 1.3 displays samples of a raw and a corrected gage record with the order of error indicated.

### 1.2.4 Calculation of Maximum Particle Velocity in Slap

Since the earth particle velocity is often of greater interest than the acceleration, it is desirable to obtain the former curve from the latter by integration. However, this process is rather laborious, and it would be desirable to obtain a simpler single measure of the particle velocity.

Here we shall be interested in the slap resulting from the passage of the air blast over an accelerometer. The later portions of the slap include not only this direct excitation but information which had already been imparted to the earth at an earlier time (see Section 1.2.1). Thus this earth motion may be edited from the gage record by using an adjustable base line. In many records this can be done, leaving as the "true" slap a wave exhibiting many of the features of a damped sine wave. In actuality, the frequency and damping are irregular, but the resemblance to a damped sine wave is clear. Now, the

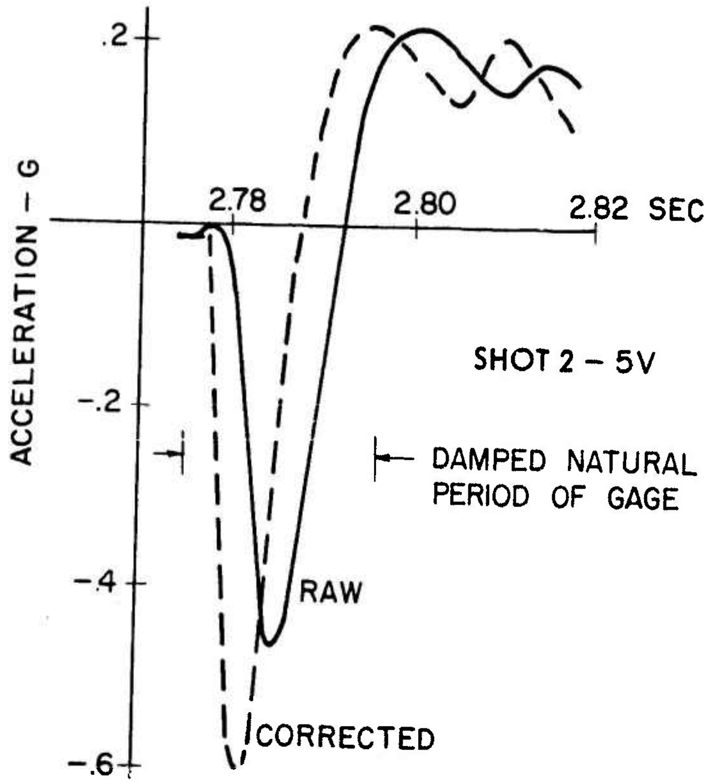


Fig. 1.3 Raw and Corrected Gage Record (Expanded time scale)

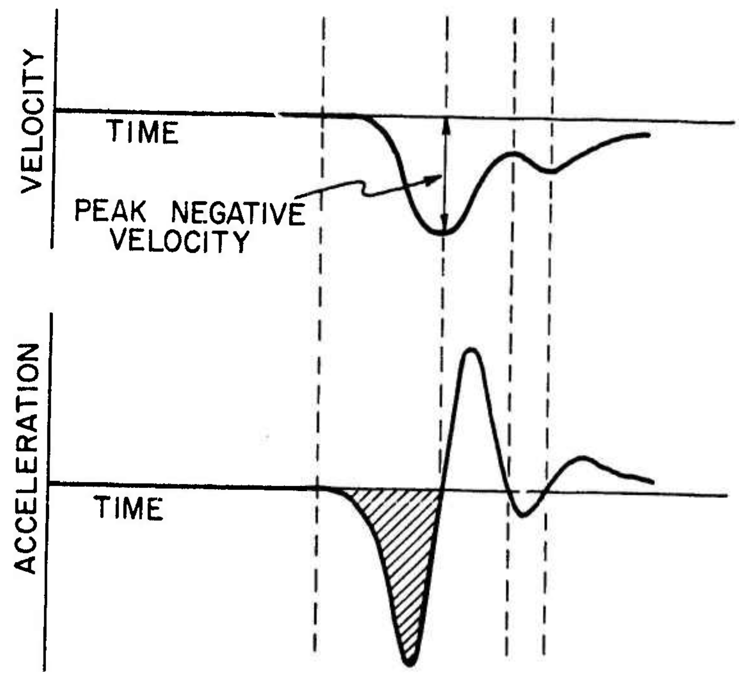


Fig. 1.4 Acceleration and Velocity Relations

particle velocities corresponding to these slaps will all be similar, since the slap accelerations are similar. Figure 1.4 indicates the general shapes of the slap acceleration and corresponding velocity. Because most of the velocity wave shapes turn out to be similar, each velocity curve may be described by the peak value and an oscillation time. From the vertical slap acceleration record and Figure 1.4, it is evident that the peak vertical velocity is negative (downward) and corresponds to the area of the first negative lobe of vertical acceleration. In addition, the duration of the negative acceleration lobe is the time for the velocity to reach peak value. For the sake of consistency, the velocity corresponding to this first lobe was used even in cases where a later lobe was somewhat larger.

# CHAPTER 2

## INSTRUMENTATION

### 2.1 GENERAL SYSTEM

The details of the instrumentation system employed have been reported elsewhere.[7,8] Here only the information essential to an understanding of the data will be presented. As before, Wiancko variable-reluctance accelerometers with associated terminal equipment were used in conjunction with Miller Model J recording oscillographs.

### 2.2 COUPLING TO THE EARTH

Accelerometers were mounted in canisters arranged for orienting three gages along cylindrical coordinates for which the axis was the vertical through the burst. The average density of canister and gage assembly was roughly that of the earth. Each canister was placed at the bottom of a hole drilled in the ground, was properly oriented, and then was cemented in place with Calseal, a quick-setting gypsum cement. Following this, the holes were filled with earth, which was then tamped to approximately the original density.

### 2.3 RESPONSE TIME

The response or rise time was determined by the high-frequency response of the gages and galvanometers used. Accelerometer natural frequencies were dependent on gage ratings, which were chosen on the basis of estimated acceleration peaks so that the instruments would be operating in their linear ranges. For most of the accelerometers, the product of damped natural frequency (in cps) and gage rating (in G units) was close to 1300. The damped natural frequencies are tabulated in Table 5.2; damping was approximately 0.7 of critical. The low-frequency response of the complete instrumentation system extended uniformly to and including zero frequency.

The natural frequency of the accelerometers limited the response time, except for some double-galvanometer channels employed on 30 G (190 cps) gages. The higher sensitivity galvanometers had damped natural frequencies of 200 cps. Thus, in these cases, the rise time was greater than for the accelerometer alone. When this occurred, no attempt was been made to correct the records for gage response by the procedure outlined in Section 1.2.3. However, in all other instances the rise time may be taken as approximately half a natural period for the accelerometer used.

2.4 CALIBRATION

Each accelerometer (and associated galvanometers) was calibrated in the field after the gage had been connected on the blast line, and again before being installed in the ground. The calibration was performed by rotation of the gage in the earth's gravitational field. Following the test program the accelerometers were removed from the ground and were again calibrated by the same technique. No significant change in sensitivity was observed.

2.5 ACCURACY

Except for frequency response errors, it is believed that the acceleration measurements are reliable to plus or minus 5 per cent. However, in these tests many records exhibit large amplitudes with equivalent frequencies close to the natural frequency of the associated accelerometers. The procedures of Sections 1.2.3 and 5.3 have been applied to estimate corrections for delay time and amplitude.

Time accuracies were determined by the tuning forks controlling the time marking synchronous motors, and by the resolution of the recording traces. The tuning fork frequency was maintained to within 0.1 per cent of the desired rate, with very good short-time stability. Arrival times could be read to plus or minus 0.001 second.

# CHAPTER 3

## OPERATIONS

### 3.1 TEST DESCRIPTION

The four nuclear explosions of Operation TUMBLER were air-dropped, air-burst weapons detonated at the Nevada Proving Grounds of the Atomic Energy Commission. The Frenchman Flat site for Shot 1 was chosen in an effort to obtain a smooth, thermally-reflecting, and dust-free surface. The area was carefully dampened and rolled prior to the test. Although the T-7 site in Yucca Flat, used for the remainder of the program, was the same as that employed in the BUSTER shots, several factors contributed to undesired differences. During the BUSTER shots in the autumn of 1951, the surface was extremely dry and powdery; the dust was ankle-deep in many places. For the TUMBLER shots of the spring of 1952, winter rains had increased the moisture content of both surface and subsurface soil to a considerable extent. Finally, at the TUMBLER blast line much of the sagebrush was removed by blading, and the many vehicles packed the soil to a more compact condition. All these factors acted to reduce the difference (if any) between the reflecting ability of the Frenchman Flat and the Yucca Flat sites.

Locations, dates, and seismic data[5] are summarized in Tables 3.1 and 3.2.

TABLE 3.1

Shot and Site Description

| Shot | Location | Date |
|---|---|---|
| 1 | FF | 1 April 1952 |
| 2 | T-7 | 15 April 1952 |
| 3 | T-7 | 22 April 1952 |
| 4 | T-7 | 1 May 1952 |

TABLE 3.2

Seismic Velocities

| Frenchman Flat | | Yucca Flat, T-7 Area | |
|---|---|---|---|
| Depth (ft) | Velocity (fps) | Depth (ft) | Velocity (fps) |
| 0 - 10 | 1200 | 0 - 5 | 800 |
| 10 - 175 | 2600 | 5 - 100 | Variable |
| 175 - 650 | 3000 | 100 - 275 | 3500 |
| 650 | 10,000 | 275 - 500 | 5000 |
| | | 500 | 6000 |

## 3.2 INSTRUMENTATION PLAN

Figure 3.1 illustrates the general gage line layout; the location of air pressure gages for the measurements of Project 1.2 are also included.

Earth acceleration vs. time measurements were made at three depths below the ground surface: at the 1-foot, 5-foot, and 50-foot levels. For Shot 1 the blast line was 3000 feet long, whereas for Shots 2, 3, and 4 the length was 9000 feet. The principal measurements were of the vertical acceleration, with a gage at the 5-foot depth located at each of the 11 primary stations, Numbers 200 through 210, on all four shots. Vertical accelerations at the 50-foot depth were measured at Stations 203 and 210 on all four shots. In addition, a few horizontal radial and horizontal tangential (or transverse) accelerometers were located at Stations 203 and 210. At the request of Mr. A. A. Thompson, formerly of AFSWP, two of the radial and tangential gages were replaced on Shots 2 and 3 by vertical ones located at a depth of 1 foot. These gave data on the effect of depth.

A gage code system was established to permit ready identification of the location of any particular gage and to furnish a convenient means of referring to the entries in the tables. A few examples will

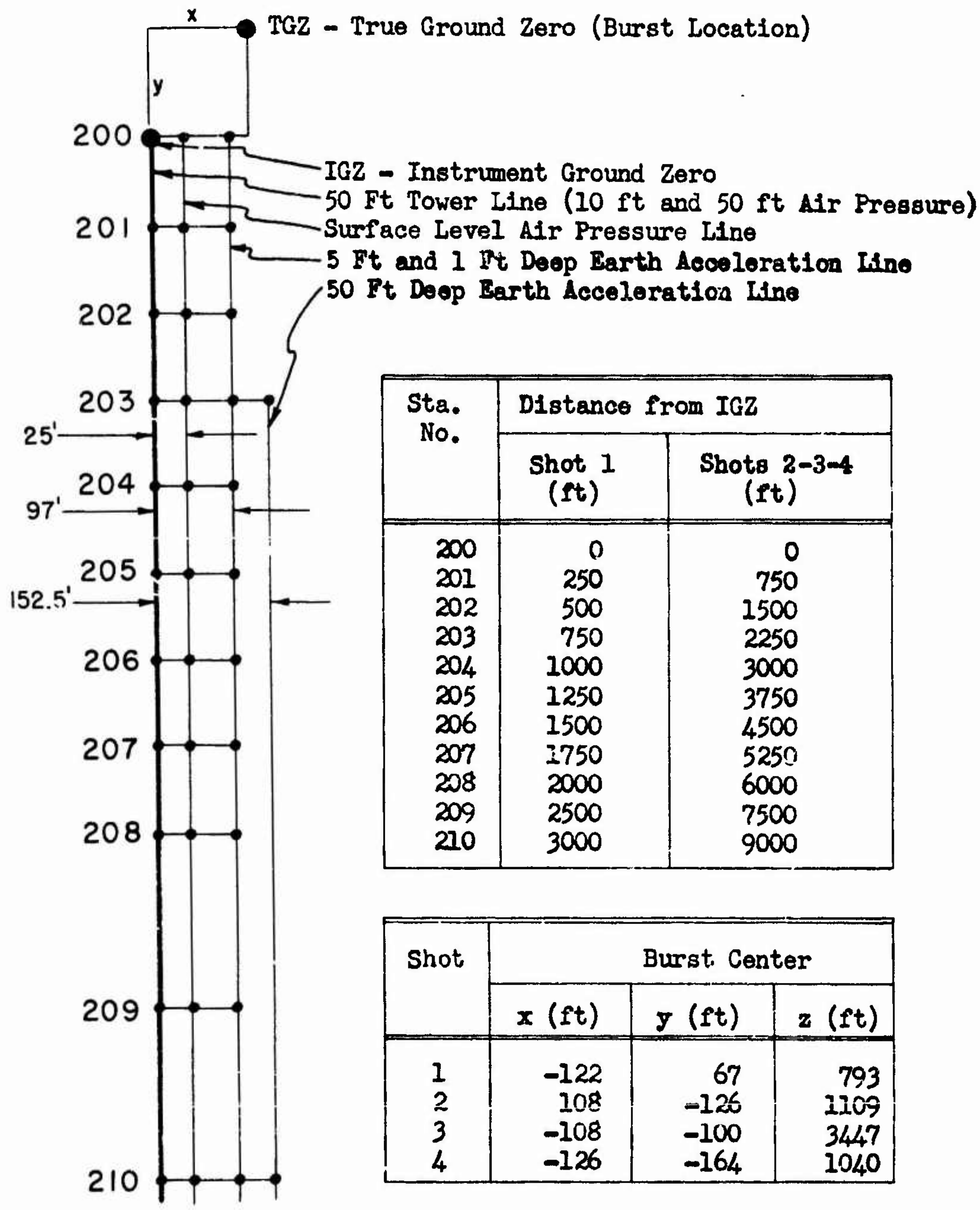


| Sta. No. | Distance from IGZ | |
|---|---|---|
| | Shot 1 (ft) | Shots 2-3-4 (ft) |
| 200 | 0 | 0 |
| 201 | 250 | 750 |
| 202 | 500 | 1500 |
| 203 | 750 | 2250 |
| 204 | 1000 | 3000 |
| 205 | 1250 | 3750 |
| 206 | 1500 | 4500 |
| 207 | 1750 | 5250 |
| 208 | 2000 | 6000 |
| 209 | 2500 | 7500 |
| 210 | 3000 | 9000 |

| Shot | Burst Center | | |
|---|---|---|---|
| | x (ft) | y (ft) | z (ft) |
| 1 | -122 | 67 | 793 |
| 2 | 108 | -126 | 1109 |
| 3 | -108 | -100 | 3447 |
| 4 | -126 | -164 | 1040 |

Fig. 3.1 Gage Line Layout

indicate how to interpret the designations. Typical gage code numbers are 3V1, 3V, 3V50, 3H, and 3T. The first number identifies the station; i.e., 3 denotes Station 203. The letter V indicates the Vertical component; H indicates the Horizontal radial component; and T indicates the Tangential component. The final number indicates the depth in feet; when no number follows the letter, the depth is the primary value of 5 feet.

# CHAPTER 4

# RESULTS

## 4.1 PERFORMANCE

A total of 79 accelerometer channels were connected on the four shots. All of these gage channels included the dual recording feature, giving a total of 158 gage traces. In dual recording, the gage feeds two galvanometers of different sensitivity, so as to increase the dynamic range that may be recorded and read.

With one exception, satisfactory records were obtained on all 79 accelerometer channels. The horizontal transverse accelerometer at gage depth of 50 feet at Station 210 (10T50) on Shot 1 became defective prior to the test. There was no opportunity to replace this gage, owing to the difficulty of recovering it from this depth. Consequently, the record obtained from it was not useful.

## 4.2 PRESENTATION OF DATA

The primary data are the gage records. Reductions of unedited tracings of all usable records form the Appendix to this report. That portion of the complete record shown in the Appendix includes all features of interest for the primary phenomena, which occurred when the air blast arrived.

In most of the records it was possible to observe certain primary features whose spatial and temporal history may be traced more or less continuously over the entire earth motion phenomenon. These are illustrated in Figure 4.1, which indicates how the values appearing in the tables of this chapter have been read from the records. Figures 4.2 through 4.6 are representative gage records from Shots 1, 2, and 3, which illustrate the variation to be expected from the idealized wave form of Figure 4.1. The notation AB indicates the arrival of the air-blast. On Shot 4, gage records from the close-in stations were far from ideal. In Figures 4.7 through 4.11 acceleration records from Shot 4 are compared directly with the surface-level air-pressure gage records.

Data read from the gage records are presented in Tables 4.1 through 4.9. Tables 4.1 and 4.2 contain, respectively, primary data and air-blast data for Shot 1. This pattern is repeated for Shots 2 and 3; on Shot 4, arrival times are tabulated separately. The primary data

include some derived information, such as the equivalent slap frequency, the vertical slap peak particl velocity (see Section 1.2.4), and the interpolated maximum air pressure.

The interpolation mentioned is necessary because the accelerometer blast line is displaced relative to the air-pressure gage blast line. Hence the ground ranges for accelerometer and air-pressure gage at the same station differ. Simple graphical interpolation gives the probable air pressure at the ground range of the accelerometer, and this is the pressure used in all comparisons.

In Chapter 5 the tabulated data are presented in a series of charts, the consideration of which forms the basis of the discussion.

## 4.3 FEATURES OF THE WAVE FORM

In Section 1.2.1 it was pointed out that at large distances the first information to arrive at a gage should be that which outruns the locally-excited air-blast slap. This early arrival is termed the direct earth wave and is noticeable on many of the representative records in Figures 4.2 through 4.11. At distant stations, the direct earth wave has often decayed to too low an amplitude to be read at the time the air-blast slap is evident.

In making the gage correction calculations, an important quantity is the maximum slope of the leading edge of the slap, dA/dt. This slope may also be described by the slap amplitude and the equivalent period. The maximum slope has been extrapolated to the axis to give an equivalent half-period; the slap frequency, which appears in the tables, is given by $f_s = 1/2T$. (See Figure 4.1.) This value is more significant than that obtained from a full slap cycle, for the two half-cycles often do not have the same duration.

It is difficult to separate, in a completely unambiguous fashion, the direct earth and slap components. The criterion used in this report is the point of maximum curvature, just before the slap. When this separation proved impossible, values were read from the base line. In most instances the error thus introduced was small.

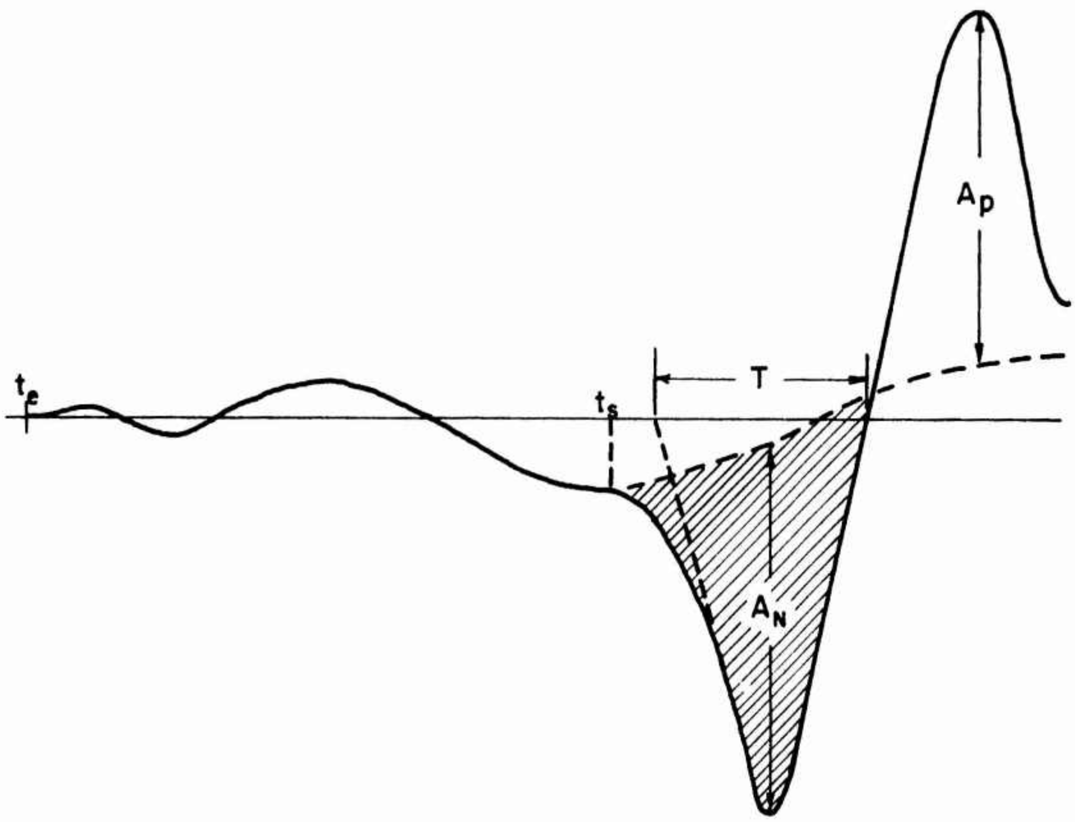


$t_e$ = ARRIVAL TIME, DIRECT EARTH WAVE
$t_s$ = ARRIVAL TIME, MAIN SLAP
$\frac{1}{2T}$ = SLAP FREQUENCY
$A_N$ = MAXIMUM NEGATIVE SLAP ACCELERATION
$A_P$ = MAXIMUM POSITIVE SLAP ACCELERATION
MAXIMUM DIRECT EARTH ACCELERATION IS ABSOLUTE MAXIMUM LYING BETWEEN $t_e$ AND $t_s$
SHADED AREA = MAXIMUM NEGATIVE VERTICAL SLAP VELOCITY

Fig. 4.1 Illustrative Wave Form

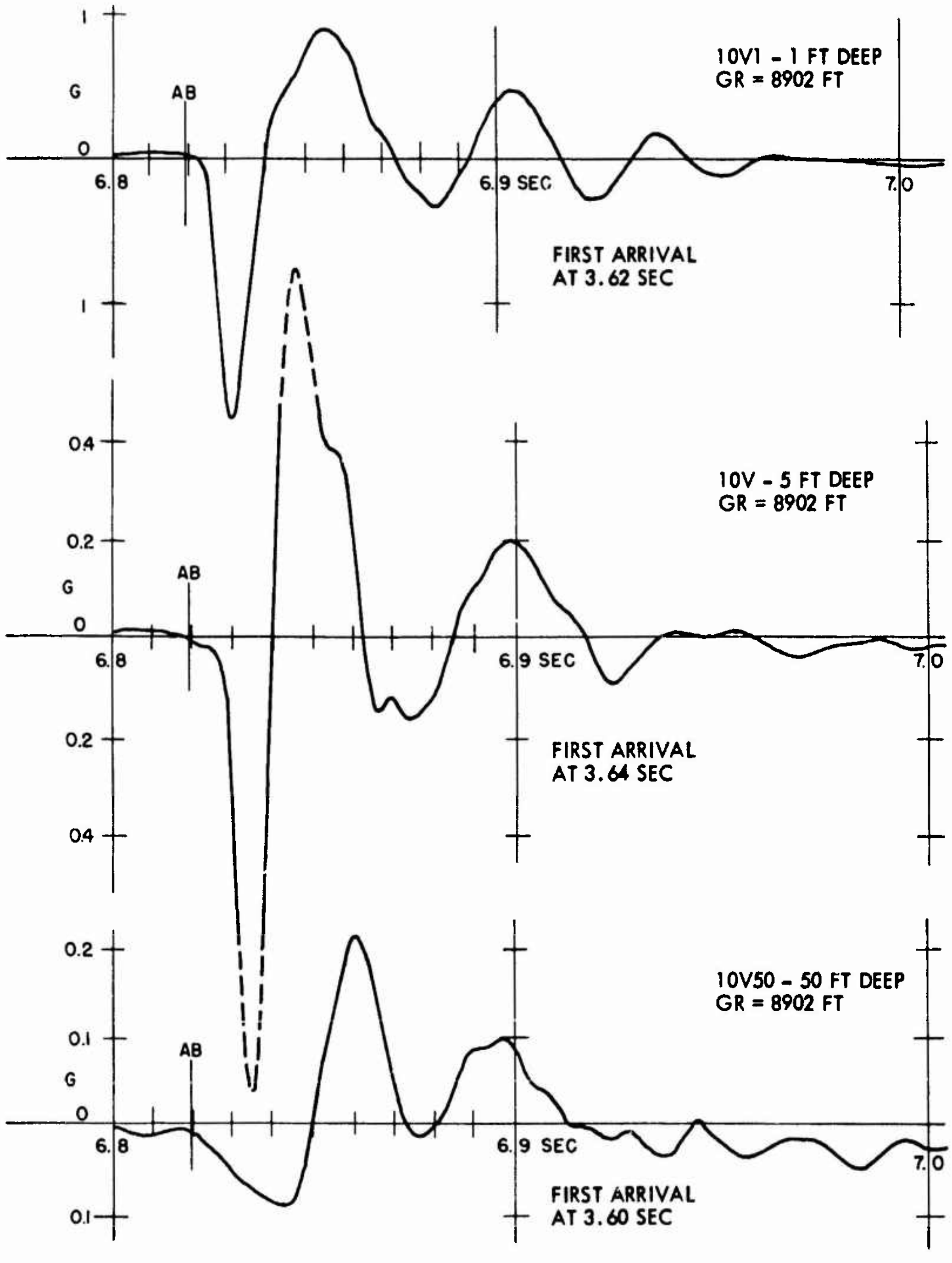


Fig. 4.2 Sample Vertical Earth Acceleration Gage Records. 1, 5, and 50 feet deep. Shot 3, Station 210

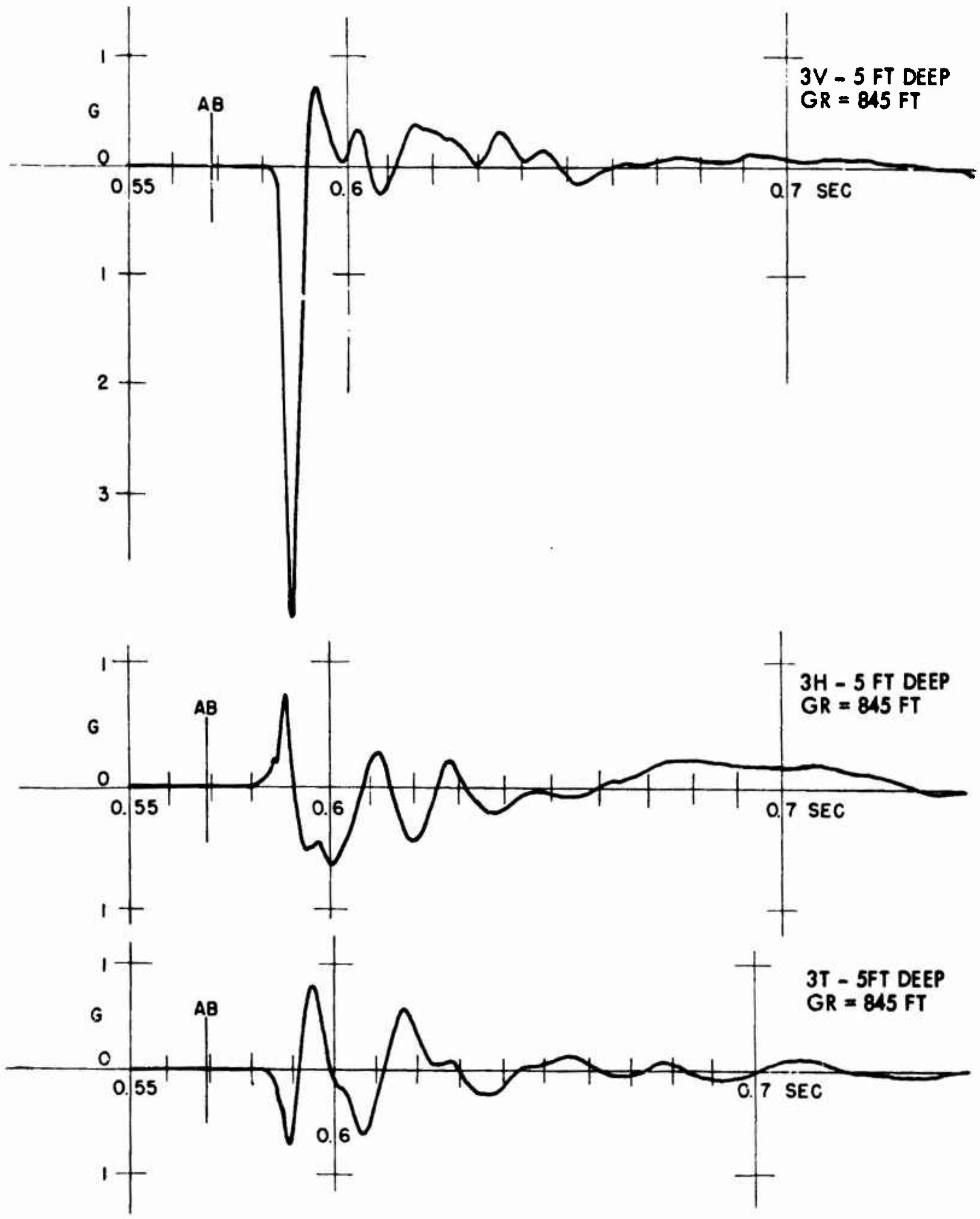


Fig. 4.3 Sample Vertical, Horizontal Radial, and Horizontal Tangential Earth Acceleration Gage Records. 5 feet deep. Shot 1, Station 203

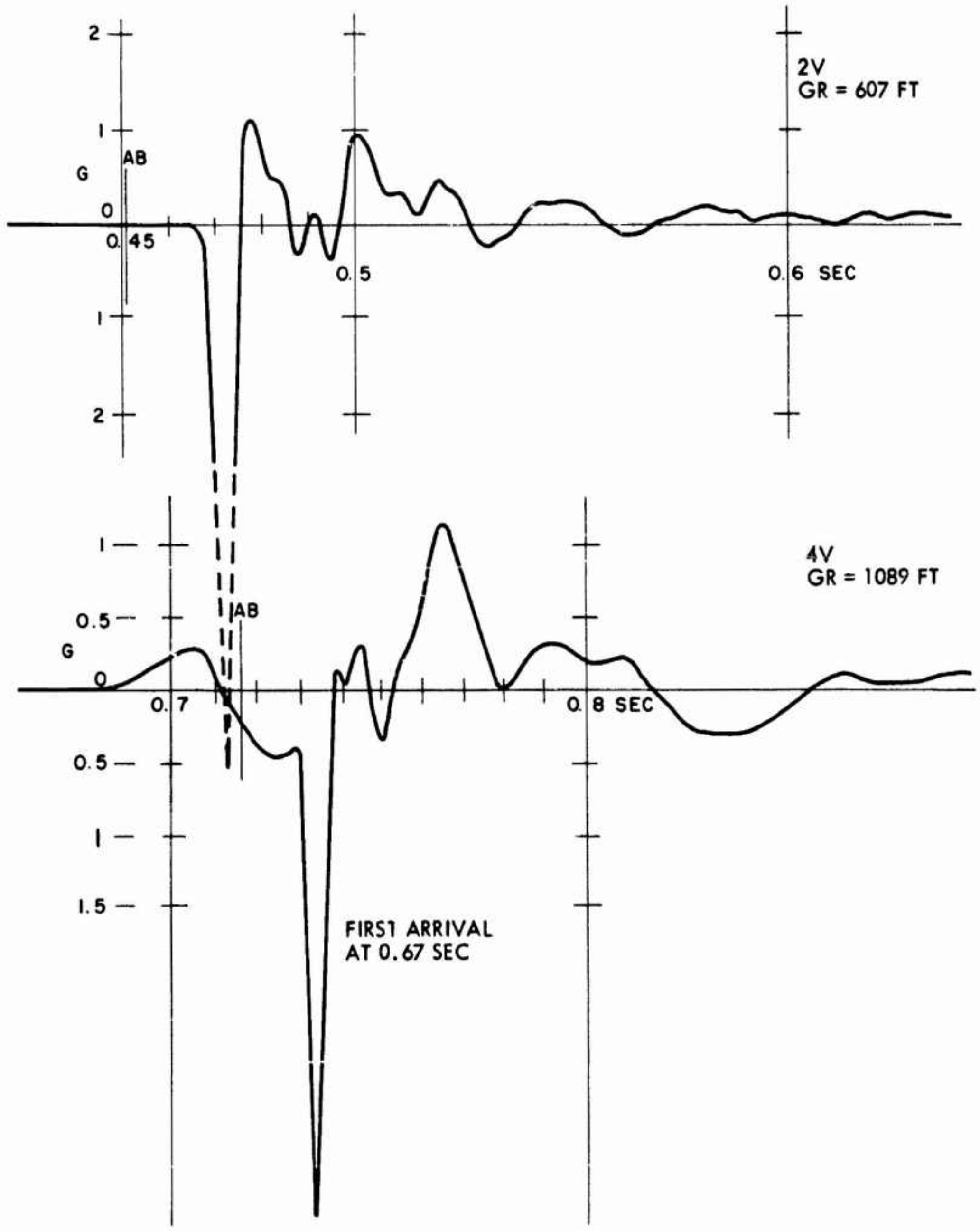


Fig. 4.4 Sample Vertical Earth Acceleration Gage Records. 5 feet deep. Shot 1, Stations 202 and 204

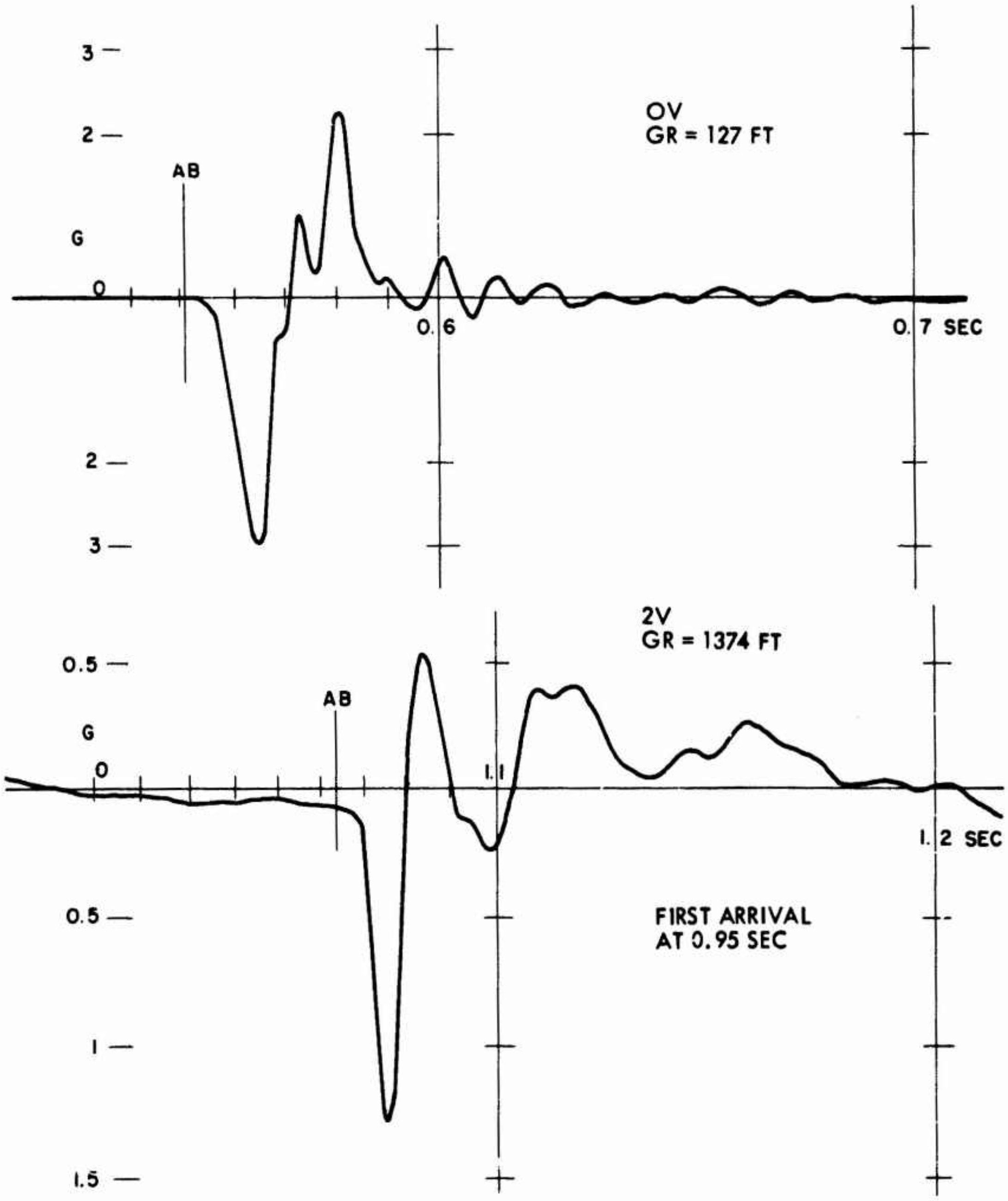


Fig. 4.5 Sample Vertical Earth Acceleration Gage Records. 5 feet deep. Shot 2, Stations 200 and 202

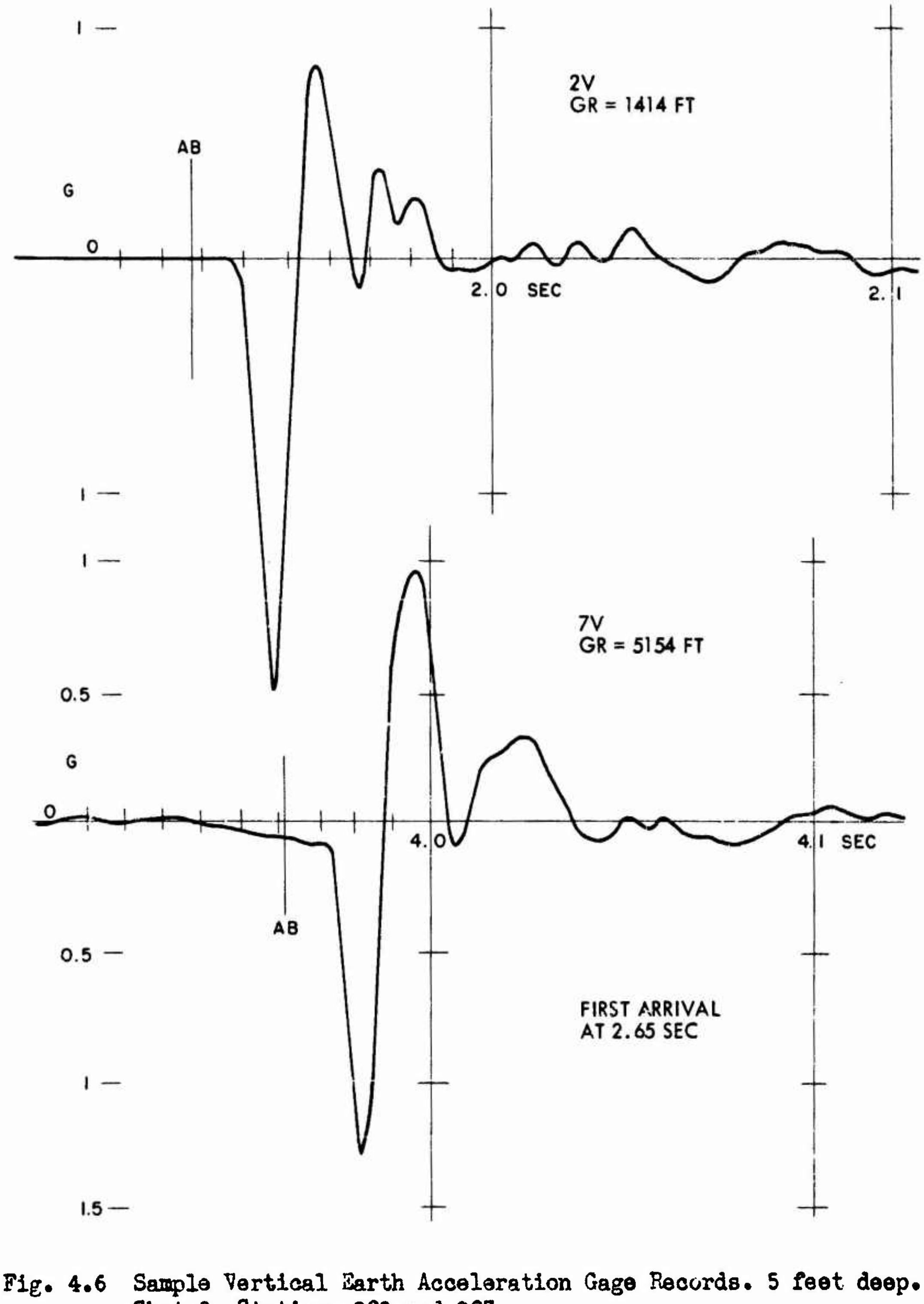


Fig. 4.6 Sample Vertical Earth Acceleration Gage Records. 5 feet deep. Shot 3, Stations 202 and 207

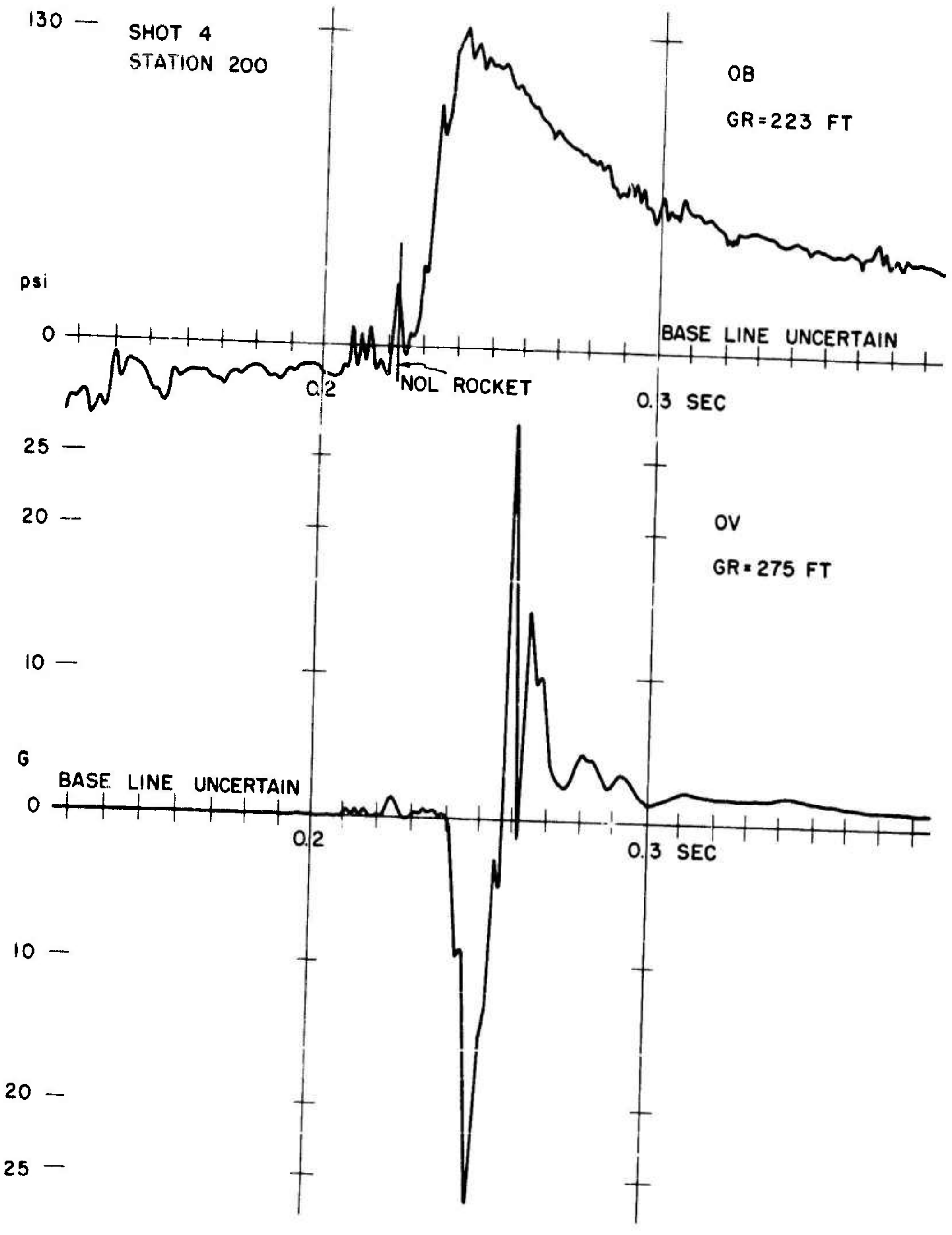


Fig. 4.7 Surface Level Air Pressure and Vertical Earth Acceleration, 5 feet deep. Shot 4, Station 200

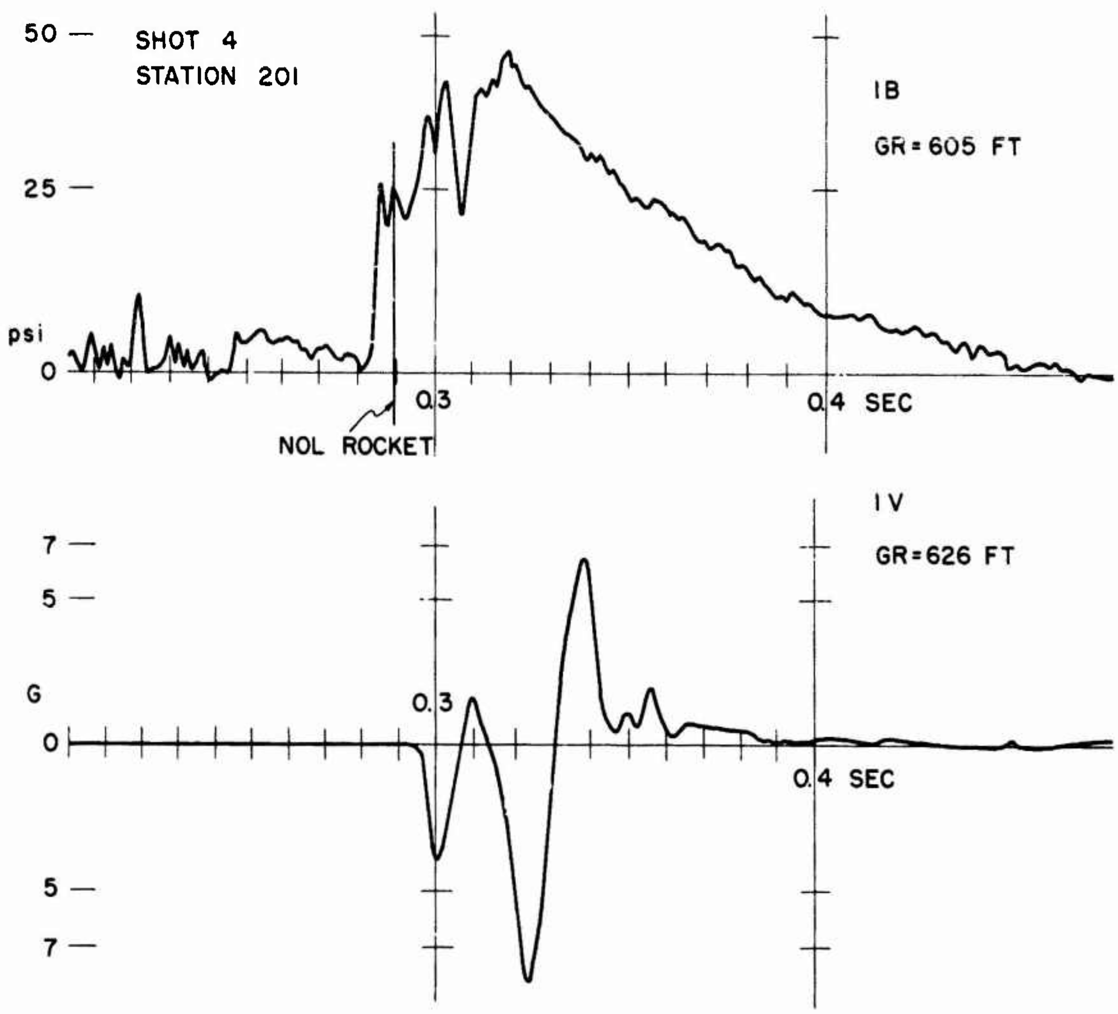


Fig. 4.8 Surface Level Air Pressure and Vertical Earth Acceleration, 5 feet deep. Shot 4, Station 201

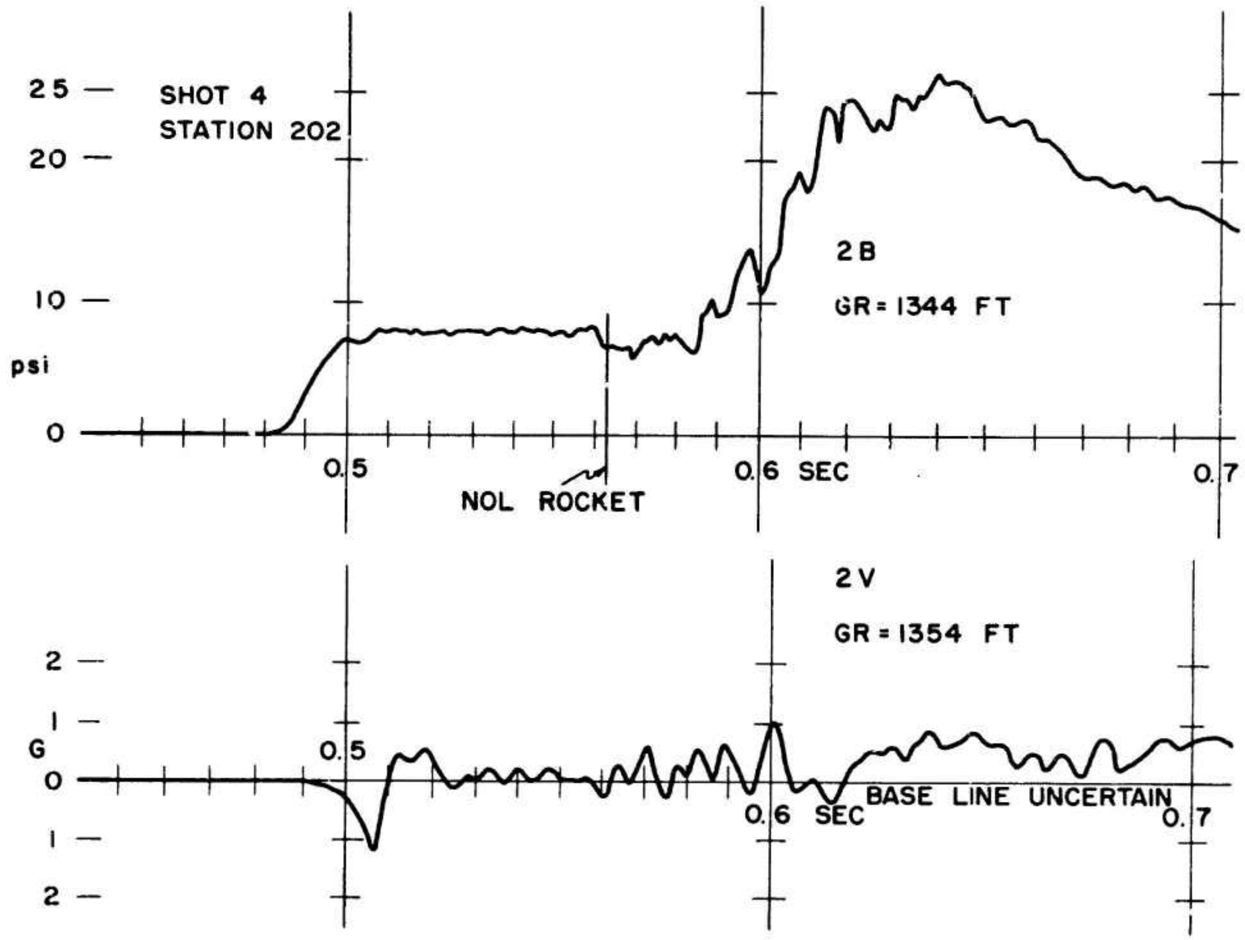


Fig. 4.9 Surface Level Air Pressure and Vertical Earth Acceleration, 5 feet deep. Shot 4, Station 202. Note that acceleration caused by precursor is greater than that caused by main blast.

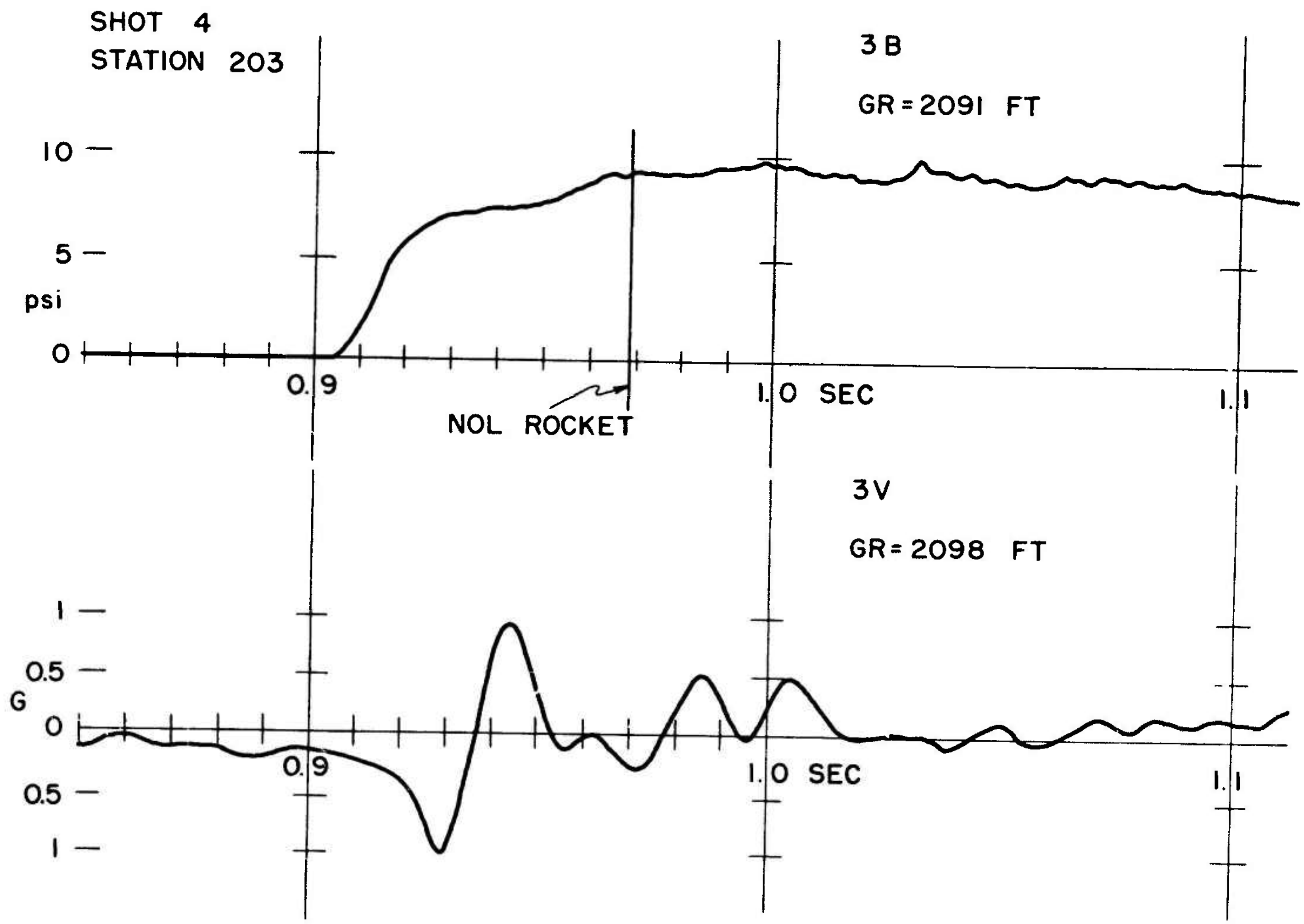


Fig. 4.10 Surface Level Air Pressure and Vertical Earth Acceleration, 5 feet deep. Shot 4, Station 203. Main blast not distinct from precursor. Note earth-transmitted acceleration has outrun direct air-blast slap.

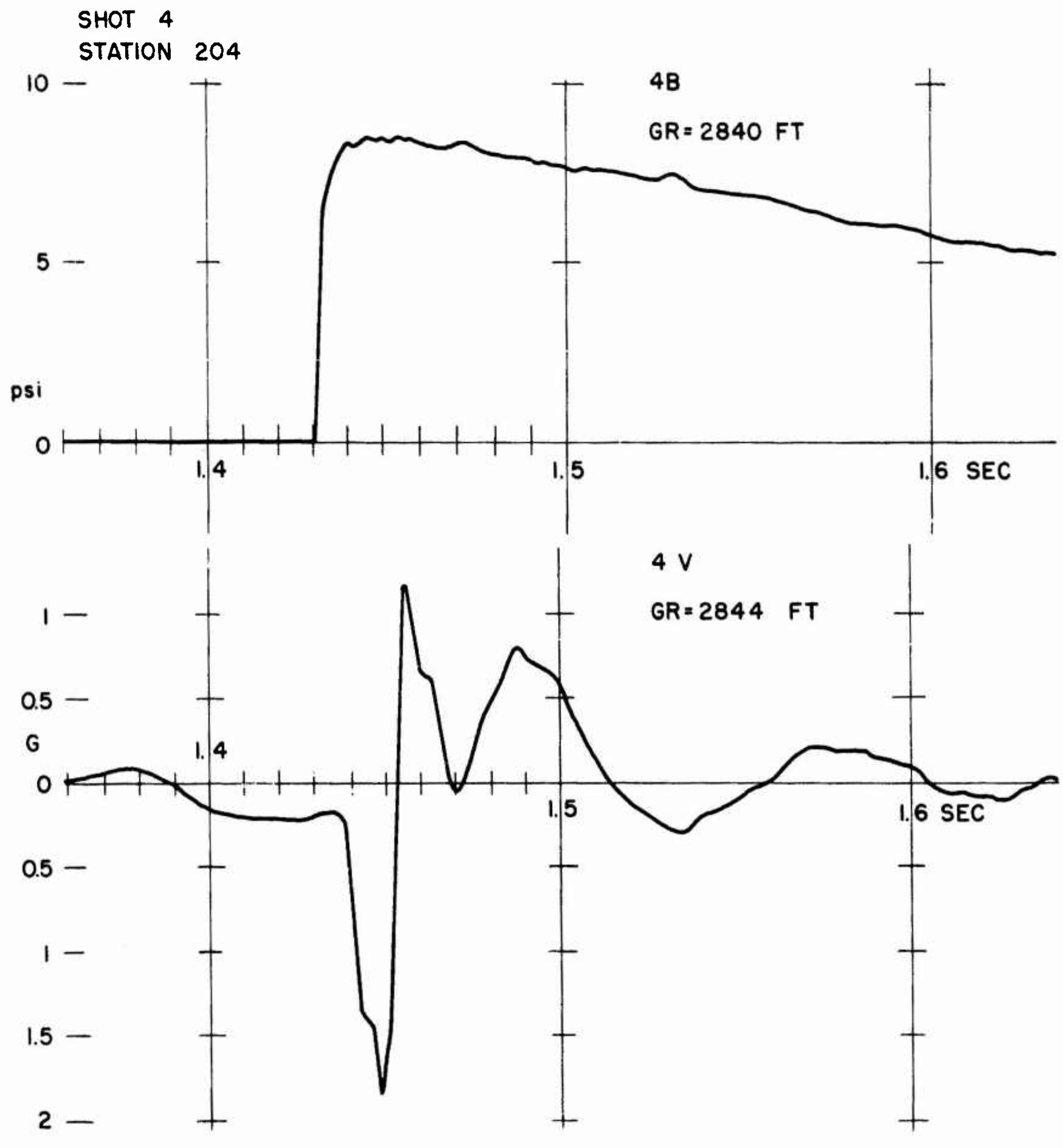


**Fig. 4.11 Surface Level Air Pressure and Vertical Earth Acceleration, 5 feet deep. Shot 4, Station 204. Precursor has disappeared; air-pressure and earth acceleration wave forms are normal.**

TABLE 4.1

Shot 1 - Preliminary Data

| Sta. No. | Gage Code No. | Grnd. Range (ft) | Depth (ft) | Acceleration (G) Max. Dir. Earth | Max. Neg. Slap | Max. Pos. Slap | Arrival Time (Sec) Earth Wave | Main Slap | Second Shock | Slap Freq (cps) | $f_s/f_n$ [j] | Max. Neg. Vel. (fps) | Max. Air Press. (psi) [k] |
|---|---|---|---|---|---|---|---|---|---|---|---|---|---|
| 200 | 0V | 227 | 5 | - | 15.0 | 3.89 | - | 0.347 | 0.986 | 119 | 0.63 | 1.1 | 25.7 |
| 201 | 1V | 384 | 5 | - | 10.53 | 1.57 | - | 0.384 | 1.04 | 96 | 0.51 | 0.97 | 22.1 |
| 202 | 2V | 607 | 5 | - | 5.57 | 1.04 | - | 0.466 | a | 81 | 0.43 | 0.77 | 13.8 |
| 203 | 3V1 | * | * | * | * | * | * | * | * | * | * | * | * |
| 203 | 3V | 845 | 5 | - | 4.10 | 0.74 | - | 0.583 | 1.476 | 76 | 0.95 | 0.41 | 10.1 |
| 203 | 3V50 | 861 | 50 | 0.03 | 0.65 | 0.19 | 0.58 | 0.598 | d | 39 | 0.49 | 0.23 | 10.2 |
| 203 | 3H | 845 | 5 | - | 0.62 | 0.75 | 0.58 | 0.581 | 1.42 | 109 | 1.36 | | 10.1 |
| 203 | 3H50 | 861 | 50 | - | 1.26 | 0.68 | 0.57 | 0.578 | d | 43 | 0.54 | | 10.2 |
| 203 | 3T | 845 | 5 | - | 0.72 | 0.81 | 0.58 | 0.583 | 1.52 | 64 | 0.79 | | 10.1 |
| 203 | 3T50 | 861 | 50 | - | 0.18 | 0.13 | 0.58 | 0.584 | d | 42 | 0.53 | | 10.2 |
| 204 | 4V | 1089 | 5 | 0.48 | 3.44 | 1.17 | 0.67 | 0.729 | 1.65 | 60 | 0.75 | 0.49 | 10.8 |
| 205 | 5V | 1335 | 5 | 0.16 | 3.72 | 1.38 | 0.76 | 0.842 | 1.86 | 82 | 1.02 | 0.47 | 9.7 |
| 206 | 6V | 1582 | 5 | 0.12 | 3.10 | 0.45 | 0.80 | 1.062 | 2.04 | 64 | 0.80 | 0.44 | 7.8 |
| 207 | 7V | 1330 | 5 | 0.12 | 2.71 | 0.85 | 0.83 b | 1.247 | 2.24 | 60 | 0.75 | 0.38 | 6.7 |
| 208 | 8V | 2078 | 5 | 0.11 | 1.92 | 0.46 | 0.95 | 1.434 | 2.46 | 58 | 0.73 | 0.29 | 5.2 |
| 209 | 9V | 2576 | 5 | 0.07 | 1.39 | 0.43 | 1.00 | 1.826 | 2.90 | 49 | 0.61 | 0.24 | 3.4 |
| 210 | 10V1 | * | * | * | * | * | * | * | * | * | * | * | * |
| 210 | 10V | 3075 | 5 | 0.05 | 1.03 | 0.44 | 1.06 | 2.226 | 3.33 | 40 | 0.89 | 0.24 | 2.47 |
| 210 | 10V50 | 3079 | 50 | 0.02 | 0.17 | 0.19 | 1.04 | 2.227 | 3.32 | 93 | 2.06 | 0.083 | 2.47 |
| 210 | 10H | 3075 | 5 | 0.04 | 0.32 | 0.38 | 1.06 | 2.234 | 3.33 | 23 | 0.51 | | 2.47 |
| 210 | 10H50 | 3079 | 50 | c | 0.07 | 0.09 | 1.05 | c | 3.33 | c | c | | 2.47 |
| 210 | 10T | 3075 | 5 | c | 0.09 | 0.12 | 1.03 | 2.240 | 3.33 | 18 | 0.40 | | 2.47 |
| 210 | 10T50 | 3079 | 50 | ** | ** | ** | ** | ** | ** | ** | ** | ** | * |

a Could not be detected
b Later arrival at 0.90 sec
c Earth wave and slap interfere; value uncertain
d Arrivals at 1.35, 1.63 and 2.12 sec
j **$f_s/f_n$ = slap frequency/damped natural frequency of gage**
k **Interpolated from original air pressure data**
* Gage not connected for this shot
** Gage out of order

TABLE 4.2

Shot 1 - Air-Blast Data

| Sta. No. | Gage Code No. | Grnd Range (ft) | Maximum Pressure (psi) | Arrival Time (sec) | |
|---|---|---|---|---|---|
| | | | | Main Blast | Second Shock |
| 200 | 0B | 166 | 26.80 | 0.331 | a |
| 201 | 1B | 352 | 22.80 | 0.369 | a |
| 202 | 2B | 587 | 14.52 | 0.451 | a |
| 203 | 3B | 831 | 10.00 | 0.569 | 1.610 |
| 204 | 4B | 1077 | 10.86 | 0.717 | 1.627 |
| 205 | 5B | 1326 | 9.74 | 0.880 | 1.826 |
| 206 | 6B | 1575 | 7.84 | 1.053 | 2.030 |
| 207 | 7B | 1824 | 6.71 | 1.236 | 2.241 |
| 208 | 8B | 2073 | 5.23 | 1.425 | 2.453 |
| 209 | 9B | 2570 | 3.43 | 1.818 | 2.884 |
| 210 | 10B | 3069 | 2.47 | 2.225 | 3.321 |

a Could not be detected

TABLE 4.3

Shot 2 - Preliminary Data

| Sta. No. | Gage Code No. | Grnd. Range (ft) | Depth (ft) | Acceleration (G) Max. Dir. Earth | Max. Neg. Slap | Max. Pos. Slap | Arrival Time (sec) Earth Wave | Main Slap | Second Shock | Slap Freq (cps) | $\frac{f_s}{f_n}$ j | Max. Neg. Vel. (fps) | Max. Air Press. (psi) k |
|---|---|---|---|---|---|---|---|---|---|---|---|---|---|
| 200 | 0V | 127 | 5 | - | 2.74 | 2.25 | - | 0.554 | 1.82 | 40 | 0.21 | 0.86 | 13.04 |
| 201 | 1V | 625 | 5 | - | 2.38 | 1.14 | - | 0.676 | 1.995 | 57 | 0.71 | 0.40 | 9.85 |
| 202 | 2V | 1374 | 5 | 0.09 | 1.22 | 0.54 | 0.95 f | 1.069 | 2.510 | 44 | 0.55 | 0.22 | 6.24 |
| 203 | 3V1 | * | * | * | * | * | * | * | * | * | * | * | * |
| 203 | 3V | 2120 | 5 | 0.07 | 1.12 | 1.28 | 1.13 f | 1.589 | 3.10 | 31 | 0.39 | 0.38 | 4.58 |
| 203 | 3V50 | 2123 | 50 | 0.03 | 0.18 | 0.47 | 1.10 f | 1.589 | 3.09 | 45 | 0.56 | 0.020 | 4.57 |
| 203 | 3H | 2120 | 5 | 0.05 | 0.68 | 0.47 | 1.10 f | 1.592 | 3.06 | 24 | 0.30 | | 4.58 |
| 203 | 3H50 | 2123 | 50 | 0.03 | 0.18 | 0.47 | 1.12 f | 1.590 | a | 77 | 0.96 | | 4.57 |
| 203 | 3T | 2120 | 5 | 0.06 | 0.20 | 0.33 | 1.13 f | 1.58 | 3.107 | 44 | 0.55 | | 4.58 |
| 203 | 3T50 | 2123 | 50 | 0.02 | 0.10 | 0.09 | 1.12 f | 1.58 | a | 48 | 0.60 | | 4.57 |
| 204 | 4V | 2874 | 5 | 0.04 | 0.74 | 0.75 | 1.27 f | 2.165 | 3.692 | 31 | 0.39 | 0.18 | 3.52 |
| 205 | 5V | 3624 | 5 | 0.03 | 0.48 | 0.20 | 1.40 f | 2.778 | 4.334 | 40 | 0.89 | 0.114 | 2.29 |
| 206 | 6V | 4374 | 5 | 0.02 | 0.37 | 0.50 | 1.52 f | c | 4.980 | 40 | 0.89 | 0.082 | 1.89 |
| 207 | 7V | 5124 | 5 | 0.02 | 0.41 | 0.36 | 1.65 f | c | 5.643 | 56 | 1.24 | 0.073 | 1.24 |
| 208 | 8V | 5875 | 5 | 0.02 | 0.55 | 0.68 | 2.10 gh | c | 6.262 | 44 | 0.98 | 0.13 | 1.07 |
| 209 | 9V | 7375 | 5 | 0.01 | 0.33 | 0.30 | 2.86 g | c | 7.625 | 55 | 1.22 | 0.063 | 0.89 |
| 210 | 10V1 | * | * | * | * | * | * | * | * | * | * | * | * |
| 210 | 10V | 8875 | 5 | 0.01 | 0.21 | 0.25 | 2.58 g | c | 8.915 | 46 | 1.02 | 0.043 | 0.48 |
| 210 | 10V50 | 8875 | 50 | 0.01 | 0.014 | 0.01 | 2.58 g | c | 8.95 | 21 | 0.47 | 0.004 | 0.48 |
| 210 | 10H | 8875 | 5 | 0.01 | 0.18 | 0.36 | 2.53 g | c | 8.962 | 33 | 0.73 | | 0.48 |
| 210 | 10H50 | 8875 | 50 | 0.01 | 0.014 | 0.01 | 2.55 g | 7.30 | a | 91 | 2.02 | | 0.48 |
| 210 | 10T | 8875 | 5 | c | 0.032 | 0.04 | 3.07 g | 7.23 | 8.926 | 31 | 0.69 | | 0.48 |
| 210 | 10T50 | 8875 | 50 | 0.001 | 0.007 | 0.006 | 2.76 g | 7.22 | a | 46 | 1.02 | | 0.48 |

a Could not be detected
c Earth wave and slap interfere: value uncertain
f Negative acceleration
g Positive acceleration
h Very faint negative acceleration at 1.76 sec
j $f_s/f_n$ = slap frequency/damped natural frequency of gage
k Interpolated from original air pressure data
* Gage not connected for this shot

TABLE 4.4

Shot 2 - Air-Blast Data

| Sta. No. | Gage Code No. | Grnd Range (ft) | Maximum Pressure (psi) | Arrival Time (sec) | |
|---|---|---|---|---|---|
| | | | | Main Blast | Second Shock |
| 200 | 0B | 151 | 12.92 | 0.551 | a |
| 201 | 1B | 629 | 9.86 | 0.674 | a |
| 202 | 2B | 1376 | 6.24 | 1.063 | a |
| 203 | 3B | 2125 | 4.57 | 1.583 | 3.1 |
| 204 | 4B | 2875 | 3.52 | 2.162 | 3.690 |
| 205 | 5B | 3625 | 2.29 | 2.771 | 4.32 |
| 206 | 6B | 4375 | 1.89 | 3.395 | 4.977 |
| 207 | 7B | 5125 | 1.24 | 4.029 | 5.634 |
| 208 | 8B | 5875 | 1.07 | 4.673 | a |
| 209 | 9B | 7375 | 0.89 | 5.968 | a |
| 210 | 10B | 8875 | 0.48 | 7.273 | 8.945 |

a Could not be detected

TABLE 4.5

Shot 3 - Preliminary Data

| Sta. No. | Gage Code No. | Grnd. Range (ft) | Depth (ft) | Acceleration (G) | | | Arrival Time (sec) | | | Slap Freq (cps) | $\frac{f_s}{f_n}$ [j] | Max. Neg. Vel. (fps) | Max. Air Press. (psi) [k] |
|---|---|---|---|---|---|---|---|---|---|---|---|---|---|
| | | | | Max. Dir. Earth | Max. Neg. Slap | Max. Pos. Slap | Earth Wave | Main Slap | Second Shock | | | | |
| 200 | 0V | 226 | 5 | - | 4.60 | 1.69 | - | 1.720 | b | 72 | 0.38 | 0.84 | [illegible]1.48 |
| 201 | 1V | 681 | 5 | - | 3.28 | 1.15 | - | 1.766 | b | 60 | 0.75 | 0.55 | 11.70 |
| 202 | 2V | 1414 | 5 | - | 1.88 | 0.84 | - | 1.932 | 7.41 | 41 | 0.51 | 0.46 | 10.15 |
| 203 | 3V1 | 2160 | 1 | - | 5.52 | 2.26 | 2.18 | 2.202 | 7.52 | 77 | 0.40 | 0.72 | 8.72 |
| 203 | 3V | 2160 | 5 | - | 1.78 | 1.03 | 2.18 | 2.210 | 7.54 | 29 | 0.36 | 0.20 | 8.72 |
| 203 | 3V50 | 2165 | 50 | - | 0.99 e | 0.50 e | 2.18 e | c,e | 7.22 e | 58 e | 0.73 e | 0.18 e | 8.72 |
| 203 | 3H | 2160 | 5 | - | 1.54 | 0.72 | 2.18 | c | 7.27 | 30 | 0.38 | | 8.72 |
| 203 | 3H50 | * | * | * | * | * | * | * | * | * | * | * | * |
| 203 | 3T | * | * | * | * | * | * | * | * | * | * | * | * |
| 203 | 3T50 | * | * | * | * | * | * | * | * | * | * | * | * |
| 204 | 4V | 2907 | 5 | 0.12 | 1.36 | 0.74 | 2.37 | 2.567 | 7.80 | 35 | 0.44 | 0.32 | 7.47 |
| 205 | 5V | 3656 | 5 | 0.06 | 1.69 | 1.11 | 2.53 | 2.992 | 8.21 | 63 | 0.79 | 0.31 | 6.34 |
| 206 | 6V | 4405 | 5 | 0.06 | 1.52 | 0.57 | 2.64 | 3.462 | 8.52 | 53 | 0.66 | 0.31 | 6.06 |
| 207 | 7V | 5154 | 5 | 0.08 | 1.22 | 0.98 | 2.65 | 3.970 | 9.15 | 38 | 0.48 | 0.32 | 4.82 |
| 208 | 8V | 5903 | 5 | 0.04 | 1.36 | 1.60 | 2.87 | 4.505 | 9.58 | 38 | 0.48 | 0.39 | 5.32 |
| 209 | 9V | 7403 | 5 | 0.05 | 1.32 | 0.89 | 3.33 | 5.637 | 10.77 | 43 | 0.54 | 0.32 | 3.93 |
| 210 | 10V1 | 8902 | 1 | 0.02 | 1.83 | 0.88 | 3.62 | 6.822 | 12.05 | 36 | 0.45 | 0.53 | 2.83 |
| 210 | 10V | 8902 | 5 | 0.02 | 0.92 | 0.76 | 3.64 | 6.825 | 12.01 | 39 | 0.87 | 0.20 | 2.83 |
| 210 | 10V50 | 8902 | 50 | 0.02 | 0.09 | 0.21 | 3.60 | c | 12.04 | 22 | 0.49 | 0.063 | 2.83 |
| 210 | 10H | 8902 | 5 | 0.03 | 0.89 | 1.20 | 3.64 | 6.833 | 12.02 | 36 | 0.80 | | 2.83 |
| 210 | 10H50 | 8902 | 50 | 0.02 | 0.09 | 0.05 | 3.62 | c | a | 51 | 1.13 | | 2.83 |
| 210 | 10T | 8902 | 5 | 0.02 | 0.15 | 0.21 | 3.7 | 6.832 | 12.04 | 39 | 0.87 | | 2.83 |
| 210 | 10T50 | * | * | * | * | * | * | * | * | * | * | * | * |

a Could not be detected
c Earth wave and slap interfere; value uncertain
e Gage rings
j $f_s/f_n$ - slap frequency/damped natural frequency of gage
k Interpolated from original air pressure data
* Gage not connected for this shot

TABLE 4.6

Shot 3 - Air-Blast Data

| Sta. No. | Gage Code No. | Grnd Range (ft) | Maximum Pressure (psi) | Arrival Time (sec) | |
|---|---|---|---|---|---|
| | | | | Main Blast | Second Shock |
| 200 | OB | 166 | 11.18 | 1.708 | a |
| 201 | 1B | 664 | 11.75 | 1.759 | a |
| 202 | 2B | 1406 | 10.15 | 1.928 | a |
| 203 | 3B | 2154 | 8.73 | 2.198 | 7.622 |
| 204 | 4B | 2903 | 7.47 | 2.561 | 7.799 |
| 205 | 5B | 3653 | 6.34 | 2.984 | 8.198 |
| 206 | 6B | 4402 | 6.06 | 3.456 | 8.646 |
| 207 | 7B | 5152 | 4.82 | 3.962 | 9.144 |
| 208 | 8B | 5902 | 5.32 | 4.498 | 9.683 |
| 209 | 9B | 7402 | 3.93 | 5.631 | a |
| 210 | 10B | 8901 | 2.83 | 6.819 | 12.038 |

a Could not be detected

TABLE 4.7

Shot 4 - Preliminary Data

| Sta. No. | Gage Code No. | Grnd. Range (ft) | Depth (ft) | Acceleration (G) Max. Dir. Earth | Pre-cursor Neg. | Pre-cursor Pos. | Max. Neg. Slap | Max. Pos. Slap | Slap Freq (cps) | $\frac{f_s}{f_n}$ j | Max. Neg. Vel. (fps) | Prec.[k] Air Press. (psi) | Main[k] Air Press. |
|---|---|---|---|---|---|---|---|---|---|---|---|---|---|
| 200 | 0V | 275 | 5 | - | - | - | 28.9 | 36.8 | 51 | 0.27 | 6.26 | - | 138 |
| 201 | 1V | 626 | 5 | - | - | - | p | p | 45 | 0.24 | p | - | p |
| 202 | 2V | 1354 | 5 | - | 1.19 | 0.53 | <0.34 | <0.97 | 50 r | 0.26 r | 0.23 r | 8.1 | 26 |
| 203 | 3V1 | 2098 | 1 | 0.12 | 2.20 | 0.48 | <0.66 | <0.93 | 41 r | 0.22 r | 0.51 r | 7.6 | 9.53 |
| 203 | 3V | 2098 | 5 | 0.22 | 0.97 | 0.90 | 0.30 | 0.50 | 28 r | 0.35 r | 0.[illegible] r | 7.6 | 9.53 |
| 203 | 3V50 | 2104 | 50 | 0.17 | 0.42 | 0.15 | <0.08 | <0.28 | 21 r | 0.26 r | b,r | 7.6 | 9.53 |
| 203 | 3H | 2098 | 5 | 0.01 | 1.44 | 0.65 | <0.39 | <0.64 | 31 r | 0.39 r | | 7.6 | 9.53 |
| 203 | 3H50 | * | * | * | * | * | * | * | * | * | * | * | * |
| 203 | 3T | * | * | * | * | * | * | * | * | * | * | * | * |
| 203 | 3T50 | * | * | * | * | * | * | * | * | * | * | * | |
| 204 | 4V | 2844 | 5 | 0.22 | - | - | 1.79 | 1.29 | 54 | 0.68 | 0.53 | - | 8.48 |
| 205 | 5V | 3593 | 5 | 0.19 | - | - | 1.72 | 0.46 | 58 | 0.73 | 0.30 | - | 6.35 |
| 206 | 6V | 4342 | 5 | 0.06 | - | - | 1.38 | 0.93 | 45 | 0.56 | 0.28 | - | 4.62 |
| 207 | 7V | 5091 | 5 | 0.07 | - | - | 1.34 | 1.28 | 44 | 0.55 | 0.30 | - | 3.75 |
| 208 | 8V | 5841 | 5 | 0.06 | - | - | 0.94 | 1.17 | 39 | 0.49 | 0.27 | - | 3.02 |
| 209 | 9V | 7339 | 5 | 0.07 | - | - | 0.80 | 0.63 | 51 | 0.64 | 0.15 | - | 2.04 |
| 210 | 10V1 | 8838 | 1 | 0.04 | - | - | 1.06 | 0.43 | 52 | 0.65 | 0.21 | - | 1.51 |
| 210 | 10V | 8838 | 5 | 0.03 | - | - | 0.49 | 0.46 | 42 | 0.93 | 0.11 | - | 1.51 |
| 210 | 10V50 | 8840 | 50 | 0.03 | - | - | 0.03 | 0.06 | 23 | 0.51 | 0.017 | - | 1.51 |
| 210 | 10H | 8838 | 5 | 0.03 | - | - | 0.54 | 0.52 | 44 | 0.98 | | - | 1.51 |
| 210 | 10H50 | 8840 | 50 | 0.03 | - | - | 0.02 | 0.05 | 42 | 0.93 | | - | 1.51 |
| 210 | 10T | 8838 | 5 | 0.01 | - | - | 0.10 | 0.12 | 36 | 0.80 | | - | 1.51 |
| 210 | 10T50 | * | * | * | * | * | * | * | * | * | * | * | * |

b  Value indefinite since wave form abnormal. Value lies between 0.03 and 0.32

j  $f_s/f_n$ - slap frequency/damped natural frequency of gage

k  Interpolated from original air pressure data

p  Gage 1V shows two shocks: air pressure, 26 and 45 psi; neg. slap accel., 3.95 and 8.13 G; pos. slap accel., 1.58 and 6.40 G; max. neg. vel., 0.74 and 2.35 fps

r  Value on precursor slap. Main slap not distinct.

*  Gage notconnected for this shot

TABLE 4.8

Shot 4 - Arrival Times

| Sta. No. | Gage Code No. | Grnd Range (ft) | Depth (ft) | Arrival Time (sec) | | | | |
|---|---|---|---|---|---|---|---|---|
| | | | | Earth Wave | Pre-cursor | Main Slap | Second Shock | Third Shock |
| 200 | 0V | 275 | 5 | - | - | 0.238 | a | a |
| 201 | 1V | 626 | 5 | - | - | p | a | a |
| 202 | 2V | 1354 | 5 | - | 0.491 | m | a | a |
| 203 | [illegible]1 | 2098 | 1 | 0.73 | 0.89 | m | a | 2.6 |
| 203 | 3V | 2098 | 5 | 0.74 | 0.91 | m | 1.549 | 2.6 |
| 203 | 3V50 | 2104 | 50 | 0.74 | 0.93 | m | 1.54 | a |
| 203 | 3H | 2098 | 5 | 0.73 | 0.925 | m | 1.55 | 2.6 |
| 203 | 3H50 | * | * | * | * | * | * | * |
| 203 | 3T | * | * | * | * | * | * | * |
| 203 | 3T50 | * | * | * | * | * | * | * |
| 204 | 4V | [illegible] | 5 | 0.91 | - | 1.438 | 2.071 | 3.37 |
| 205 | 5V | 3593 | 5 | 1.05 | - | 1.980 | 2.640 | 4.080 |
| 206 | 6V | 4342 | 5 | 1.19 | - | 2.542 | 3.229 | 4.788 |
| 207 | 7V | 5091 | 5 | 1.19 | - | 3.131 | 3.843 | 5.498 |
| 208 | 8V | 5841 | 5 | 1.24 | - | 3.731 | 4.456 | 6.197 |
| 209 | 9V | 7339 | 5 | 1.34 | - | 4.967 | 5.766 | 7.585 |
| 210 | 10V1 | 8838 | 1 | 2.11 | - | 6.226 | 6.979 | 8.966 |
| 210 | 10V | 8838 | 5 | 1.47 | - | 6.228 | 6.983 | 8.969 |
| 210 | 10V50 | 8840 | 50 | 1.47 | - | c | 6.99 | 8.97 |
| 210 | 10H | 8838 | 5 | 1.94 | - | 6.230 | 6.974 | 8.98 |
| 210 | 10H50 | 8840 | 50 | 1.84 | - | c | a | a |
| 210 | 10T | 8838 | 5 | 1.93 | - | 6.237 | 6.992 | 8.97 |
| 210 | 10T50 | * | * | * | * | * | * | * |

a Could not be detected
c Earth wave and slap interfere; value uncertain
m No distinct main shock
p Gage IV shows two shocks; arrival times, 0.295 and 0.314 sec.
* Gage not connected for this shot

TABLE 4.9

Shot 4 - Air-Blast Data

| Sta. No. | Gage Code No. | Grnd Range (ft) | Pressure (psi) | | Arrival Time (sec) | | | |
|---|---|---|---|---|---|---|---|---|
| | | | Pre-cursor | Main Shock | Pre-cursor | Main Shock | Second Shock | Third Shock |
| 200 | 0B | 223 | - | 140 | - | 0.225 | a | a |
| 201 | 1B | 605 | q | p | q | p | a | a |
| 202 | 2B | 1344 | 8.1 | 26 | 0.483 | 0.585 | a | 1.86 |
| 203 | 3B | 2091 | 7.6 | m | 0.904 | m | 1.528 | 2.50 |
| 204 | 4B | 2840 | - | 8.3 | - | 1.431 | 2.061 | 3.30 |
| 205 | 5B | 3589 | - | 6.35 | - | 1.972 | 2.630 | 4.04 |
| 206 | 6B | 4338 | - | 4.62 | - | 2.538 | 3.223 | 4.77 |
| 207 | 7B | 5087 | - | 3.75 | - | 3.126 | 3.831 | 5.48 |
| 208 | 8B | 5837 | - | 3.02 | - | 3.728 | 4.449 | 6.18 |
| 209 | 9B | 7337 | - | 2.04 | - | 4.962 | 5.700 | 7.58 |
| 210 | 10B | 8837 | - | 1.51 | - | 6.222 | 6.975 | 8.76 |

a Could not be detected

m No distinct main shock.

p Gage 1B has three separate shocks; arrival times, 0.284, 0.295, and 0.307 sec; pressures, 26, 42, and 45 psi.

q Record not clear; possibly a precursor exists with arrival time of 0.246 sec and pressure of 5.2 psi.

# CHAPTER 5

# DISCUSSION

## 5.1 GENERAL

The topics treated in this discussion may be grou under three general headings. First, the primary data are modified to bring out more clearly the fundamental phenomena involved. This requires consideration of the following:

Transmission process
Gage correction process

The primary data are then discussed under the following headings:

Air blast slap
TUMBLER Shot 4 precursor
Particle velocity
Effects of depth
Energy absorption

Finally, data of subsidiary importance to the main objectives are considered:

Secondary disturbances
Horizontal radial and tangential accelerations

## 5.2 TRANSMISSION PROCESS

In Section 1.2.1 the process of transmitting energy from the air blast to the earth has been considered on a qualitative basis. Somewhat more quantitative information is added by constructing for each of the four shots the time of arrival diagram idealized in Figure 1.2. These constitute Figures 5.1 through 5.4; the curves labeled secondary and tertiary are discussed in Section 5.9. Data derived from the curves appear in Table 5.1.

The curves for the main slap relate to the time at which locally generated information from the air blast starts being received at the gage. The accelerometers are all 5 feet deep. There is a 5 to 10 millisecond average delay between arrival at the surface and at the gage, indicating a transmission velocity at the surface of between 1000 and 500 feet per second for both the Frenchman Flat and the Yucca Flat

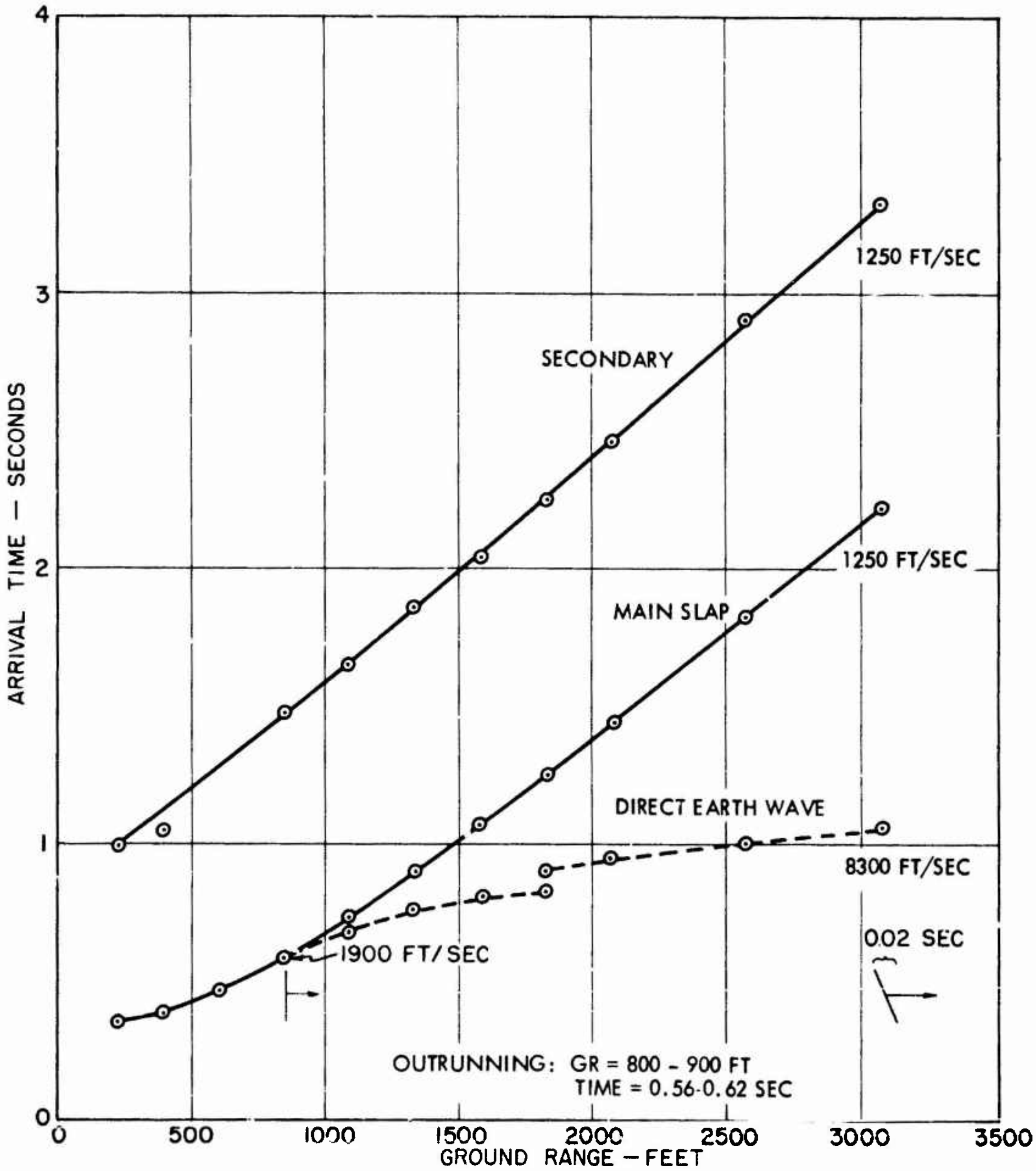


Fig. 5.1 Earth Acceleration Arrival Times. 5 feet deep. Shot 1

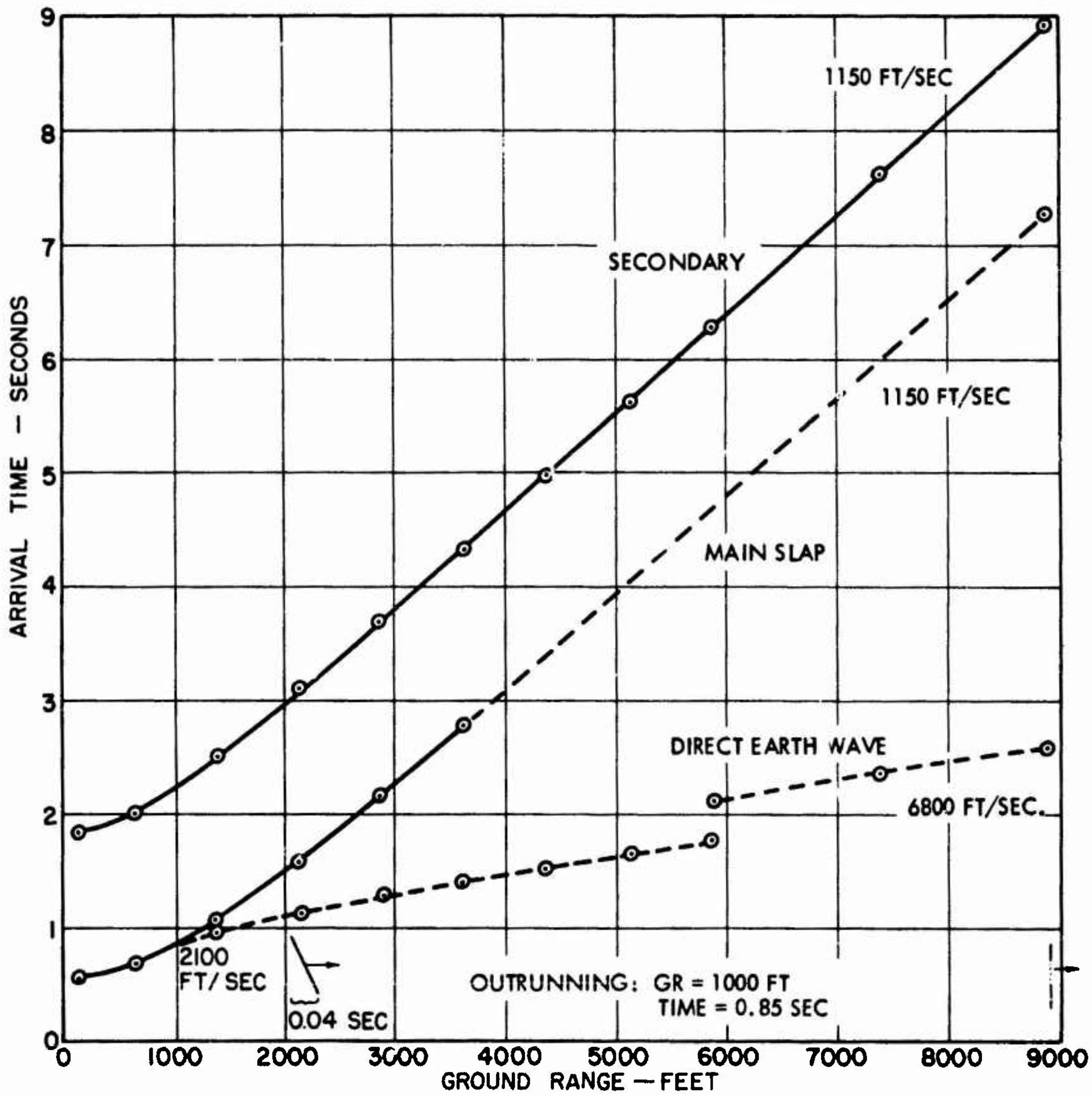


Fig. 5.2 Earth Acceleration Arrival Times. 5 feet deep. Shot 2

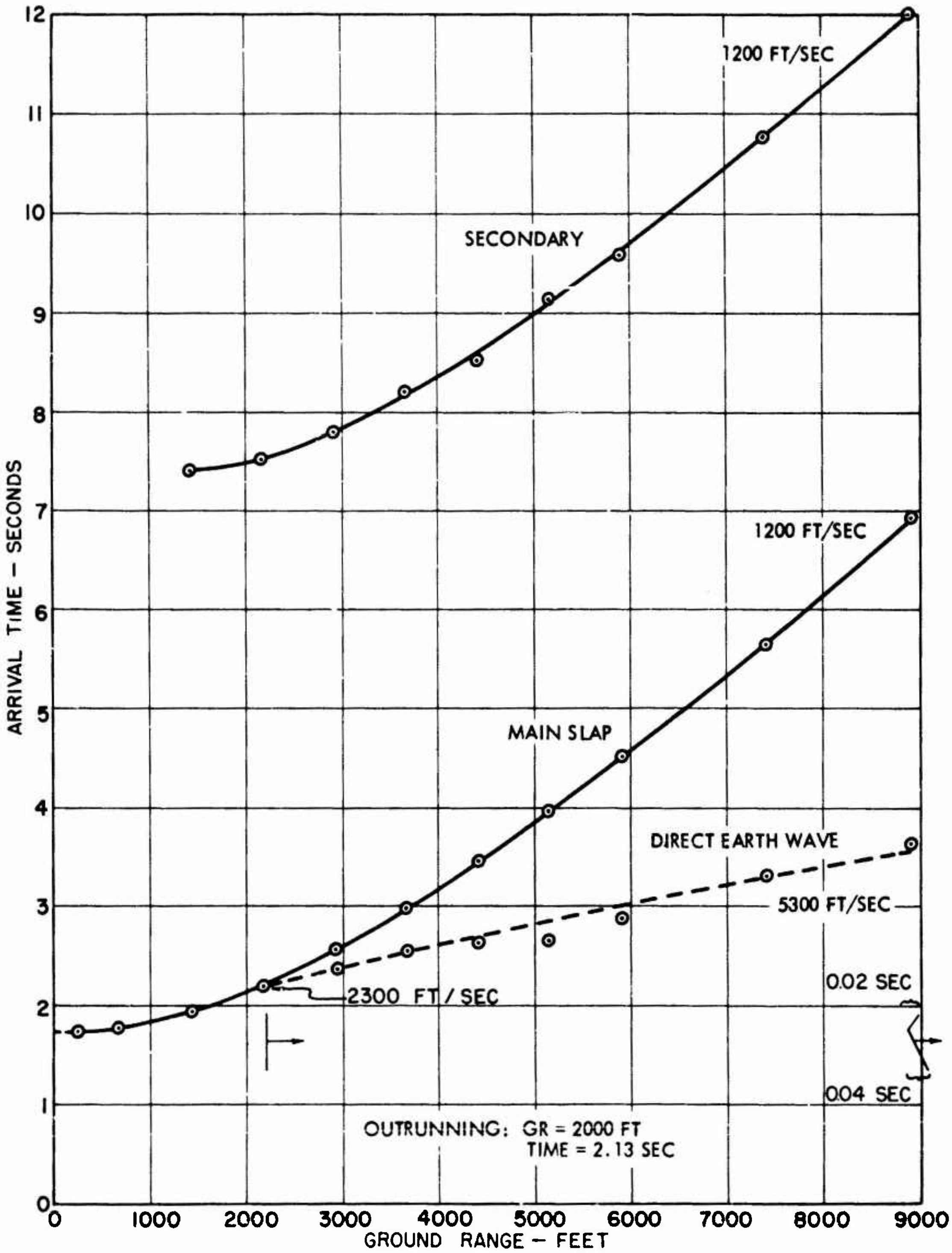


Fig. 5.3 Earth Acceleration Arrival Times. 5 feet deep. Shot 3

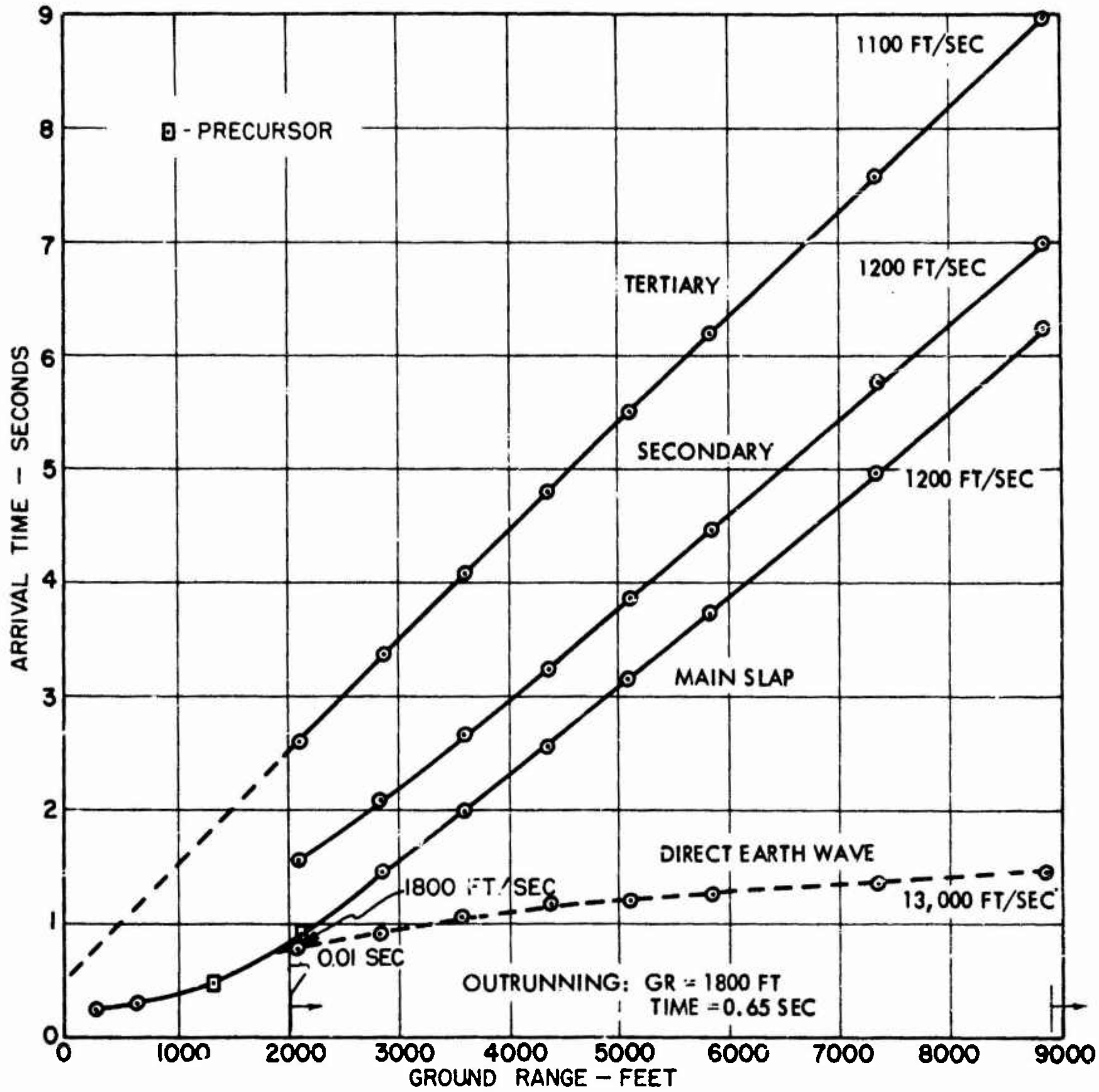


Fig. 5.4 Earth Acceleration Arrival Times. 5 feet deep. Shot 4

TABLE 5.1

Transmission Process Data

| Shot | Outrunning | | | Final Velocity | | |
|---|---|---|---|---|---|---|
| | Range (ft) | Time (sec) | Vel. (fps) | Range (ft) | Air (fps) | Earth (fps) |
| 1 | 850 | 0.59 | 1900 | 3000 | 1250 | 8300 |
| 2 | 1000 | 0.85 | 2100 | 9000 | 1150 | 6800 |
| 3 | 2000 | 2.13 | 2300 | 9000 | 1200 | 5300 |
| 4 | 1800 | 0.65 | 1800 | 9000 | 1200 | 13000 |

sites. This is not inconsistent with the known nature of the surface. Within the limits of this time delay, the "main slap" curves coincide in shape with those for the surface level air pressure.[2]

The "direct earth wave" curves refer to information arriving before that of the main slap. This wave increases in amplitude until the main slap arrives. No characteristic frequency was observed, though all frequencies were lower than the slap frequency. The outrunning (or breakaway) ground ranges are somewhat uncertain, but appear to be 850, 1000, 2000, and 1800 feet, respectively, for the four shots. The outrunning ranges for Shots 2 and 3 will not scale unless the propagation velocities in air and earth are the same at the same scaled distance. However, the earth arrival curves are slightly concave downward, indicating a general increase of velocity with depth. Thus the velocity in earth will not scale unless the velocity gradient scales as $W^{-1/3}$. Since this happy situation cannot be conveniently contrived, the apparent horizontal earth velocity will increase with distance and hence will tend to increase with yield, when measured at constant scaled distance. A consequence is that the ground range for outrunning in a larger scaled test will be less than predicted by conventional scaling, since the apparent horizontal earth wave velocity increases with scaled distance. In Shot 3, 3000 feet would have been predicted if the earth velocity had been constant, whereas 2000 feet was observed.

The earth wave curves in Shots 1 and 2 are seen to consist of two segments. This type of behavior is also observed in seismic methods of geophysical prospecting. As noted in Section 1.2.1, the attenuation in earth is greater than in air. Hence the initial arrival may be so attenuated at large ranges as to be unreadable. The arrival first noticed may be that of a later oscillation, when the first arrival has dropped below the noise level.

The initial and final velocities of the earth waves are indicated on the curves. All propagation velocities increase with range, attaining values of about 8300, 6800, 5300, and 13,000 feet per second at ranges of 3500, 9000, 9000, and 9000 feet, respectively, for the four shots. The first three appear plausible, but the velocity for Shot 4 is too high. A thermal explosion theory of precursor formation would predict high velocities such as this. In such a theory the precursor is assumed to be a rise in air pressure corresponding to a rapid heating of the air by radiation; the apparent velocity of the pressure rise would be very great. However, much lower arrival times and also a noticeable precursor at the distant stations would be expected, neither of which is observed. Except for Shot 4, the velocities are in the order that might be expected for the soils at the two sites; Frenchman Flat had a much more homogeneous and compact soil and larger near-surface seismic velocities (Table 3.2).

The initial earth wave velocities at outrunning are measured at the common point of tangency of the two curves. The approximate values are 1900, 2100, 2300, and 1800 feet per second for the four shots. The average value is about 2000 feet per second and, within the limits of the shots, may be taken as the effective initial surface propagation velocity for wave motion of the type excited in the earth by the air blast.

From Figure 1.1, the inclination of the wave fronts in the earth is seen to change after the earth wave outruns the air blast. From the two deep arrays of accelerometers, the wave front orientation between the 1- and 5-foot and the 5- and 50-foot deep gages may be obtained from time of arrival differences. These differences and the wave fronts are also displayed in Figures 5.1 through 5.4. In general, the inclination is opposite to that expected for an earth with uniform velocity.[1] However, because of the observed velocity gradient, the deeper portions of the wave fronts will travel faster, so that the orientation of the wave front will become as indicated in Figures 5.1 to 5.4.

## 5.3 GAGE CORRECTION

The procedure outlined in Section 1.2.3 may now be applied to calculating the correction of the slap wave forms due to gage response limitations. Table 5.2 lists the damped natural frequencies of the accelerometers used at various depths in the tests. Each accelerometer was connected to a high sensitivity galvanometer with a natural frequency of 200 cycles per second and to a low sensitivity galvanometer with a natural frequency of 300 cycles per second. Shot 2 was selected as the best one to correct, since most of its gage records were clean and readable, but the peak negative vertical slap acceleration versus ground range curve appeared peculiar.

TABLE 5.2

Accelerometer Damped Natural Frequencies

| Sta. No. | Gage Code No. | Damped Natural Frequency (cps) | | | |
|---|---|---|---|---|---|
| | | Shot 1 | Shot 2 | Shot 3 | Shot 4 |
| 200 | OV | 190 | 190 | 190 | 190 |
| 201 | 1V | 190 | 80 | 80 | 190 |
| 202 | 2V | 190 | 80 | 30 | 190 |
| 203 | 3V1 | * | * | 190 | 190 |
| 203 | 3V | 80 | 80 | 80 | 80 |
| 203 | 3V50 | 80 | 80 | 80 | 80 |
| 203 | 3H | 80 | 80 | 80 | 80 |
| 203 | 3H50 | 80 | 80 | * | * |
| 203 | 3T | 80 | 80 | * | * |
| 203 | 3T50 | 80 | 80 | * | * |
| 204 | 4V | 80 | 80 | 80 | 80 |
| 205 | 5V | 80 | 45 | 80 | 80 |
| 206 | 6V | 80 | 45 | 80 | 80 |
| 207 | 7V | 80 | 80 | 80 | 80 |
| 208 | 8V | 80 | 80 | 80 | 80 |
| 209 | 9V | 80 | 80 | 80 | 80 |
| 210 | 10V1 | * | * | 80 | 80 |
| 210 | 10V | 45 | 45 | 45 | 45 |
| 210 | 10V50 | 45 | 45 | 45 | 45 |
| 210 | 10H | 45 | 45 | 45 | 45 |
| 210 | 10H50 | 45 | 45 | 45 | 45 |
| 210 | 10T | 45 | 45 | 45 | 45 |
| 210 | 10T50 | 45 | 45 | * | * |

* Gage not connected for this shot

Points for the correction process were taken at millisecond intervals. The necessary derivatives were computed from these data points, using finite differences. It was found that the concept of slap frequency had to be modified. The correction depends to a great extent on the maximum slope of the leading edge. First the half-period, T, was found by extrapolation of the maximum slope and was employed to obtain the slap frequency, $f_s$, by

$$f_s = \frac{1}{2T} \tag{5.1}$$

The corrected slap curve was computed point by point, assuming a value of the damping ratio

$$\beta = 0.7 \tag{5.2}$$

The original and corrected curves were plotted with a more open time scale than the original records, as in Figure 1.3; the earth wave was edited out, as in Figure 4.1; and the corrected amplitude and frequency were read off. These are compared with the as-read values in Table 5.3. As an independent variable, the ratio of slap frequency to damped natural frequency of the gage is chosen. The undamped gage natural frequency would serve as well.

The correction factors are displayed graphically as functions of the above frequency ratio in Figure 5.5, together with an estimate of the maximum error in the amplitude correction. Corrections up to 60 per cent are calculated at a frequency ratio near unity. It is expected that the amplitude correction will always be positive (see the curves of Reference 6), so the spread into the negative correction region is unlikely. The slap frequency correction is more erratic but shows a tendency to increase with frequency ratio. Values in the range from 15 per cent to 35 per cent are calculated.

These same correction functions may be applied to the slap frequency and amplitude for the other shots, because the ratio of air-blast duration to equivalent slap period is so large (about 20 to 1). However, the large region of probable error makes this procedure somewhat doubtful. The ratio of slap frequency to gage frequency for every gage is given in Tables 4.1, 4.3, 4.5, and 4.7, providing a rough check on the reliability of the accelerations tabulated. To reduce the error, the raw data would have to be read at much smaller time intervals than was possible here. The values do confirm, however, that the corrected curve generally has a larger peak amplitude occurring sooner than in the raw curve. The time delay was small, amounting to only 2 to 5 milliseconds.

The ratio of slap frequency to damped natural gage frequency

TABLE 5.3

Gage Correction Data, Shot 2

| Gage Code No. | Grnd Range (ft) | $f_m$[a] (cps) | $f_s$ (cps)[b] | | $A_n$ (G)[c] | | $\frac{f_{s1}}{f_n}$ | $\frac{f_{s2}}{f_{s1}}$ | $\frac{A_{n2}}{A_{n1}}$ |
|---|---|---|---|---|---|---|---|---|---|
| | | | $f_{s1}$ as rd. | $f_{s2}$ corr. | $A_{n1}$ as rd. | $A_{n2}$ corr. | | | |
| 0V | 127 | 190 | 40 | - | 2.74 | - | - | - | - |
| 1V | 625 | 80 | 57 | 63 | 2.38 | 2.58 | 0.71 | 1.10 | 1.08 |
| 2V | 1374 | 80 | 44 | - | 1.22 | 1.33 | 0.55 | - | 1.09 |
| 3V | 2120 | 80 | 31 | 36 | 1.12 | 1.14 | 0.39 | 1.16 | 1.02 |
| 3V50 | 2123 | 80 | 45 | 55 | 0.18 | 0.18 | 0.36 | 1.22 | 1.00 |
| 4V | 2874 | 80 | 31 | 34 | 0.74 | 0.74 | 0.39 | 1.10 | 1.00 |
| 5V | 3624 | 45 | 40 | 50 | 0.48 | 0.61 | 0.89 | 1.25 | 1.27 |
| 6V | 4374 | 45 | 40 | 50 | 0.37 | 0.49 | 0.89 | 1.25 | 1.32 |
| 7V | 5124 | 80 | 56 | 69 | 0.41 | 0.44 | 0.70 | 1.23 | 1.07 |
| 8V | 5875 | 80 | 44 | 52 | 0.55 | 0.58 | 0.55 | 1.18 | 1.05 |
| 9V | 7375 | 80 | 55 | 60 | 0.33 | 0.37 | 0.69 | 1.09 | 1.12 |
| 10V | 8875 | 45 | 46 | 63 | 0.21 | 0.34 | 1.02 | 1.37 | 1.62 |

a $f_n$ = damped natural frequency of gage
b $f_s$ = slap frequency
c $A_n$ = maximum negative slap acceleration

TABLE 5.4

Minimum Ideal Gage Frequencies

| | Surface Level Air Pressure (psi) | Damped Natural Frequency of Gage (cps) |
|---|---|---|
| Shot 1 | 30<br>10<br>3 | 400<br>240<br>150 |
| Shots 2, 3, and 4 | 100 to 6<br>6 to 1 | 240<br>180 |

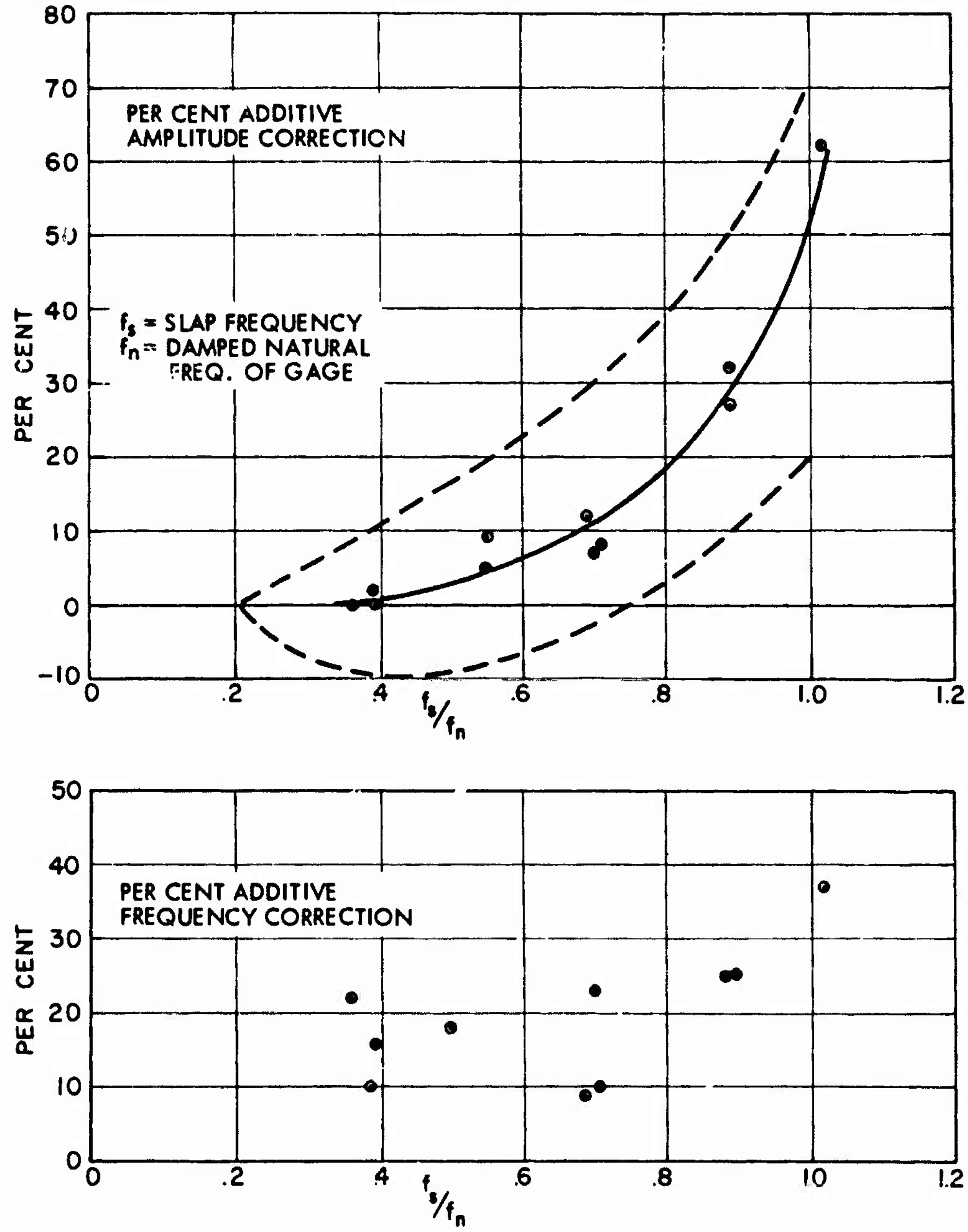


Fig. 5.5 Corrections for Gage Response, Shot 2

should be less than 0.3 if the recorded amplitude is to be free of significant error. If both accelerometers and galvanometer had had the natural frequencies given in Table 5.4, corrections for gage response would have been unnecessary. However, gage sensitivity decreases as natural frequency increases. A different terminal equipment, not available to us at the time of the TUMBLER shots, would be required by gages with such high natural frequencies.

## 5.4 SLAP ACCELERATION

If there is a one-to-one correspondence between earth motion and air-blast pressure, then the relation should be more evident when the peak negative slap vertical earth acceleration is plotted as a function of the peak surface level air pressure than if each is plotted separately against ground range. The validity of the assumption may be judged by the scatter of the data points. This method of plotting proves useful in predicting phenomena in the earth when the air pressure is known.

In Figures 5.6 and 5.7 these functions are displayed for the 5-foot deep acceleration and the surface level air pressure for the four shots; a composite appears in Figure 5.8. The slap accelerations plotted are as-read, uncorrected values from Tables 4.1, 4.3, 4.5, and 4.7. Owing to the fact that the accelerometers were laterally displaced from the blast line, the ground ranges for accelerometers and air pressure gages were appreciably different at the first few stations. The air pressures plotted are the interpolated values corresponding to the same ground range as the accelerometers. The data points corrected for gage response are added for Shot 2, but the consistency of the relation is not thereby improved. The curve at low pressures may be raised about 50 per cent by the correction. However, these accelerations were of lower magnitude than for the other shots and hence are subject to greater instrumental error.

On Shot 4 the acceleration wave forms in the high-pressure region showed the arrival of two or even three pressure waves, instead of one. Only the first arrival can be expected to show a consistent ratio of peak acceleration to peak pressure; in later arrivals this ratio is affected by the time interval between shocks and by the non-linearity of the earth. The curve drawn for Shot 4 in Figure 5.7 leaves out of consideration the points corresponding to the second shock at Station 201 and the true incident shock at Stations 202 and 203.

The slope of the curves on these log-log plots is also the exponent in the power-law relation between acceleration and pressure. The values of the exponent are smallest for small pressures. In the four shots, the exponents at the two ends of the curves have the following

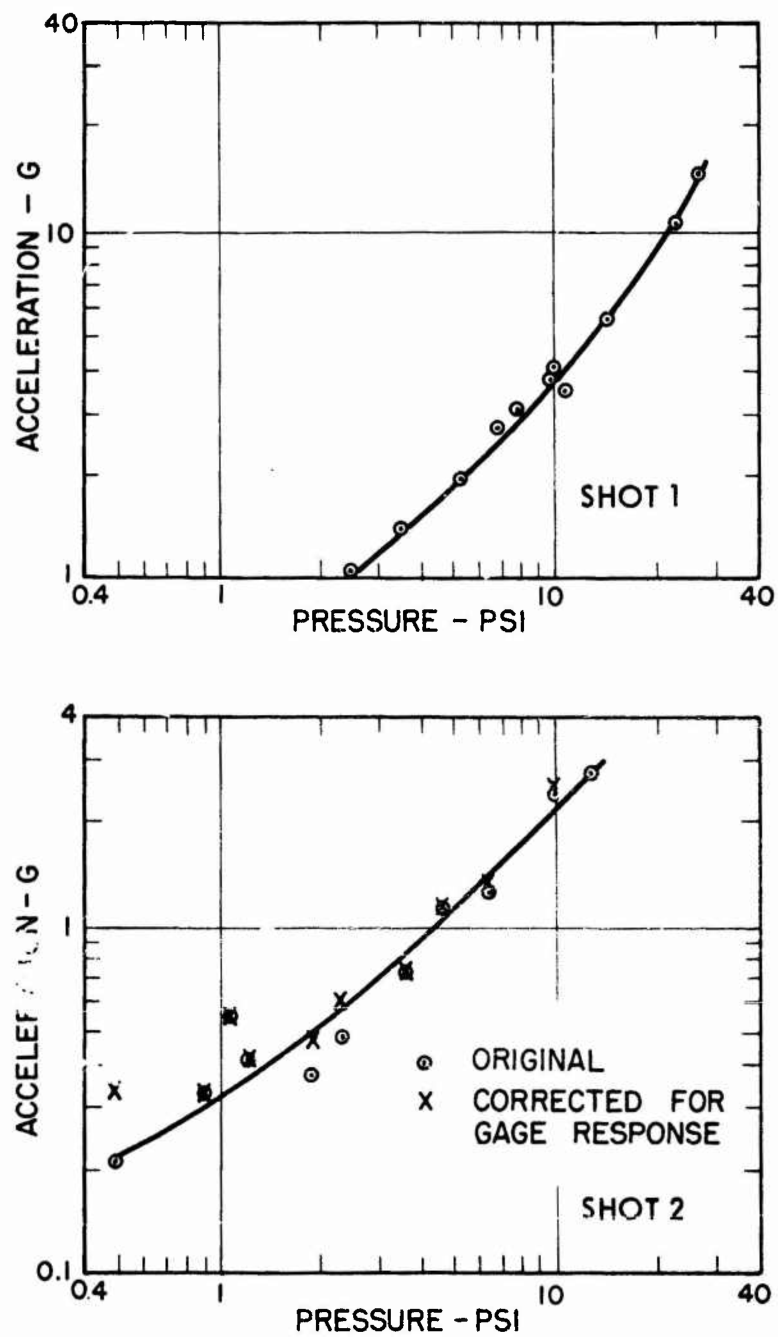


Fig. 5.6 Maximum Negative 5-foot Vertical Slap Acceleration vs. Maximum Surface Level Air Pressure, Shots 1 and 2

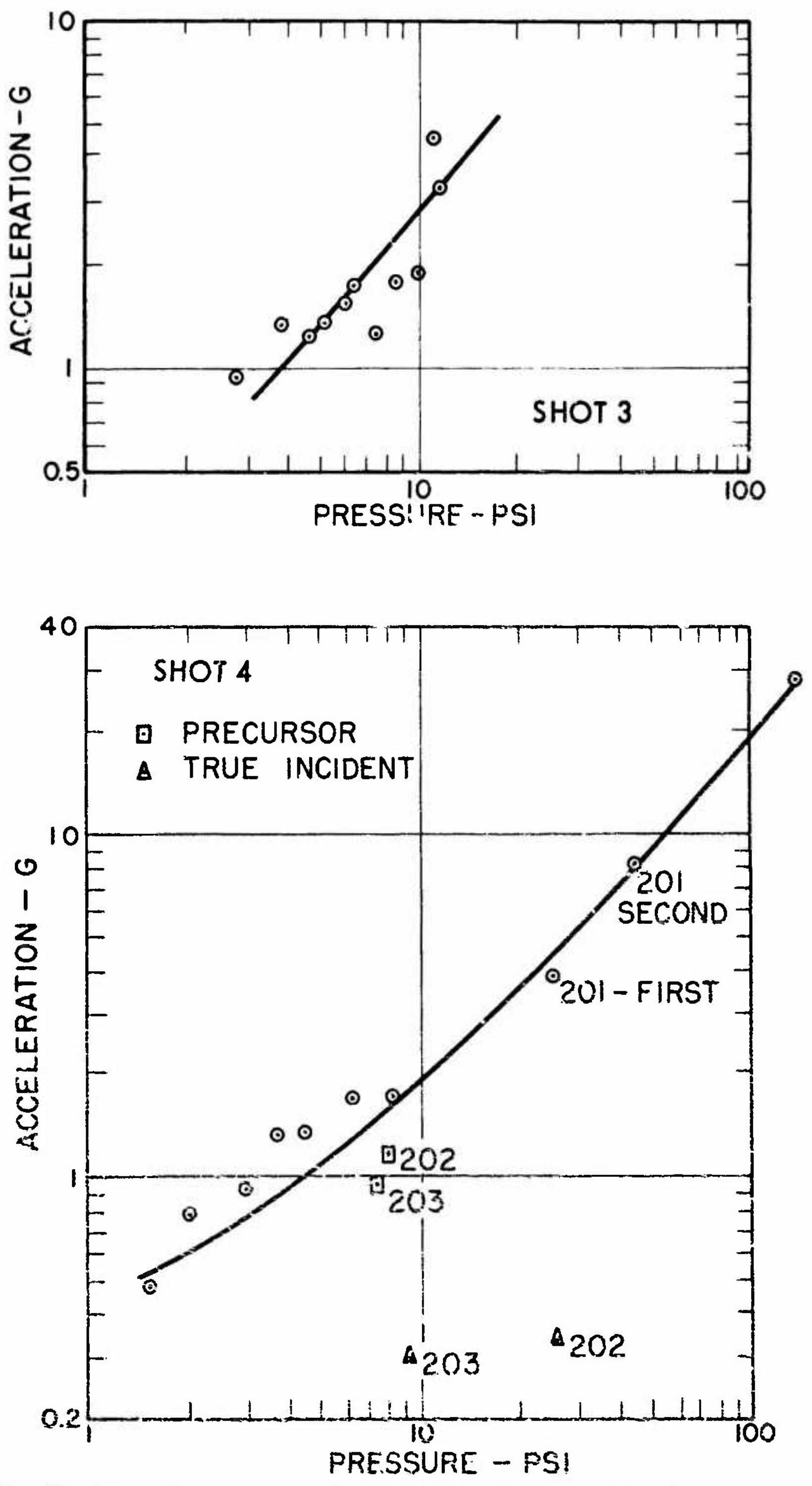


Fig. 5.7 Maximum Negative 5-foot Vertical Slap Acceleration vs. Maximum Surface Level Air Pressure, Shots 3 and 4

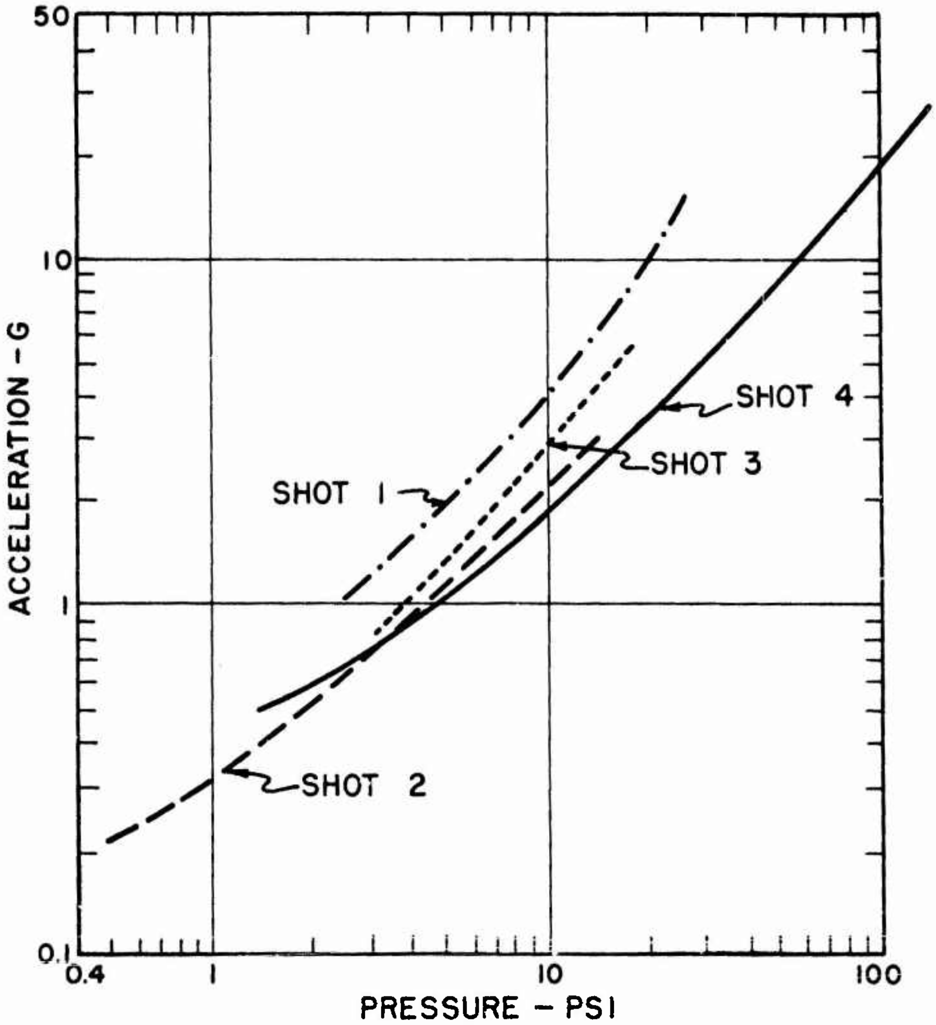


**Fig. 5.8 Composite Maximum Negative 5-foot Vertical Slap Acceleration vs. Maximum Surface Level Air Pressure**

approximate values: Shot 1, 0.87 and 1.33; Shot 2, 0.52 and 0.96; Shot 3, 1.00 and 1.19; and Shot 4, 0.51 and 1.15. The general increase of exponent with pressure implies that the earth becomes a somewhat better transmitter at larger pressures. This may be due to the compression of air in the surface layer, which would introduce the greatest attenuation at low air pressures and less attenuation as the pressure increases.

If one composite relation were required for all shots at Yucca Flat, then the straight line with exponent 0.89, with a slap acceleration of 2.5 g at 10 psi overpressure, might suffice. The equation is

$$A = 0.32\, p^{0.89} \quad , \tag{5.3}$$

where the units are g and psi, and a spread of plus or minus 50 per cent will include almost all the points. It must be emphasized, however, that this functional relationship is severely limited in its generality: it applies specifically to the yields, burst heights, and soil conditions of the shots at Yucca Flat. It is interesting that Shot 1, at Frenchman Flat, shows the expected greater earth response to pressure. There the soil was much more homogeneous and compact than at Yucca Flat. In the 10 psi region the slap accelerations produced were about 60 per cent greater than the average at Yucca Flat.

The data on uncorrected slap frequency, given in Tables 4.1, 4.3, 4.5, and 4.7, display considerable scatter if plotted as a function of surface level peak air pressure. For this reason, no curves are presented here. For Shots 2 and 4, the frequency appears to be more or less independent of air pressure, whereas on Shot 1 there is a definite trend toward an increase of frequency with pressure. A similar but less marked tendency is present in Shot 3. Shot 1 displays somewhat higher frequencies than the other three shots; this may possibly be a result of the more compact and higher velocity soil at Frenchman Flat. However, the large scatter of data points for all four shots renders these statements quite vague; they must be regarded as impressions gleaned from data insufficient in amount to treat statistically. The frequency increase on Shot 1 at Frenchman Flat probably indicates the type of non-linearity in the soil: an increase in effective modulus with pressure. In Figure 5.8 the corresponding amplitude curve exhibits slightly more curvature than do those for the average of the shots at Yucca Flat; this behavior, however, is not too pronounced. A safe qualitative conclusion is that the Frenchman Flat soil shows less attenuation and is somewhat more non-linear than that at Yucca Flat.

## 5.5 TUMBLER SHOT 4 PRECURSOR

On Shot 4 of the TUMBLER tests there existed at close-in gage

stations a unique air-pressure wave, called the precursor, which preceded the ordinary incident wave. A discussion of the various explanations suggested for this phenomenon is given in the report on Project 1.2.2/

Vertical earth acceleration as a function of time is compared with the surface level air pressure in Figures 4.7 through 4.11. Since the accelerometer blast line was displaced relative to the air-pressure gage blast line, the ground ranges for the two types of gage differ; thus arrival times are comparable only to several milliseconds. The vertical lines marked "NOL rocket" indicate incident wave arrival times obtained from rocket-trail photography.9/

In Figure 5.7 peak acceleration is plotted against peak air pressure; the relation is the same for the precursor as for other first arrivals. The incident wave following the precursor does not follow this relation but is affected by the natural frequency of the earth and its non-linear characteristics.

It was shown in Section 1.2.1 that the "round trip" pressure ratio for transmission from air to earth to air again would be given by Equation 1.4. The ratio may be computed from the known unit weight of air and earth, and the average velocity at outrunning found in Section 5.2. Use for air (at the site elevation and pressure), 0.66 lb/cu ft and 1100 fps; for earth, 100 lb/cu ft and 2000 fps. The round trip pressure ratio is then about 1/1400. Thus precursor formation by this mechanism alone is extremely unlikely.

In Section 5.8 the fraction of blast energy absorbed by the earth from the air is calculated to be about 0.2 per cent for Shot 4, showing again that precursor formation by the action of the earth on the air is unlikely.

## 5.6 SLAP PARTICLE VELOCITY

Maximum vertical earth particle velocities were calculated by the procedure outlined in Section 1.2.4, from the as-read vertical 5-foot slap accelerations. These values appear in Tables 4.1, 4.3, 4.5, and 4.7. Because of the expected close relation between earth motion and air pressure, these velocities are compared with the interpolated surface level air pressures given in the same tables. The curves for velocity versus air pressure appear in Figures 5.9 and 5.10, with Figure 5.11 affording a comparison by composite curves. The curves for all four shots can be approximated by the relation

$$v = 0.06\ p^{0.89} \qquad (5.4)$$

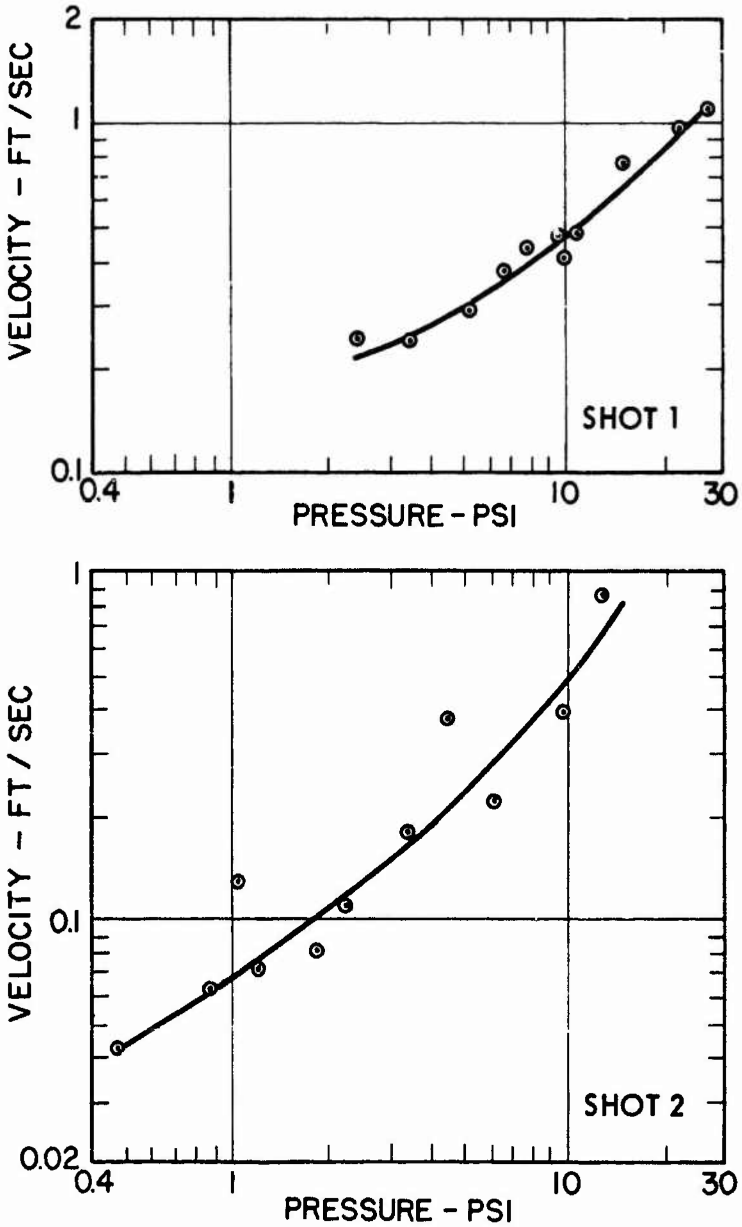


Fig. 5.9 Maximum Negative 5-foot Vertical Slap Particle Velocity vs. Maximum Surface Level Air Pressure, Shots 1 and 2

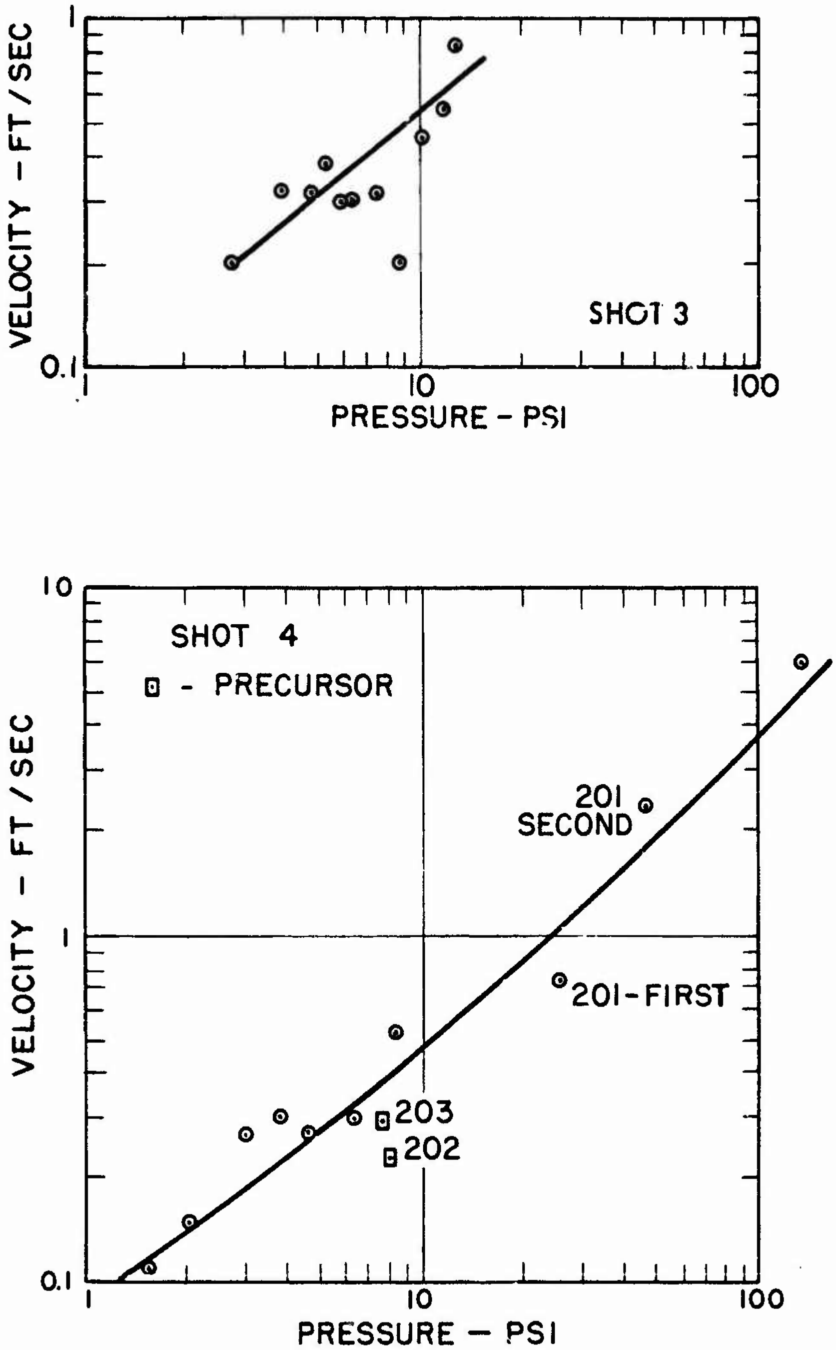


Fig. 5.10 Maximum Negative 5-foot Vertical Slap Particle Velocity vs. Maximum Surface Level Air Pressure, Shots 3 and 4

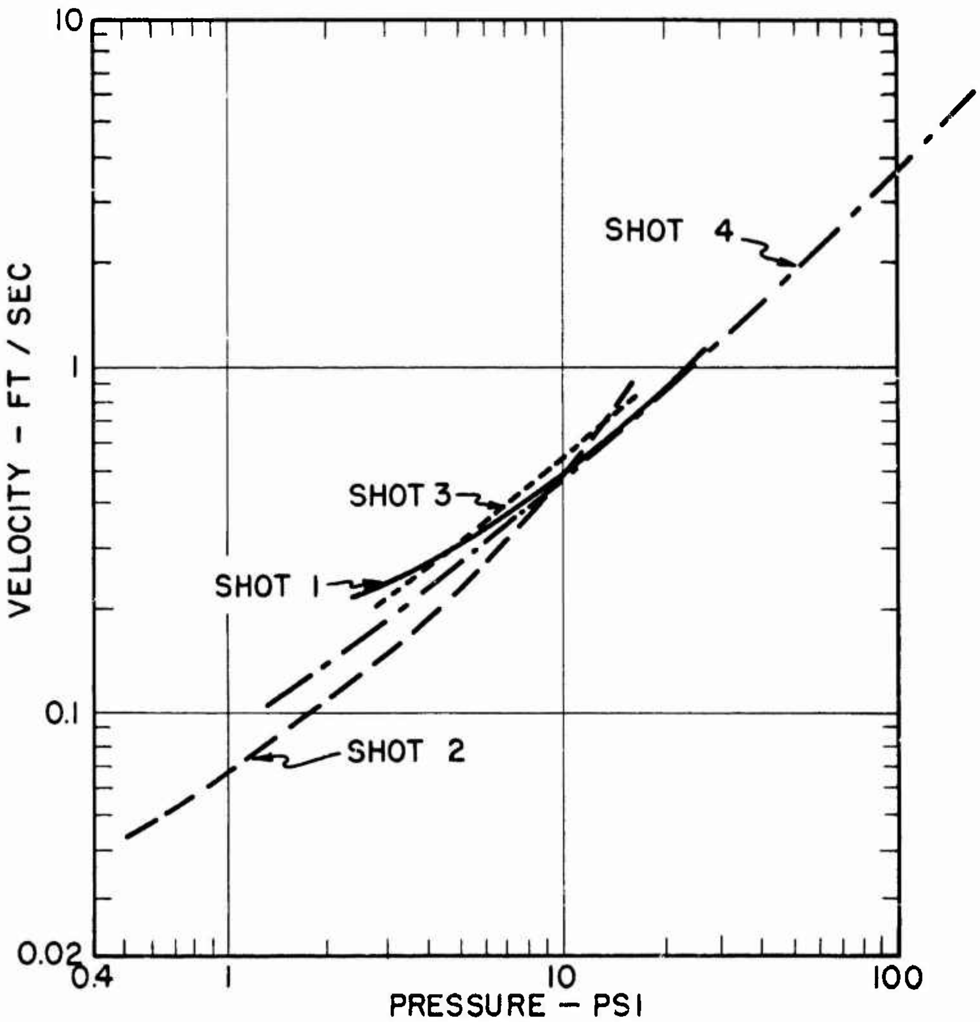


Fig. 5.11 Composite Maximum Negative 5-foot Vertical Slap Particle Velocity vs. Maximum Surface Level Air Pressure

where the units are fps and psi, and where a spread of plus or minus 60 per cent will include most points.

When the lower-pressure portions of the curves are compared, the ratio of peak pressure in psi to peak velocity in fps is in the neighborhood of 15 to 1 for all shots. Shot 1 shows somewhat more variation than the others, but the average ratio is about the same. In English units of pounds per square foot for pressure, the ratio is about 2200 lb-sec/cu ft. If the earth acts as a perfectly elastic fluid under the excitation of the air blast, then this ratio should be equal to the characteristic wave impedance $z$ or $\rho c$, as discussed in Section 1.2.1. In addition, the air pressure should be transmitted undiminished to the surface of the earth. With these assumptions, the velocity of vertical transmission, c, should be given by the characteristic impedance divided by the density. For Nevada Proving Grounds soil, a reasonable near-surface value of density is three slugs (about 96 pounds) per cubic foot. Thus c is about 700 fps on this basis. This may be compared with the value obtained by dividing the accelerometer depth (5 feet) by the time delay between arrival of the air blast at the surface and its initial appearance at the gage. This delay is indefinite but lies between 5 and 10 milliseconds. Thus the velocity of vertical transmission near the surface is directly calculated as between 500 and 1000 fps, agreeing well with the 700 fps calculated from the air pressure to earth particle velocity ratio. Note that this vertical propagation velocity is considerably less than the horizontal velocity obtained from time of arrival data discussed in Section 5.2. The average horizontal velocity at outrunning was about 2000 fps, about three times the vertical velocity. This discrepancy probably reflects the marked change in transmission characteristics for the first few feet of earth near the surface.

## 5.7 EFFECTS OF DEPTH

At Stations 203 and 210, vertical accelerometers were installed at depths of 1 foot and 50 feet in addition to gages at the standard depth of 5 feet. On Shots 1 and 2, no 1-foot accelerometers were connected. The slap accelerations and particle velocities as functions of depth constitute the data discussed here. Besides the general behavior, it is also desired to estimate the relation between peak slap velocity at 5 feet and at the surface.

Figure 4.2 displays representative vertical acceleration records at the 1-, 5-, and 50-foot depths at Station 210 on Shot 3. There the attenuation with depth is easily seen.

Figures 5.12 and 5.13 present these peak slap accelerations vs. depth for the four shots at the two stations instrumented in depth.

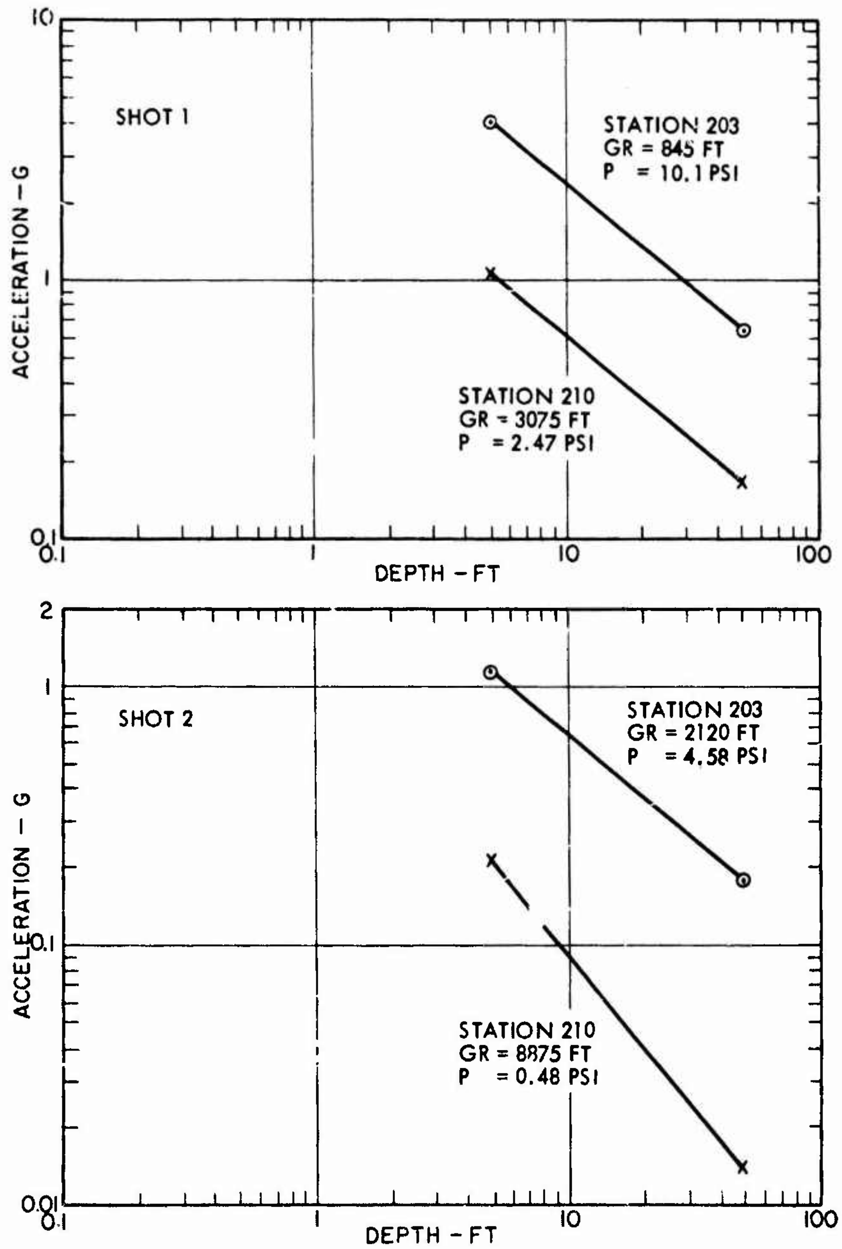


**Fig. 5.12** Maximum Negative 5-foot Vertical Slap Acceleration vs. Depth, Shots 1 and 2

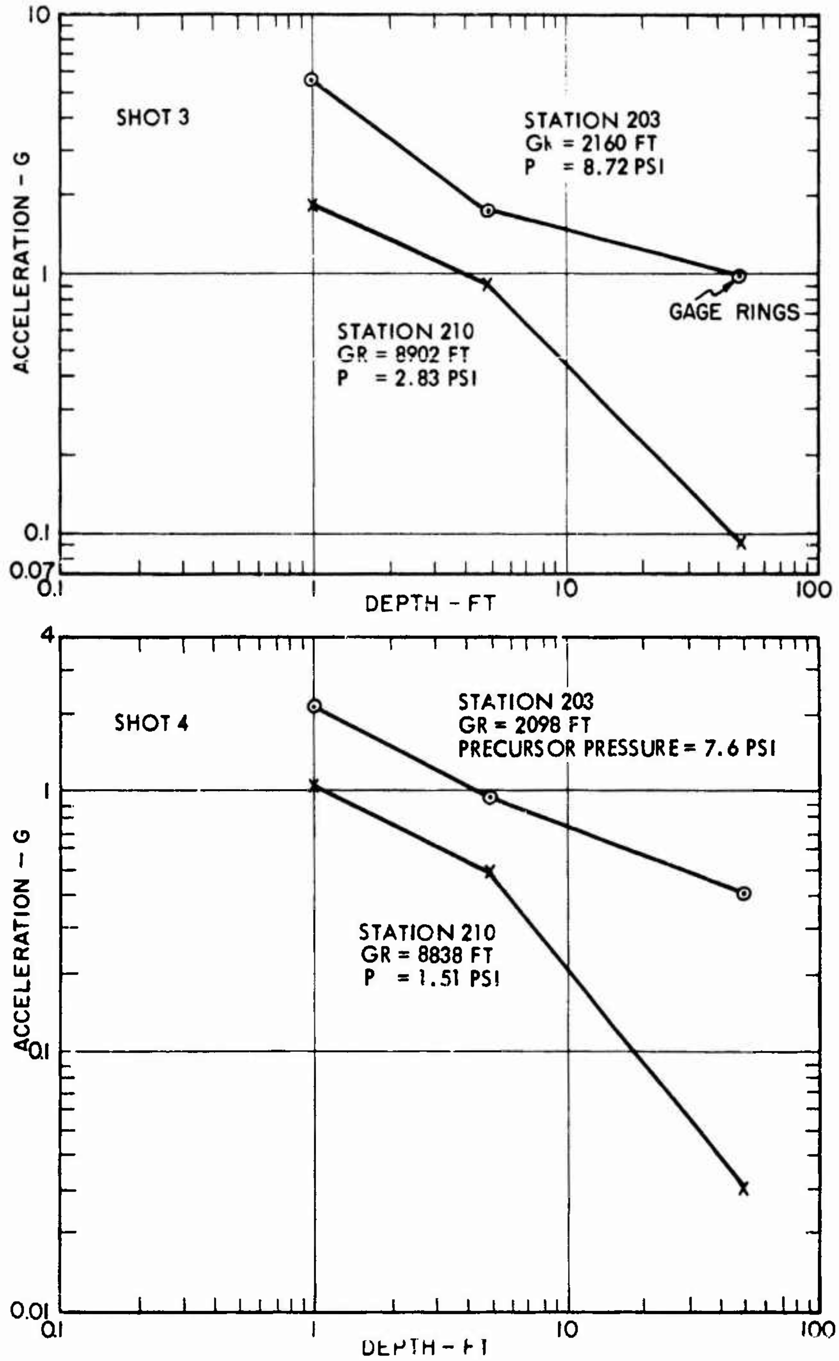


Fig. 5.13 Maximum Negative 5-foot Vertical Slap Acceleration vs. Depth, Shots 3 and 4

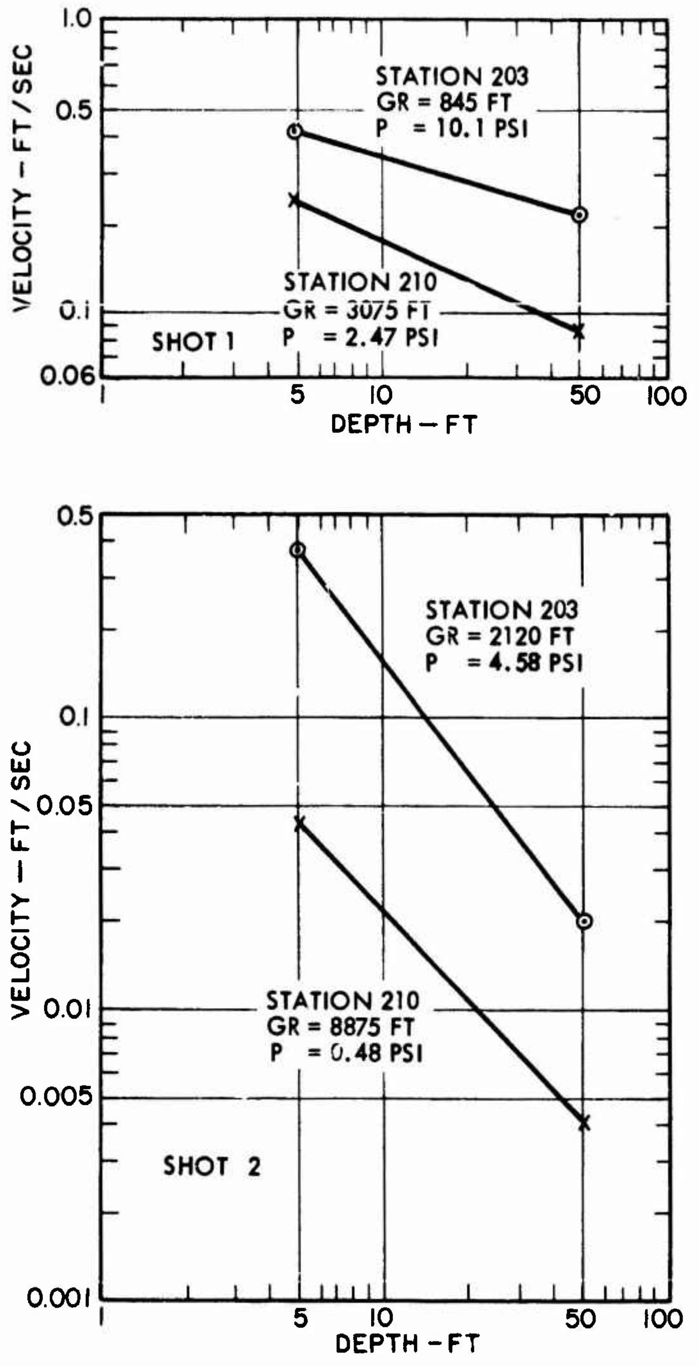


Fig. 5.14 Maximum Negative 5-foot Vertical Slap Velocity vs. Depth, Shots 1 and 2

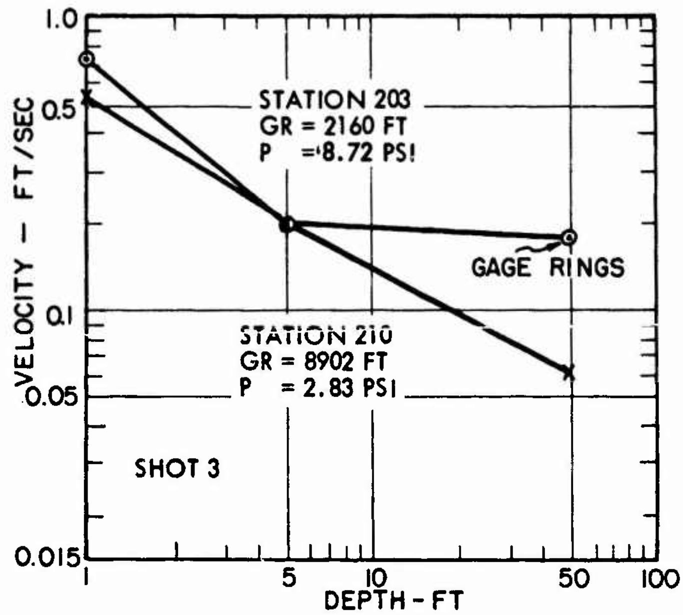


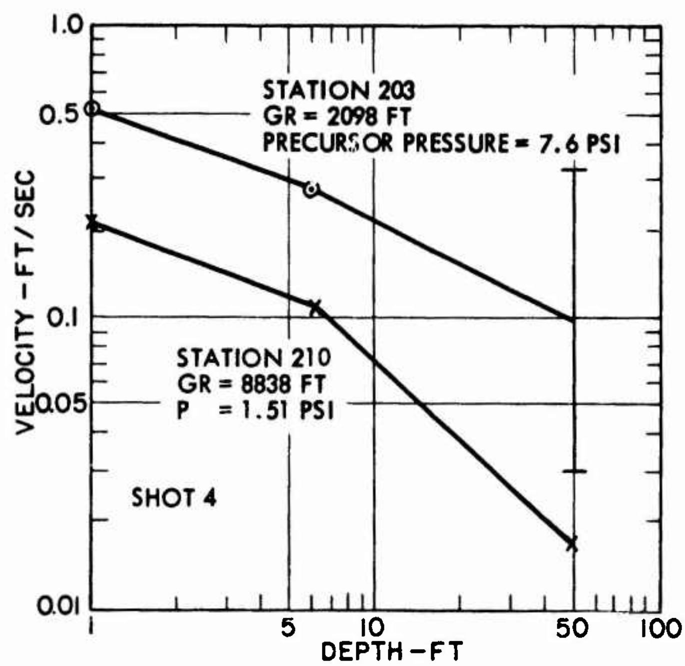


Fig. 5.15 Maximum Negative 5-foot Vertical Slap Velocity vs. Depth, Shots 3 and 4

Indicated on each curve are the ground range and surface-level maximum air pressure. On Shot 3 one 50-foot gage showed considerable ringing, and on a similar gage on Shot 4 it was difficult to separate the slap from the earth motion which started to arrive before the slap. In general, the attenuation rate appears to increase with depth, although the data are too sparse for any firm conclusion.

The peak vertical slap particle velocities are plotted against depth in Figures 5.14 and 5.15. The peak velocity does not seem to attenuate as fast as do the corresponding accelerations between 5 and 50 feet.

In order to calculate energy absorption by the earth (Section 5.8), an estimate must be made of the ratio between particle velocities at 5 feet and at the surface. The only satisfactory records at all three depths were those at Station 210 for Shots 3 and 4. For these, extrapolation to surface particle velocity was somewhat uncertain. The approximate ratio of surface to 5-foot velocities appeared to lie between 3 and 4 for Shot 3, and between 2 and 3 for Shot 4. The surface level air pressures were respectively 2.8 psi and 1.4 psi. A fairly consistent variation of earth motion with depth was observed on all shots by comparing gage records at the two stations. The slap accelerations and velocities between 5 and 50 feet showed greater attenuation rates for the more distant (low air pressure) stations. The only exception was the velocity for Shot 2. The meaning of this general behavior is not clear; at large distances the slap contains a large and uncertain contribution from earth information which has outrun that directly from the air blast.

## 5.8 ENERGY ABSORPTION

This section has been prepared from material furnished by Mr. A. A. Thompson, formerly of the Armed Forces Special Weapons Project. The principles of the analysis were developed by Mr. Thompson, and he performed the mechanical integrations and the numerical calculations involved.

It is of interest to examine the energy transfer between the air pressure wave and the ground. This will aid in estimating the reflectivity of earth, the alteration of air pressure wave form due to this mechanical absorption, and the possibility of the absorbed energy later contributing to the formation of a precursor.

It is assumed that the surface of the earth acts as an impervious diaphragm subjected to an overpressure due to the passage of the air shock wave.

The total energy, W, absorbed by the earth is given by the double integral

$$W = 2\pi \int_0^\infty \left[ \int_0^\infty p\, v_s\, dt \right] r\, dr \quad , \tag{5.5}$$

where

r is the ground range,

$p = p(r,t)$ is the surface level overpressure, and

$v_s = v_s(r, t)$ is the vertical earth particle velocity at the surface; positive is upwards.

The evaluation of the integral of Equation 5.5 requires a knowledge of the earth particle velocity at the surface. However, the principal earth motion instrumentation was at a depth of 5 feet. The stations instrumented at additional depths of 1 foot and 50 feet were intended to provide data by extrapolation for estimating the surface velocities from the 5-foot data. Thus the integral may be written

$$W = 2\pi \int_0^\infty \left[ \int_0^\infty p(q\, v_5)\, dt \right] r\, dr \tag{5.6}$$

where

$v_5 = v_5(r, t)$ is the vertical earth particle velocity at a depth of 5 feet and

$q = q(r, t) = v_s(r, t)/v_5(r, t)$ is a function of r and t transforming the 5-foot velocity to the value at the surface.

The variable, q, comprises a time delay and amplitude change between the two levels. The time delay is small; as noted in Section 5.2, it is of the order of 5 to 10 milliseconds. Experimentally, it is known that the duration of the air blast is larger than that of the significant portion of the velocity (see Figure 5.16 for typical velocity wave forms). Thus the time delay is very small compared with the air-blast duration, and the overpressure changes very little during this delay time.

The assumption may now be made that, aside from the small delay, the velocity wave forms at 5 feet and at the surface differ only by a multiplicative constant, $q_0$. Then Equation 5.6 becomes

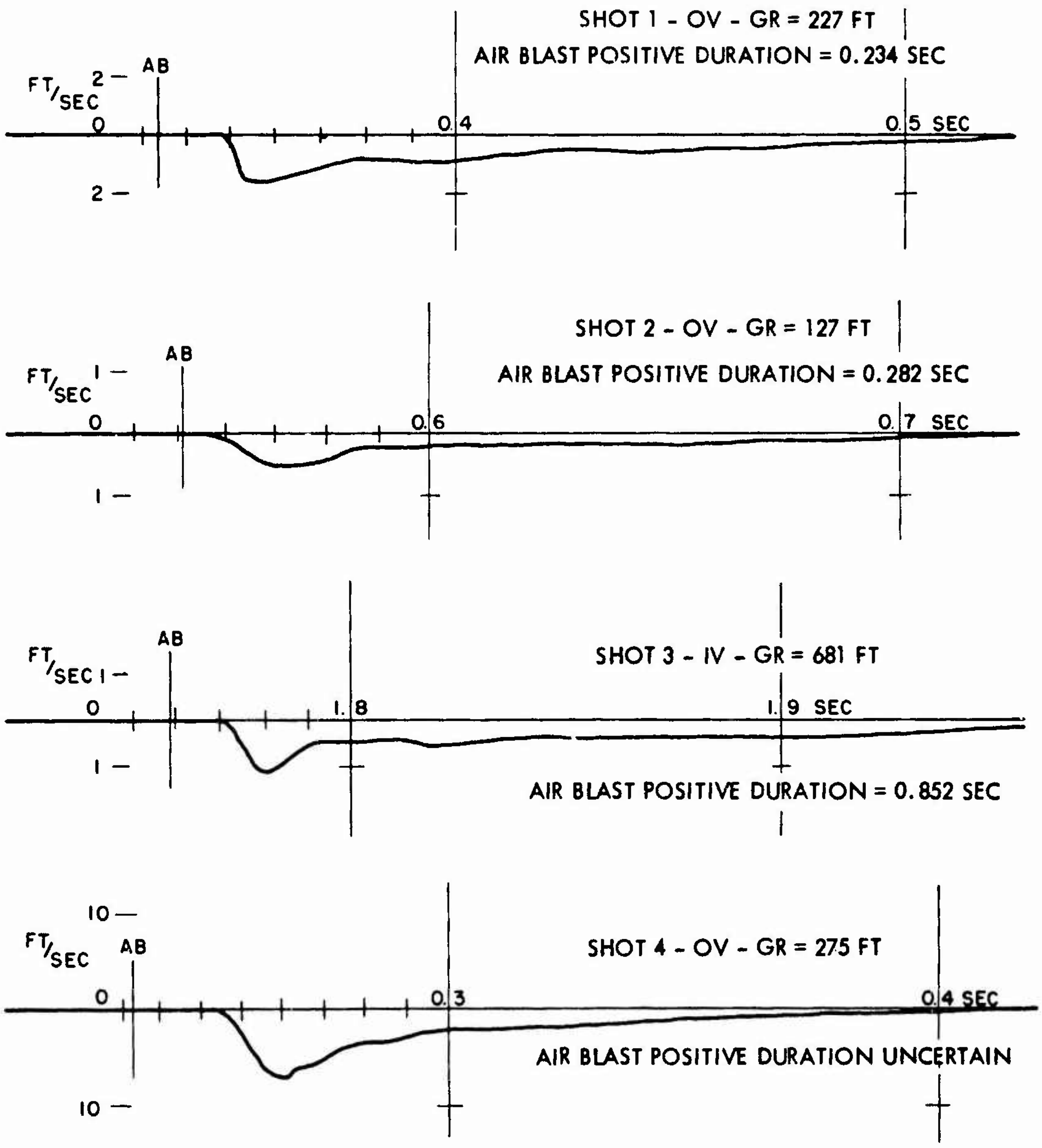


Fig. 5.16 Vertical Earth Particle Velocity vs. Time. 5 feet deep, positive upward

$$\frac{W}{q_0} = 2\pi \int_0^{\infty} \left[ \int_0^{\infty} p \, v_5 \, dt \right] r \, dr \quad . \qquad (5.7)$$

The vertical earth accelerations were integrated by Mr. Thompson at the California Institute of Technology, using a mechanical integraph supplied through the cooperation of Professor B. W. Housner. No corrections were introduced for gage response limitations, so that the actual velocities will be somewhat greater than those obtained by simple integration of the gage records. The value of $W/q_0$ was computed using only those stations having air pressures greater than 5 psi. These include the major portion of the integral. As an intermediate step, values of

$$\frac{T}{q_0} = 2\pi \, r \int_0^{\infty} p \, v_5 \, dt \qquad (5.8)$$

were calculated at various ground ranges. In the final integration for W, conventional graphical interpolation was used to get a smooth function. Values are tabulated in Table 5.5, listing the ground range, r; the integral

$$\int_0^{\infty} p \, v_5 \, dt \quad ; \qquad (5.9)$$

the quantity $T/q_0$ as given by Equation 5.8; and the final value of $W/q_0$ obtained by Equation 5.7 out to the value of r at the 5-psi limit. Although there is still an appreciable contribution beyond this limit, it is decreasing because the pressure and velocity are each decreasing faster than 1/r.

The above integration procedure may be simplified by noting from the representative velocity-time curves of Figure 5.16 that the principal earth velocity pulse occurs in a time fairly short compared with the positive duration of the air blast. This is particularly true for Shots 3 and 4, in which it was felt that earth motion might withdraw appreciable energy from the air blast. As a very rough approximation, assume that the pressure p can be replaced by an equivalent constant average value $\alpha p_m$ somewhat less than the maximum $p_m$. Thus Integral 5.9 becomes

$$\int_0^{\infty} p \, v_5 \, dt \simeq \alpha \, p_m \int_0^{\infty} v_5 \, dt = \alpha \, p_m \, d_5 \quad , \qquad (5.10)$$

TABLE 5.5

Ground Absorption Information

| Shot | Sta. No. | Grnd Range (ft) | $\int_0^\infty pv_5dt$ (ft-lb/in$^2$) | $2\pi r\int_0^\infty pv_5dt$ ($10^{12}$ergs) | $W/q_o$ ($10^{16}$ergs) |
|---|---|---|---|---|---|
| 1 | 200 | 232 | 1.3 | 3.7 | |
| | 201 | 387 | 1.1 | 5.2 | |
| | 202 | 609 | 1.0 | 7.5 | |
| | 203 | 847 | 0.79 | 8.2 | |
| | 204 | 1089 | 0.61 | 8.2 | |
| | 205 | 1335 | 0.59 | 9.5 | |
| | 206 | 1583 | 0.28 | 5.5 | 1.5 |
| 2 | 200 | 127 | 0.32 | 0.5 | |
| | 201 | 625 | 0.25 | 1.9 | |
| | 202 | 1374 | 0.15 | 2.5 | |
| | 203 | 2123 | 0.03 | 0.79 | |
| | 204 | 2874 | 0.02 | 0.71 | 0.3 |
| 3 | 200 | 226 | 0.77 | 2.1 | |
| | 201 | 681 | 0.75 | 6.3 | |
| | 202 | 1414 | 0.47 | 8.1 | |
| | 203 | 2160 | 0.32 | 8.4 | |
| | 204 | 2907 | 0.26 | 9.1 | 4 |
| 4 | 200 | 275 | 32 | 110 | |
| | 201 | 626 | 10 | 78 | |
| | 202 | 1354 | 3.3 | 55 | |
| | 203 | 2098 | 0.50 | 13 | 15 |

where $d_5$ is the permanent displacement at a depth of 5 feet. The factor $q_o$ enters as before; here its time variation is again not important, the principal assumption being that it is independent of r and $p_m$.

It is evident that the whole calculation hinges on the factor $q_o$. In the previous section, rough estimates were made in terms of velocity ratios. For Shot 3 the ratio of surface to 5-foot velocity peaks appeared to be between 3 and 4; for Shot 4, between 2 and 3. When $q_o$ is obtained by comparing permanent displacement ratios between the 1-foot and 5-foot levels by double integration of acceleration records, the

values are near 2.4 for Shot 3 and 2.0 for Shot 4. Assuming a ratio of 2 for surface to 1-foot displacements, values of 4.8 and 4.0 result. Surface level air pressures were 2.8 and 1.4 psi, respectively, for these two sets of conditions. Thus $q_o$ is not a very constant quantity. For purposes of comparison, it appears reasonable to use $q_o$ equal to 4 for all shots. Then the energy absorbed out to the 5-psi contour may be obtained from the data in Table 5.5. When expressed as a fraction of the equivalent TNT energy to obtain the same air blast,[2] the values given in Table 5.6 are obtained.

The relatively larger value of absorption for Frenchman Flat (Shot 1) is surprising, because maximum absorption would be expected if there were a gradual transition from air to earth. The initially fluffy surface at Yucca Flat is closer to this condition than the hard, watered, and rolled surface at Frenchman Flat. Of course, rain, blading, and packing by vehicles reduced this difference. It must again be emphasized that the whole procedure rests, as it must, on assumptions which are necessary because of the small amount of effect-of-depth data available. However, even with generous allowances for error, the energy absorbed would still be a small fraction of the total blast energy. Hence it appears safe to conclude that the blast wave will not be appreciably altered by this absorption mechanism alone.

From acoustic considerations similar to those used in calculating the round trip pressure ratio in Section 1.2.1, the ratio of the intensities in air and in earth may be obtained by assuming each to be a linear fluid. The intensity ratio, for the extreme mismatch actually existing, is the acoustic impedance ratio. On the basis of Section 5.5, the average value for all shots is about 1/700, or 0.14 per cent.

TABLE 5.6

Energy Absorbed by Ground

| Shot. | Energy Absorbed out to 5-psi Contour ($10^{16}$ ergs) | Per Cent of Equivalent TNT Air-Blast Energy |
|---|---|---|
| 1 | 1.5 | 0.3 |
| 2 | 0.3 | 0.06 |
| 3 | 4 | 0.03 |
| 4 | 15 | 0.18 |

This agrees in rough order of magnitude with the energy absorption calculations above. For tests under other conditions, the acoustic impedance ratio can provide a useful measure of the absorption; this may be of interest in blasts over loose snow, which is highly absorbing.

## 5.9 SECONDARY DISTURBANCES

The report on air pressure measurements[2] discussed certain secondary shocks or blips of small amplitude which were observed in the wave forms. Similar disturbances were sought in the earth acceleration records; they were found to be present at the expected times. Arrival times are given in Tables 4.1, 4.3, 4.5, and 4.8. However, the oscillation did not have as sudden an onset as did the slap, so readings of its time of arrival were subject to more error. The disturbance was unmistakable, however, since the earth motion had usually almost died out before the blip arrived.

Times of arrival of these secondary earth disturbances are plotted in Figures 5.1 through 5.4, together with main disturbance information. In each shot, the secondary and primary (slap) time of arrival curves displayed a time displacement which was usually smaller at outrunning than at the maximum range instrumented. These extreme values were approximately: Shot 1, 0.9 second and 1.1 seconds; Shot 2, 1.3 and 1.6 seconds; Shot 3, 5.3 and 5.0 seconds; and Shot 4, 0.7 and 0.8 second. In every shot, the final propagation velocity of the secondary disturbances was that of the slap.

A tertiary disturbance was observed on Shot 4 which agreed in time of arrival with the slowly rising tertiary air pressure increases. The final propagation velocity of this disturbance was 1100 feet per second, as compared with 1200 feet per second for both secondary and slap phenomena.

A surprising feature of all secondary disturbances is the relative magnitude of the earth motion. The ratio of locally induced peak acceleration to the air pressure rise causing it was some 3 to 10 times greater for the secondary blips than for the slap. No quantitative evaluation was attempted, owing to the difficulty of reading the low values of air pressure in the blips.

## 5.10 HORIZONTAL RADIAL AND HORIZONTAL TANGENTIAL ACCELERATIONS

At Stations 203 and 210 horizontal radial and horizontal tangential accelerometers were installed at depths of 5 and 50 feet. Figure 4.3 displays representative vertical, horizontal radial, and horizontal tangential acceleration records at 5-foot depth at Station 203 on Shot 1.

Little is known of the mechanisms causing the horizontal radial component of the acceleration. In a very simple view, the air-blast pressure can exert only a normal force on the surface. The flow behind the reflected shock front is parallel to the surface and can exert a drag force on the earth. A complete solution of the problem in the simplest, most idealized case would require consideration of the vibration of a semi-infinite elastic solid from the excitation of a point source in a fluid above it. A start toward work on this problem has been made by Ott.[4]

The tangential acceleration should be small, as presumably it is due only to the asymmetry of the actual explosion or the test medium.

Any comparison of peak values on the vertical, horizontal radial, and horizontal tangential accelerations is misleading for three reasons:

(a) The peak accelerations occur at different times and hence cannot be regarded as components of an acceleration vector.

(b) Many of the horizontal radial and tangential records do not show a well-defined earth wave and slap. The earth wave could not be edited out as in the vertical acceleration; the accelerations read were the absolute maximum negative and positive accelerations shown on the record.

(c) On most of the records used in the comparison, the half-period associated with the maximum acceleration is near the natural half-period of the gage. As Shown in Section 5.3, these maxima may be 60 per cent or more smaller than the actual maxima.

For comparison purposes we shall use the peak-to-peak acceleration (the sum of the absolute values of the maximum negative and positive accelerations), as this will minimize the effect of varying wave forms. Table 5.7 gives these quantities and also the ratio of horizontal and tangential components to the vertical component.

The size of the horizontal radial component relative to the vertical increased with increasing ground range. The size of the tangential component relative to the vertical decreased slightly with ground range. Nothing can be said as to the effects of depth. The relative size of the horizontal radial component increased in the same order as that of the shots, indicating that both yield and burst height are involved.

TABLE 5.7

Comparison of Vertical, Horizontal, and Tangential Accelerations

| Shot | Sta. No. | 5 feet deep V | 5 feet deep H | 5 feet deep T | 50 feet deep V | 50 feet deep H | 50 feet deep T |
|---|---|---|---|---|---|---|---|
| Maximum Peak-to-Peak Acceleration (G) | | | | | | | |
| 1 | 203 | 4.84 | 1.37 | 1.53 | 0.84 | 1.94 | 0.31 |
| | 210 | 1.47 | 0.70 | 0.21 | 0.36 | 0.46 | - |
| 2 | 203 | 2.40 | 1.15 | 0.53 | 0.65 | 0.65 | 0.19 |
| | 210 | 0.46 | 0.54 | 0.07 | 0.024 | 0.024 | 0.013 |
| 3 | 203 | 2.81 | 2.26 | - | 1.49 | - | - |
| | 210 | 1.68 | 2.09 | 0.36 | 0.30 | 0.14 | - |
| 4 | 203 | 1.79 | 2.33 | - | 0.84 | - | - |
| | 210 | 0.95 | 1.06 | 0.22 | 0.09 | 0.07 | - |
| Ratio to Vertical Component | | | | | | | |
| 1 | 203 | 1.00 | 0.28 | 0.32 | 1.00 | 2.31 | 0.37 |
| | 210 | 1.00 | 0.48 | 0.14 | 1.00 | 0.45 | - |
| 2 | 203 | 1.00 | 0.48 | 0.22 | 1.00 | 1.00 | 0.29 |
| | 210 | 1.00 | 1.17 | 0.15 | 1.00 | 1.00 | 0.54 |
| 3 | 203 | 1.00 | 0.80 | - | 1.00 | - | - |
| | 210 | 1.00 | 1.24 | 0.21 | 1.00 | 0.47 | - |
| 4 | 203 | 1.00 | 1.30 | - | 1.00 | - | - |
| | 210 | 1.00 | 1.12 | 0.23 | 1.00 | 0.78 | - |

# CHAPTER 6

# SUMMARY, CONCLUSIONS, AND RECOMMENDATIONS

## 6.1 SUMMARY AND CONCLUSIONS

### 6.1.1 Energy Absorption

By consideration of particle velocities, the fraction of blast energy absorbed from the air by the earth was calculated to be for Shot 1, 0.3 per cent; Shot 2, 0.06 per cent; Shot 3, 0.03 per cent; Shot 4, 0.18 per cent. Acoustic considerations would give an average value of 0.14 per cent, agreeing in order of magnitude with the above. The true values are probably less than the calculated ones, as simplifying assumptions were made with this in mind. It seems likely that the absorption of such a small fraction of the total blast energy would not appreciably affect the blast wave.

### 6.1.2 Transmission Process

Outrunning by the direct earth wave in front of the main slap took place at an average velocity of 2000 feet per second and ground ranges of 850, 1000, 2000, and 1800 feet for the four shots. The velocity of the direct earth wave increased with range, attaining values of 8300, 6800, 5300, and 13,000 feet per second at ranges of 3500, 9000, 9000, and 9000 feet for the four shots. The velocity of the main slap decreased with range to a constant average value of 1200 feet per second for all four shots.

The inclination of wave fronts in the earth was opposite to that expected for earth with uniform velocity; this may be due to the observed gradient of velocity vs. depth.

### 6.1.3 Slap Acceleration

As expected from the character of the soils, Shot 1 showed greater values of earth acceleration for the same air pressure than did the shots at Yucca Flat. All curves of acceleration vs. pressure on a log-log plot were concave upward, indicating the earth is a better transmitter at high pressures than at low. For Shots 2, 3, and 4 the curves can be approximated by the relation

$$A = 0.32\ p^{0.89}$$

where A is in g, and p is in psi. A spread of plus or minus 50 per cent would include almost all points. This relation applies specifically to the yields, burst heights, and soil conditions of the shots at Yucca Flat.

### 6.1.4 TUMBLER Shot 4 Precursor

Earth acceleration as a function of air pressure follows the same relation for the precursor as for shock waves with no precursor. The incident wave following the precursor does not observe this relation.

The round trip pressure ratio from air to earth back to air was calculated as 1/1400. The fraction of energy absorbed from the air by the earth was calculated as 0.18 per cent on Shot 4. Hence precursor formation by the action of earth on air is unlikely.

### 6.1.5 Slap Particle Velocity

All four curves of slap velocity vs. air pressure can be approximated by

$$v = 0.06\ p^{0.89}$$

(where v is in fps and p is in psi), with a spread of plus or minus 60 per cent.

Vertical propagation velocity, calculated from the ratio of pressure to velocity, was about 700 feet per second near the surface.

### 6.1.6 Gage Correction

On many of the 80 and 45 cps accelerometers the slap frequency was near the natural frequency of the gage. Shot 2 peak accelerations and frequencies were corrected for the effect of gage response. The correction was 0 per cent at a frequency ratio of 0.3 and 60 per cent at a frequency ratio of 1.0. The damping ratio of the gages was 0.7.

### 6.1.7 Effects of Depth

The data on effect of depth are too sparse and uncertain to permit any firm conclusions. In general, the attenuation rate for both acceleration and velocity is greater at greater ground range (lower air pressure). For both, the attenuation rate increases with depth, but velocity does not attenuate as fast as the corresponding acceleration.

6.1.8 Horizontal Radial and Tangential Accelerations

The horizontal radial component of the acceleration is of the same order of magnitude as the vertical component but shows greater variation in wave form. Its relative size increases with ground range and is greater for each succeeding shot. The horizontal tangential component is small compared to the vertical component, and its relative size decreases with ground range.

6.1.9 Secondary Disturbances

The acceleration records showed secondary (and on Shot 4, tertiary) disturbances corresponding to those noted in the air blast.[2] It is surprising that the relative magnitude of earth acceleration to air pressure rise of these later disturbances is some 3 to 10 times greater than for the main slap.

## 6.2 RECOMMENDATIONS

It is recommended that this report be accepted as an indication that, for air bursts on a scale and over surfaces similar to those of the TUMBLER shots, earth absorption of air blast energy and re-radiation of the energy back into the air blast are both negligible. Further work is needed to determine the energy absorption of other types of surfaces; loose snow, for example, is known to be very absorbent.

The analysis used in this report to calculate energy absorption requires a knowledge of the vertical earth velocity at surface level. More knowledge of the attenuation of velocity with depth is needed to permit extrapolation to the surface. A knowledge of the horizontal tangential component of acceleration is probably unnecessary; these measurements could be dispensed with. It is important that all gages and the equipment associated with them have resonant frequencies three times as great as the frequency of any oscillation whose amplitude is important.

## BIBLIOGRAPHY

1. Armed Forces Special Weapons Project, "Data Furnished by AFSWP," 15 May 1952. SECRET SI, RESTRICTED DATA.

2. V. Salmon, "Air Pressure vs. Time," Stanford Research Institute, Final Report, Project 1.2, Operation TUMBLER. SECRET SI, RESTRICTED DATA, (WT-512).

3. O. v. Schmidt, "Über Knallwellenausbreitung in Flüssigkeiten und festen Körpern," Physikalische Zeitschrift 39, 868 (1938). UNCLASSIFIED.

4. H. Ott, "Reflexion und Brechung von Kugelwellen; Effekte 2. Ordung," Annalen der Physik 41, 443 (1942). UNCLASSIFIED.

5. M. S. Johnson and D. E. Hibbard, "Geology of the Nevada Proving Grounds," U. S. Geological Survey, Operation TUMBLER Report WT-518, February, 1953. RESTRICTED SI.

6. S. Levy and W. D. Kroll, "Response of the Accelerometers to Transient Accelerations," J. Research Nat. Bur. Standards 45, (October, 1950). UNCLASSIFIED.

7. E. B. Doll and V. Salmon, "Scaled HE Tests," Stanford Research Institute, Operation JANGLE Report WT-377, April, 1952. SECRET SI, RESTRICTED DATA.

8. E. B. Doll and V. Salmon, "Ground Acceleration, Ground and Air Pressures for Underground Test," Stanford Research Institute, Operation JANGLE Report WT-380, April, 1952. SECRET SI, RESTRICTED DATA.

9. C. J. Aronson et al., "Free-Air and Ground-Level Pressure Measurements," Naval Ordnance Laboratory, Operation TUMBLER Report WT-513, November, 1952. SECRET SI, RESTRICTED DATA.

# APPENDIX

## GAGE RECORDS

Reductions (1 : 2.5) of tracings of the interesting portions of all gage records comprise this appendix. The portion shown is that immediately following the arrival of the air blast at the surface. Features of the direct earth wave and secondary shocks do not appear in these reductions; accelerations and times associated with them appear in the tables.

The records are arranged first by shot, then by ground range, gage type (vertical, horizontal, tangential), and depth.

Each record is provided with time and acceleration coordinate locations, and with line AB indicating arrival of the air blast at the surface. The time interval on each gage record labeled "DNP" is the damped natural <u>half</u>-period of the gage. Camera corrections needed to reduce all records to a common time base are indicated by the notation, "Add x milliseconds." Labeling includes shot number, gage code symbol, ground range, slant range to point on surface above gage, and other information as required. The gage code system is explained in Section 3.2.

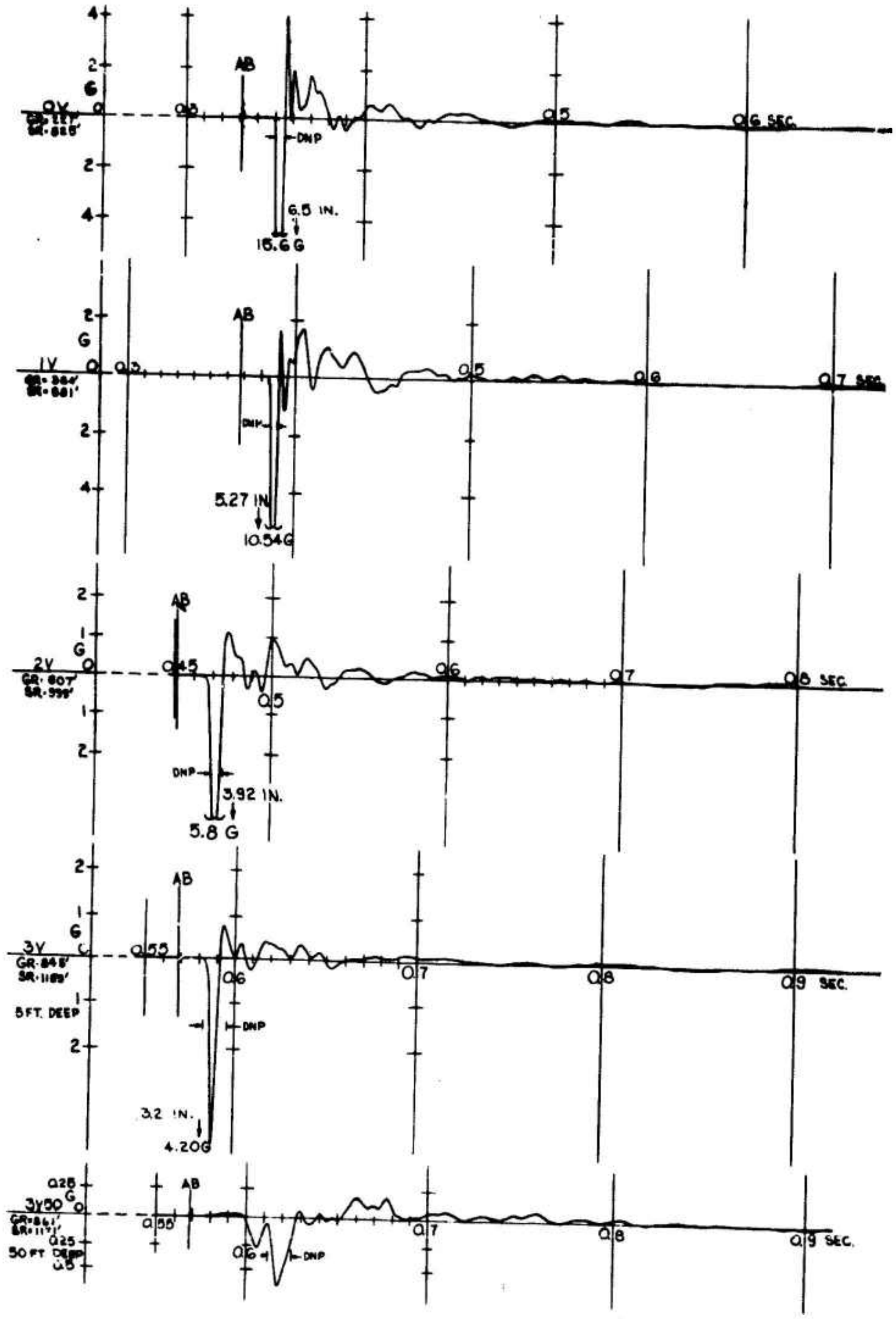

Fig. A.1 Shot 1, Gages 0V through 3V50

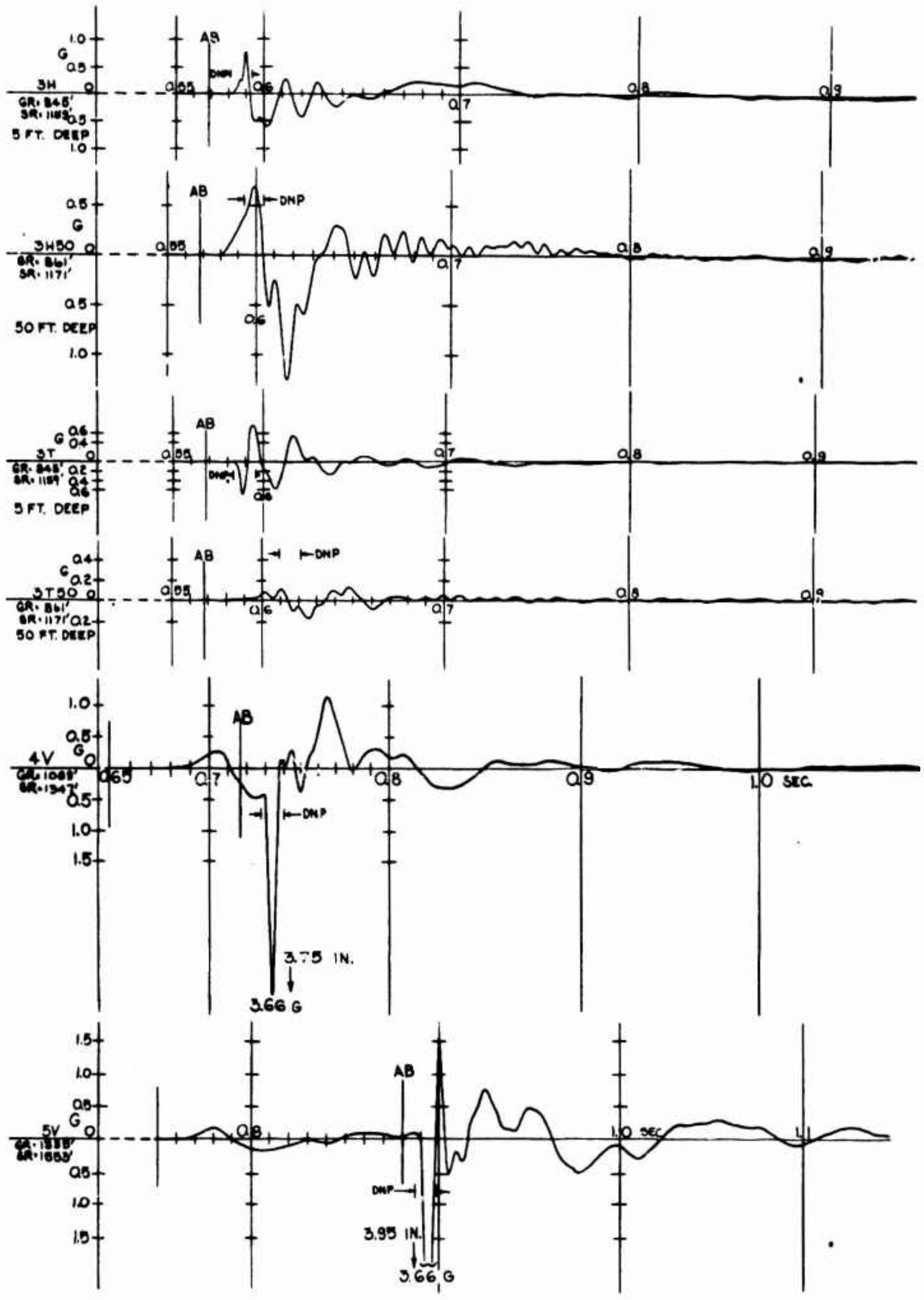


Fig. A.2  Shot 1, Gages 3H through 5V

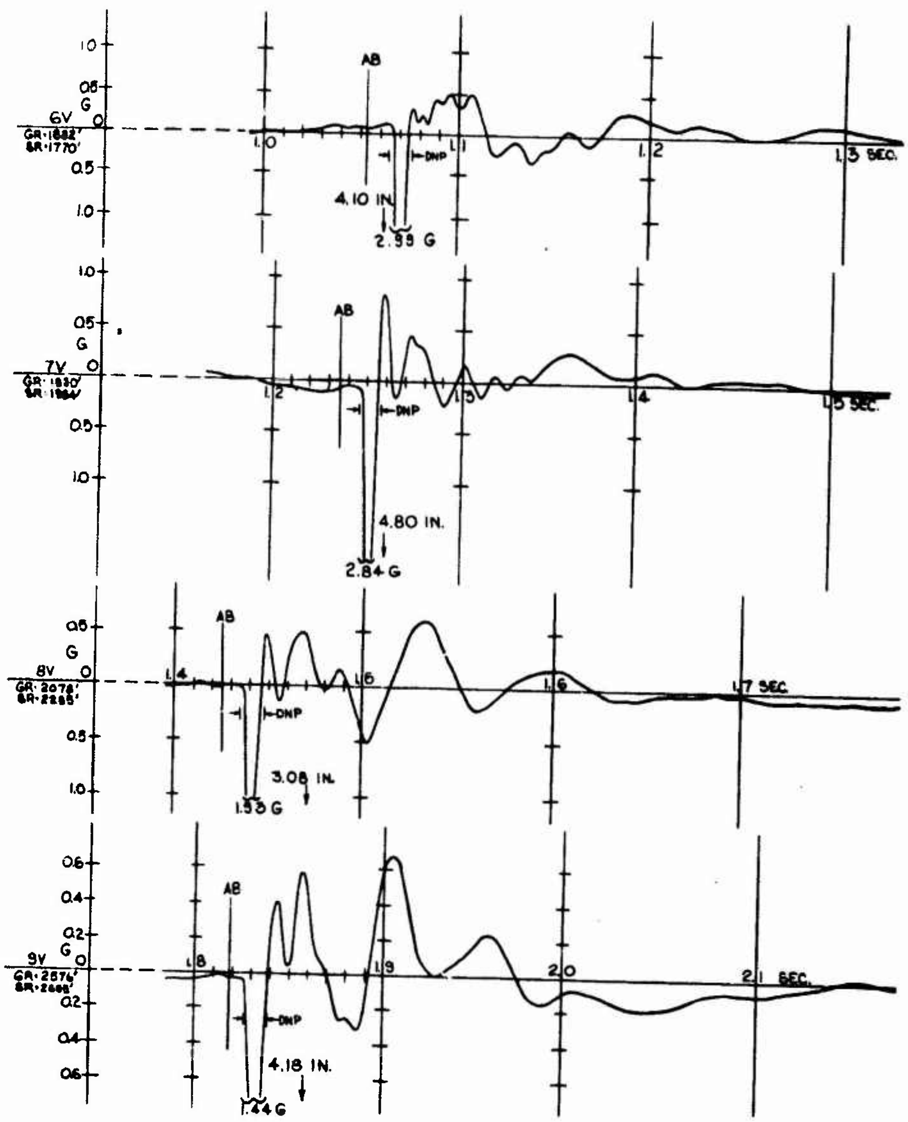


Fig. A.3 Shot 1, Gages 6V through 9V

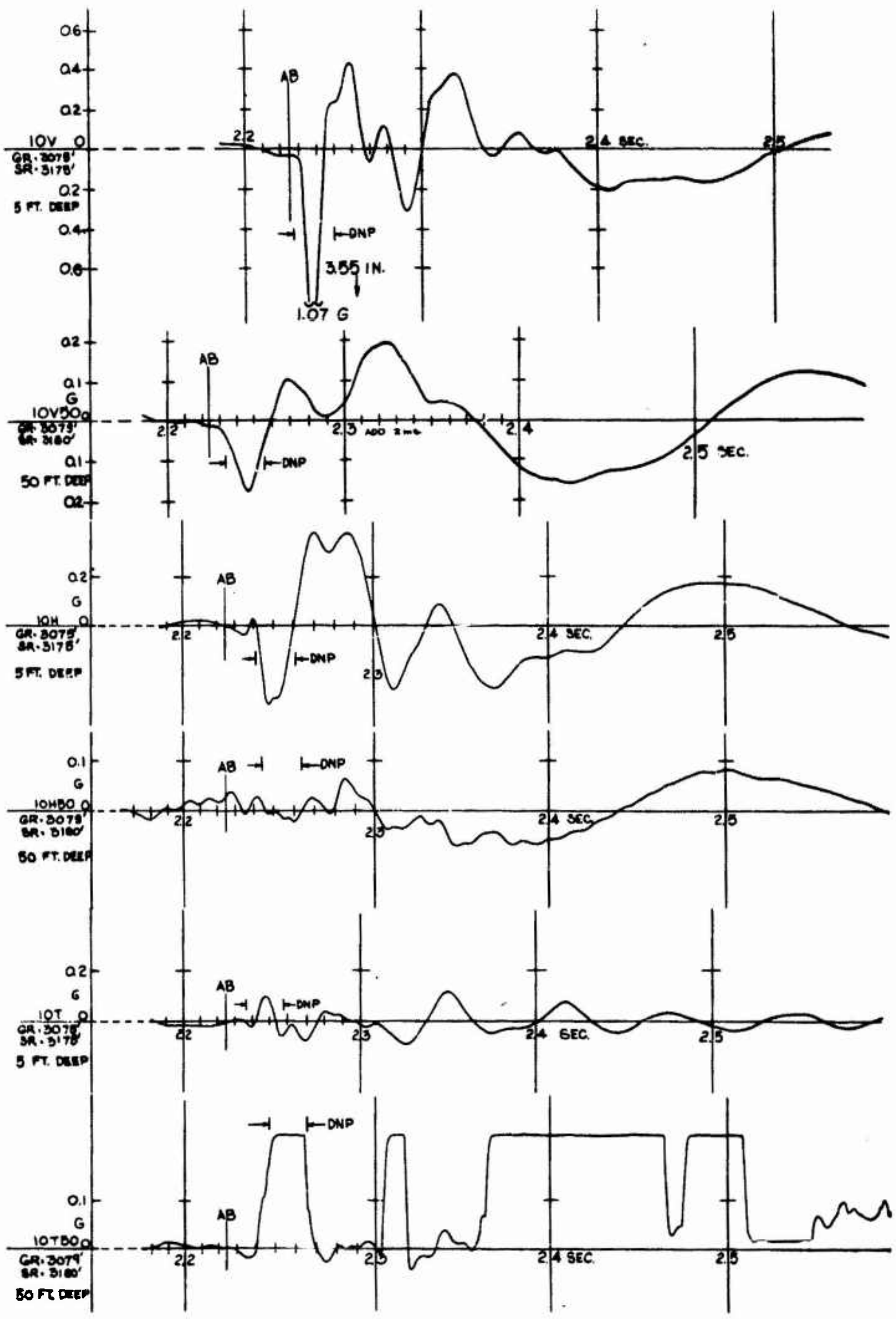


Fig. A.4 Shot 1, Gages 10V through 10T50

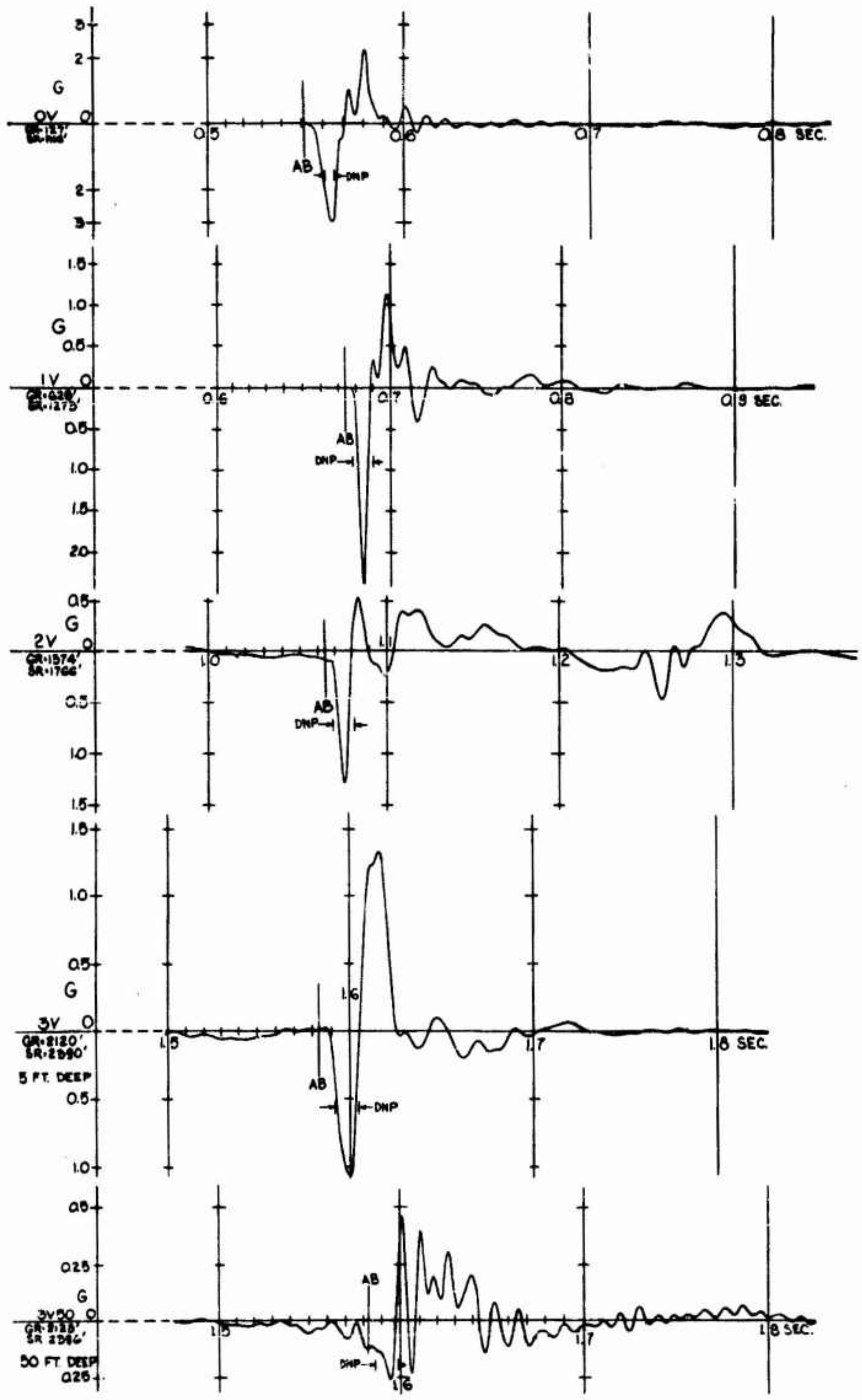


Fig. A.5 Shot 2, Gages 0V through 3V50

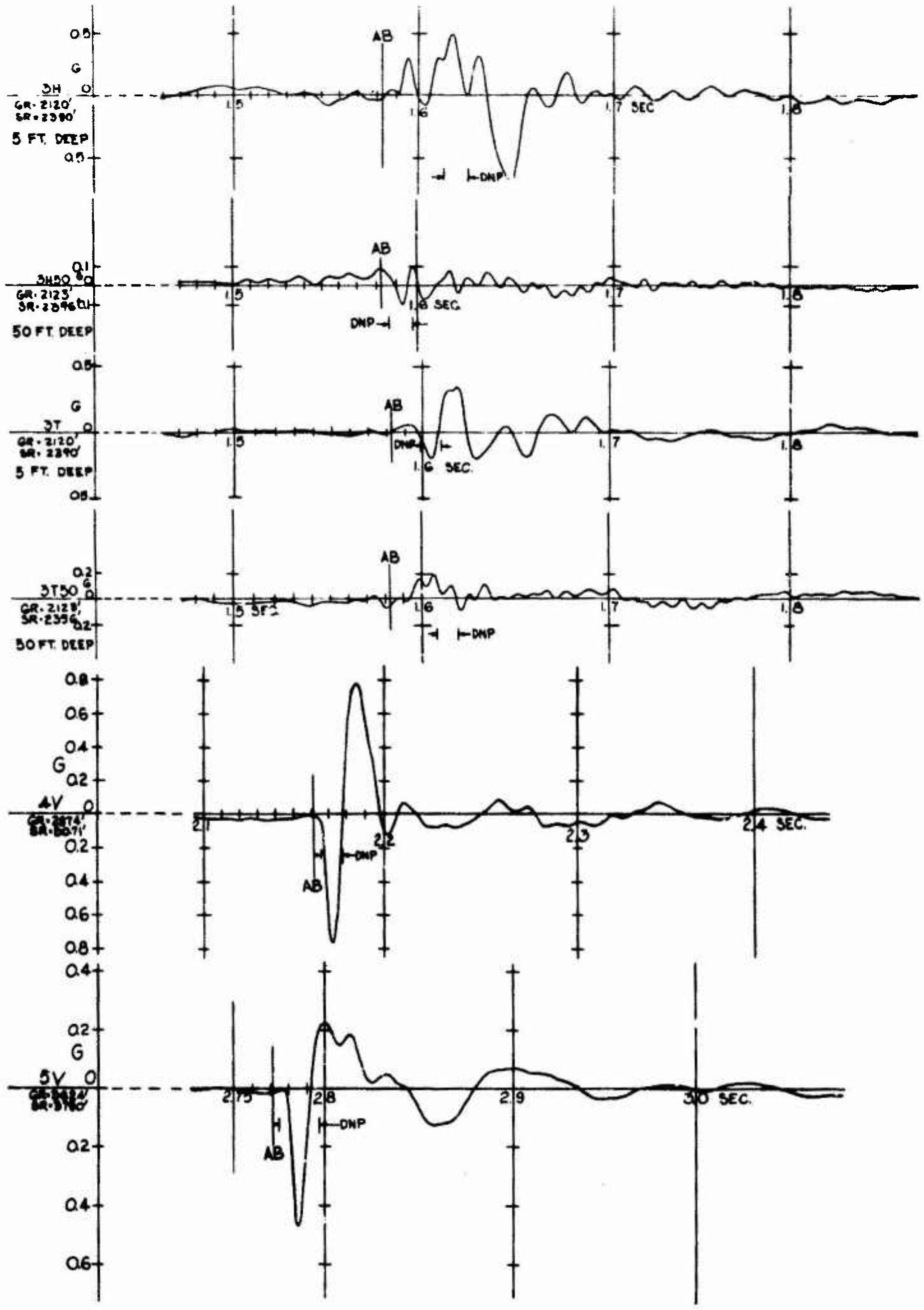

Fig. A.6 Shot 2, Gages 3H through 5V

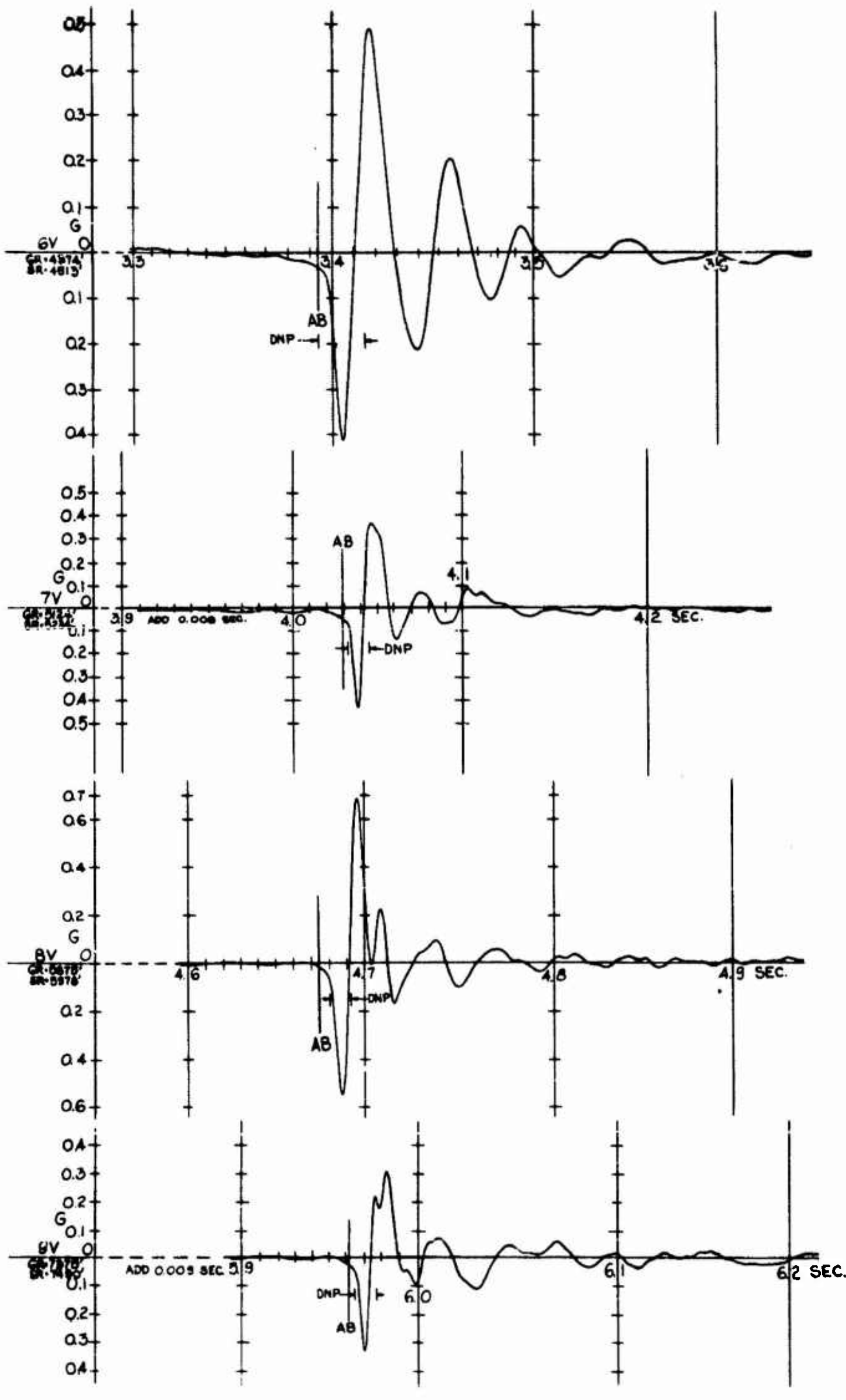

Fig. A.7 Shot 2, Gages 6V through 9V

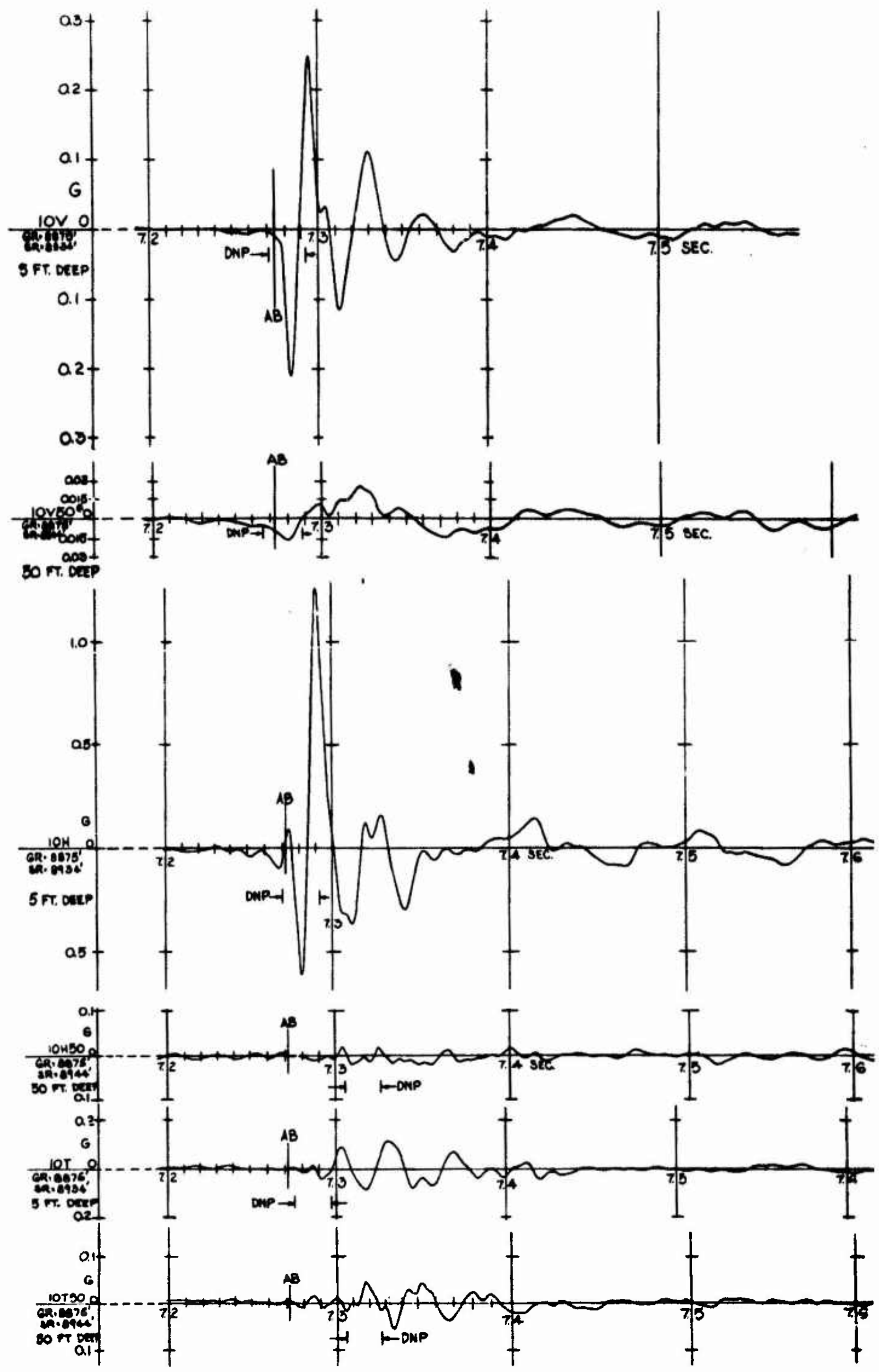

Fig. A.8 Shot 2, Gages 10V through 10T50

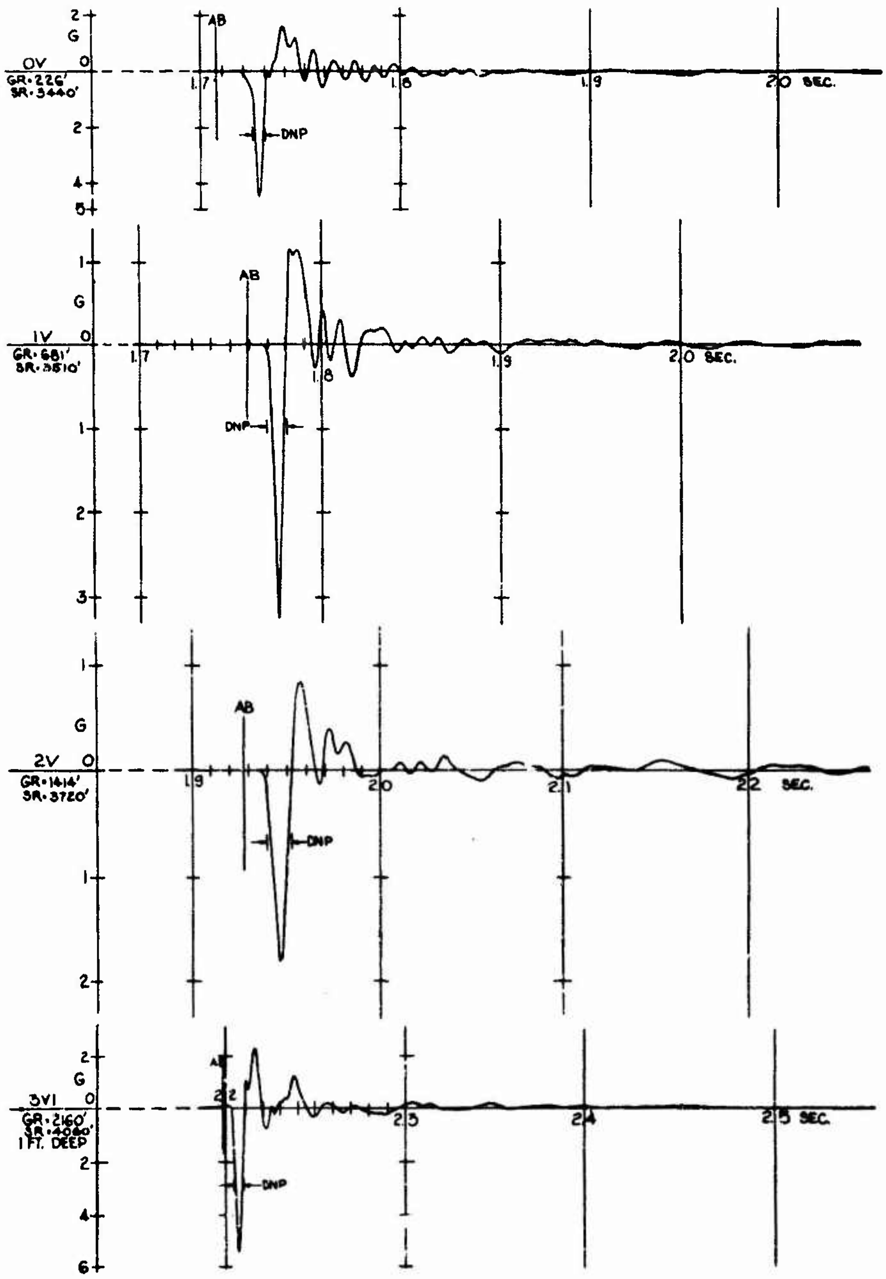


Fig. A.9 Shot 3, Gages OV through 3V1

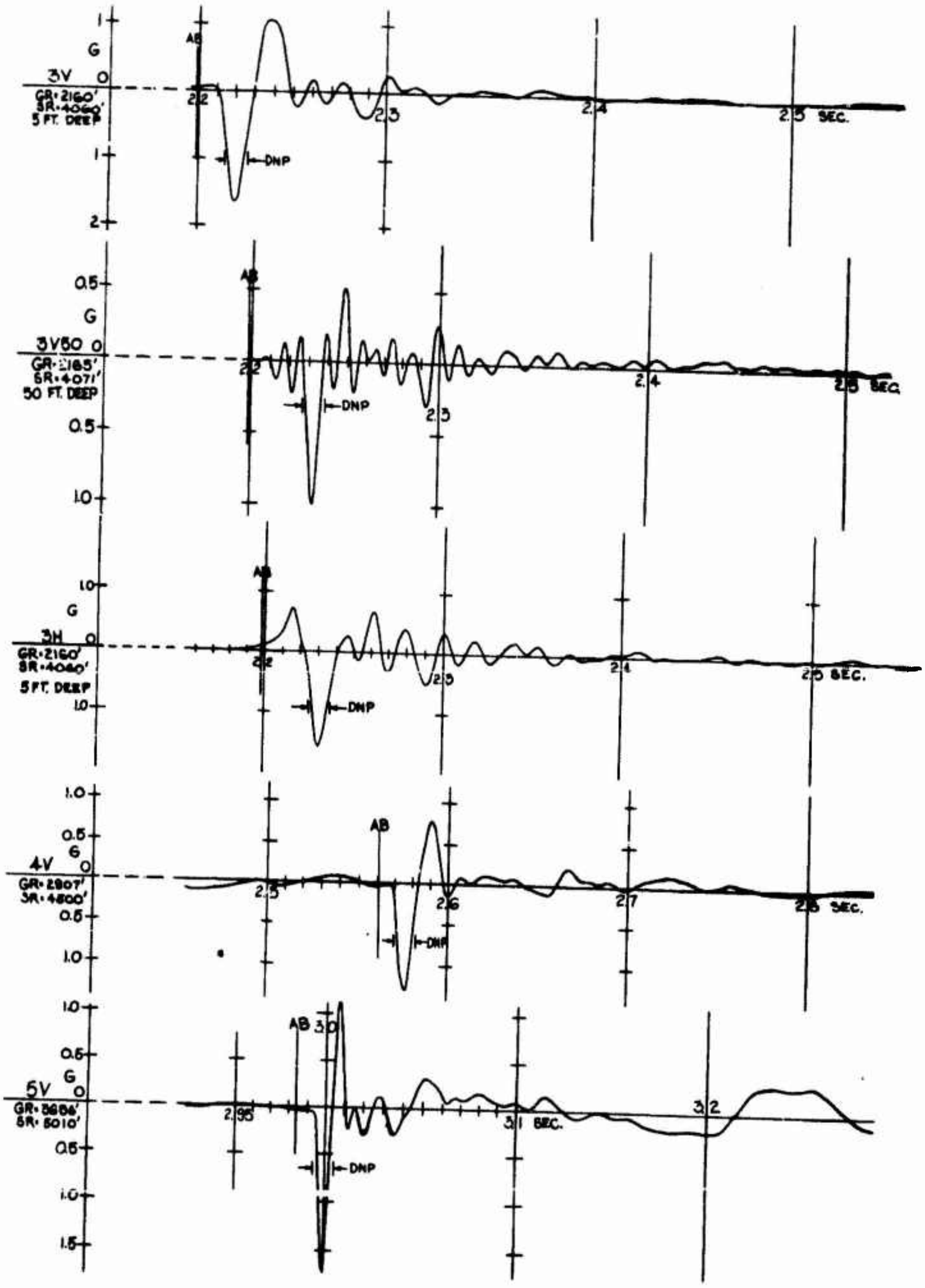


Fig. A.10 Shot 3, Gages 3V through 5V

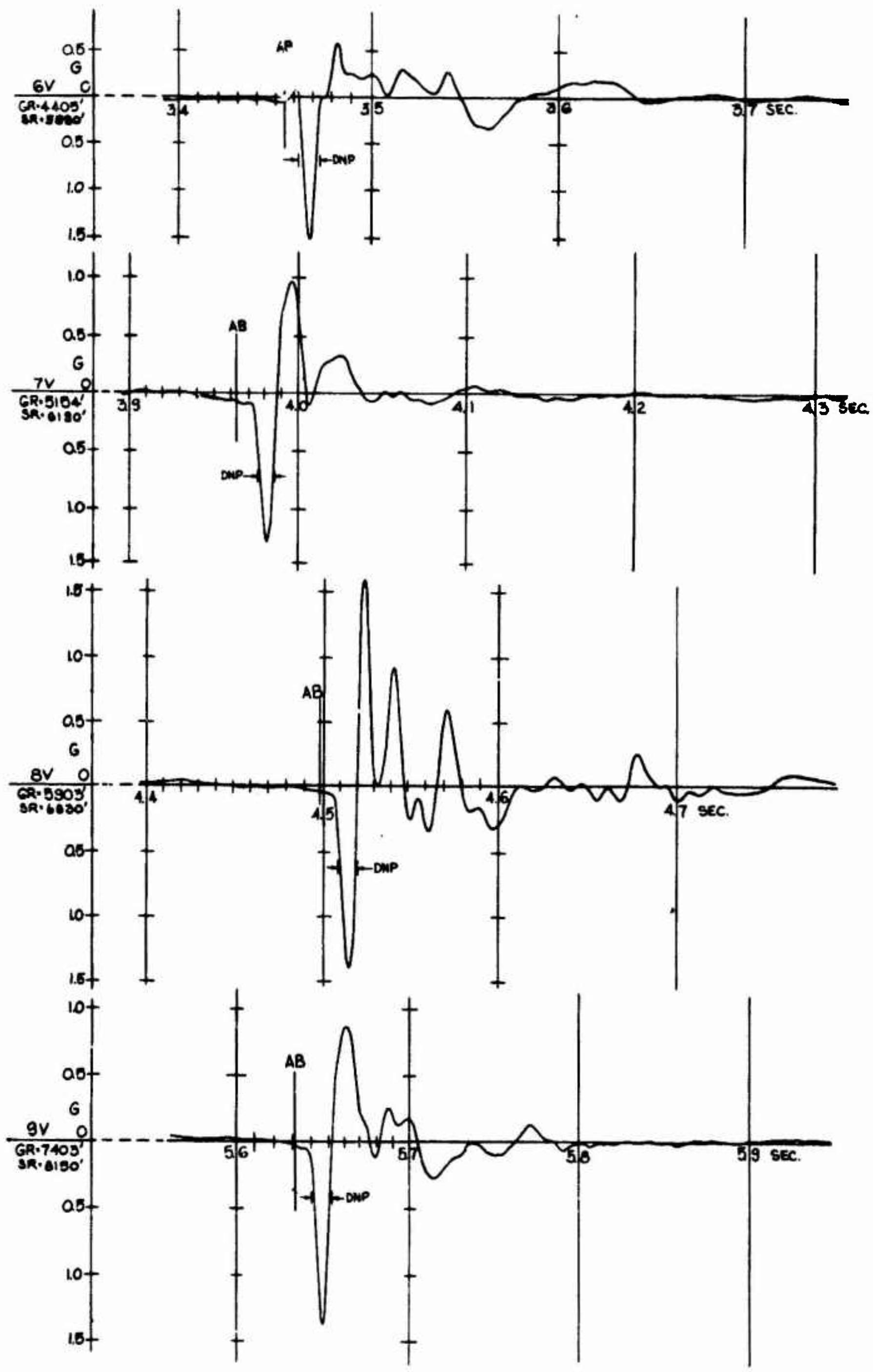


Fig. A.11 Shot 3, Gages 6V through 9V

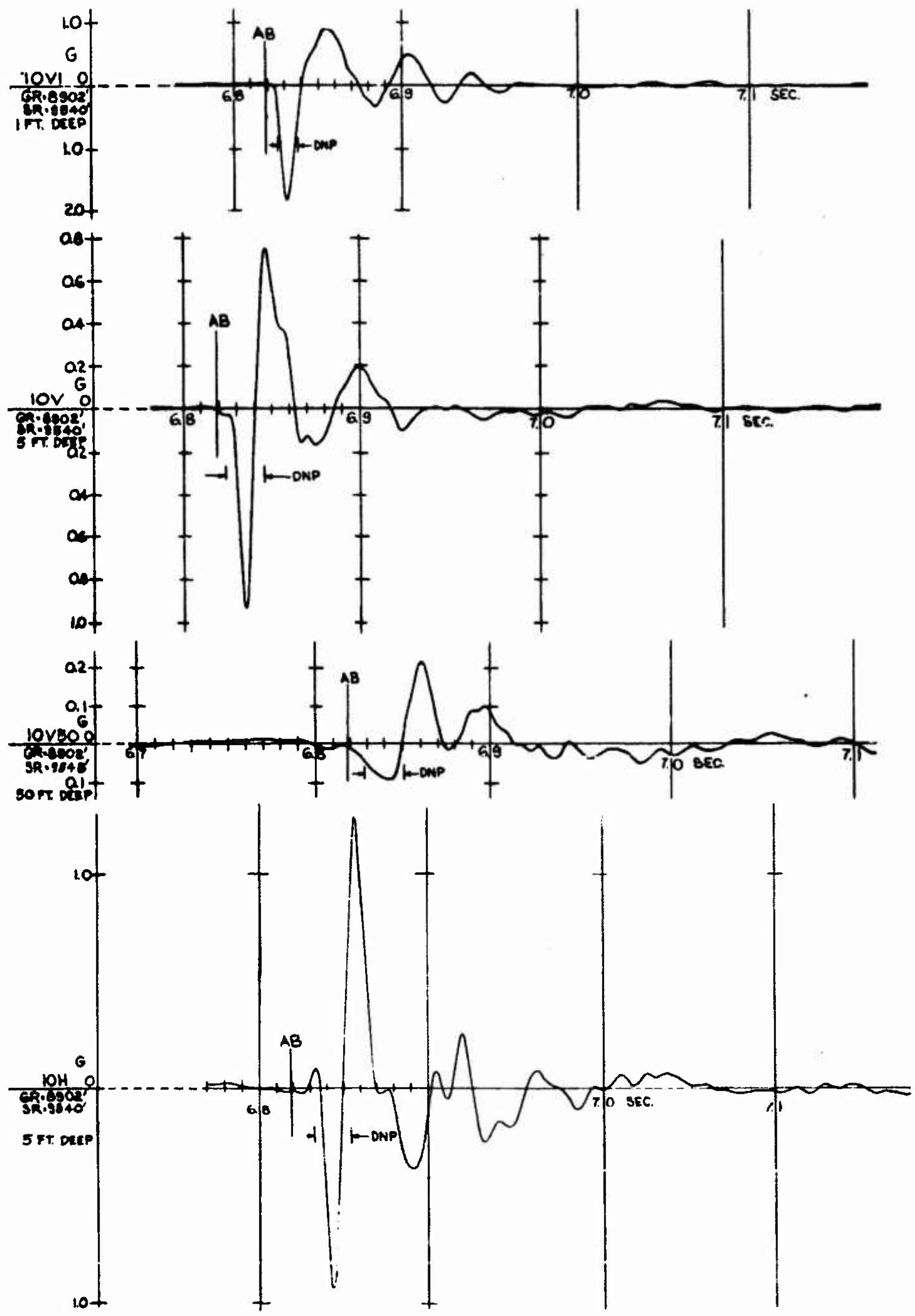


Fig. A.12 Shot 3, Gages 10V1 through 10H

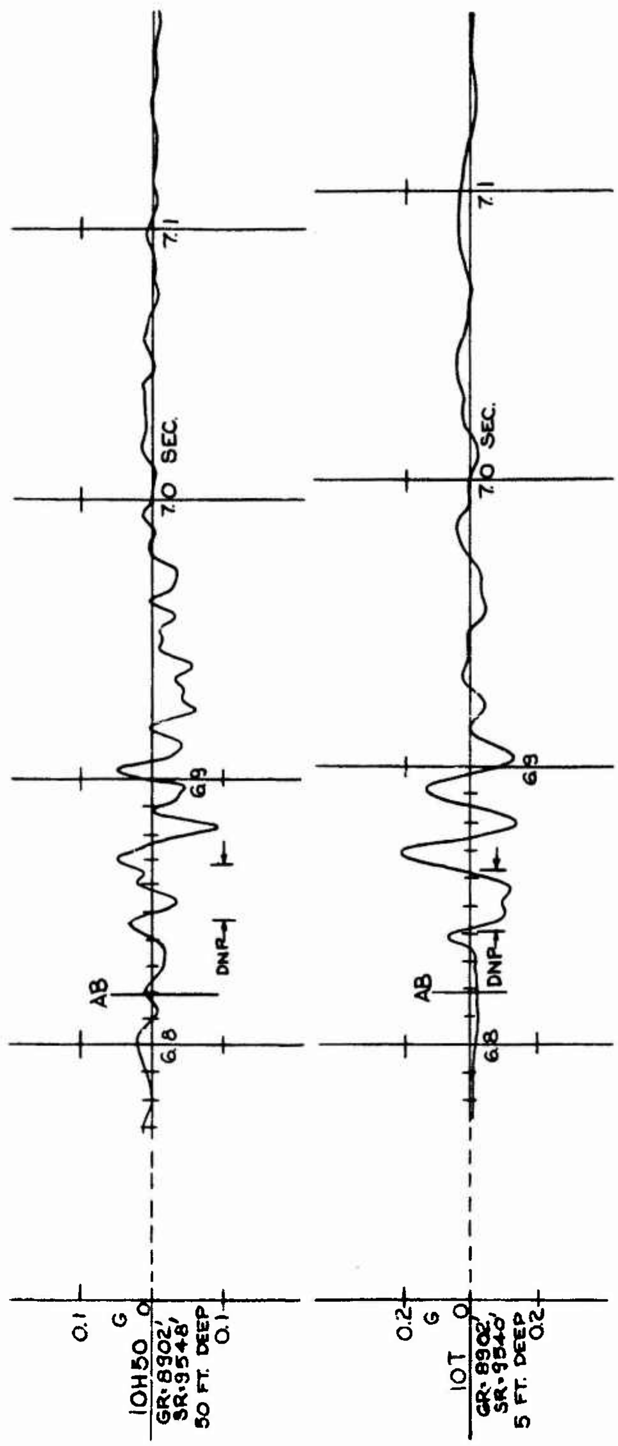


Fig. A.13 Shot 3, Gages 10H50 and 10T

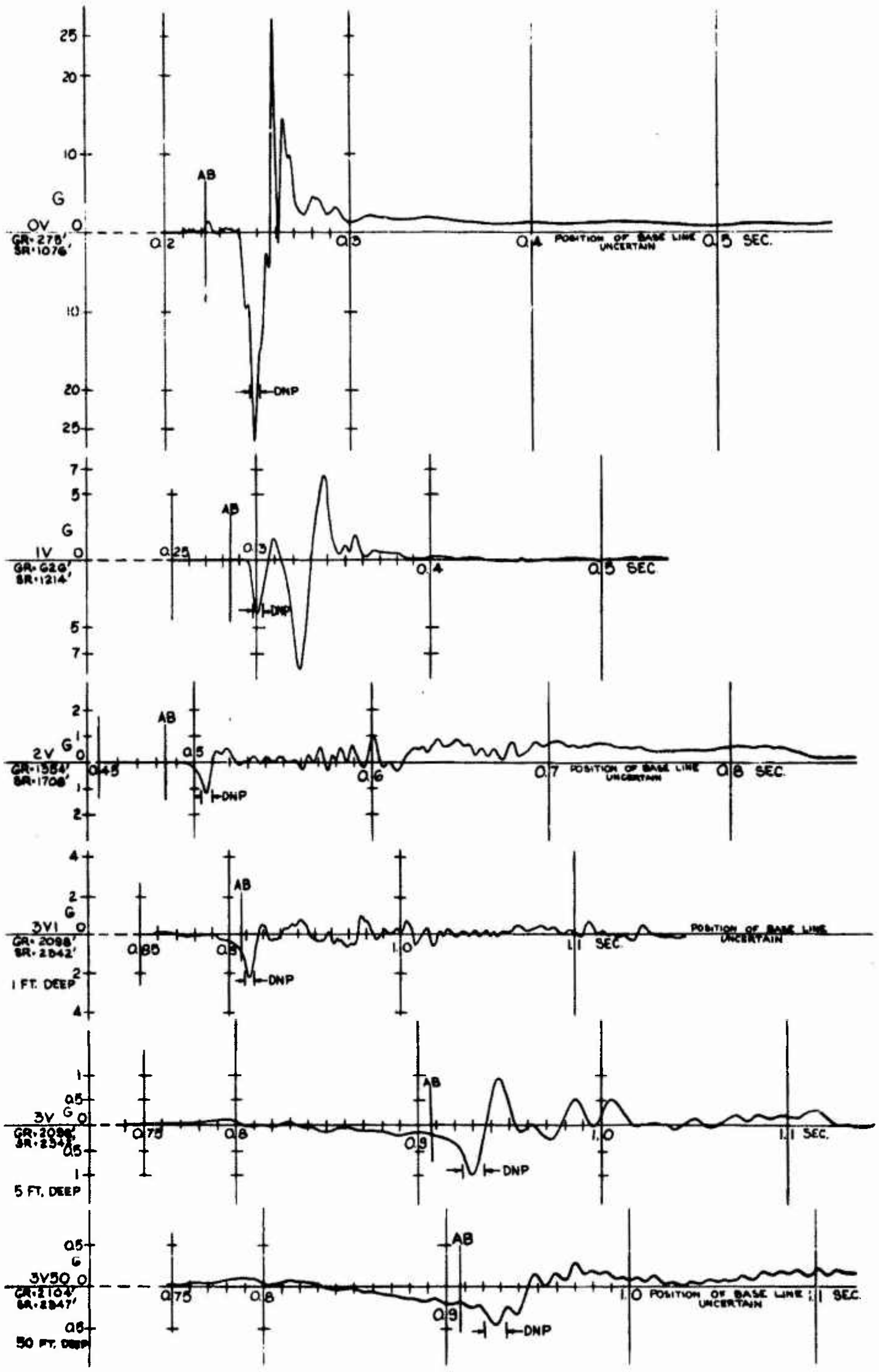

Fig. A.14 Shot 4, Gages OV through 3V50

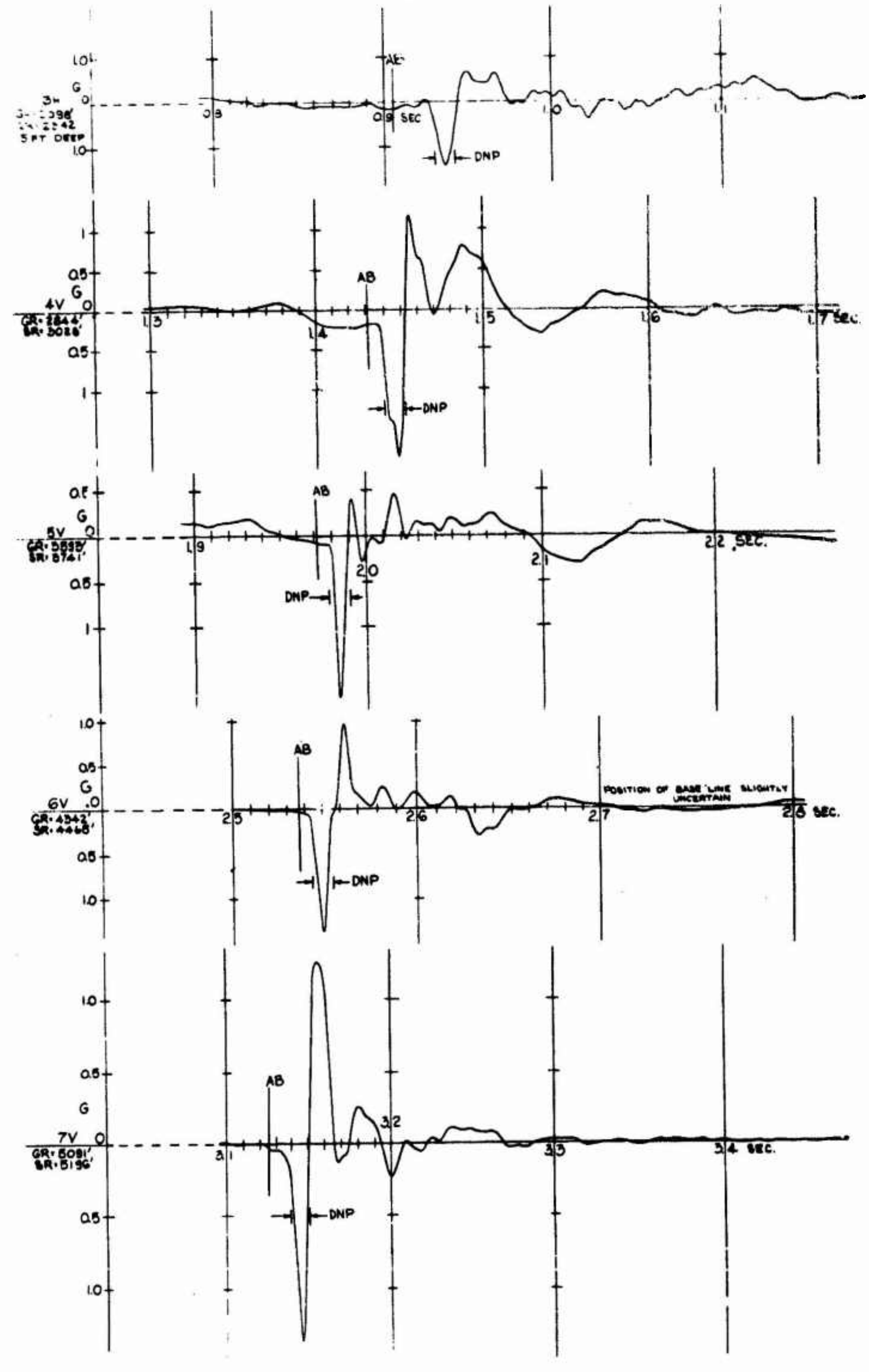

Fig. A.15 Shot 4, Gages 3H through 7V

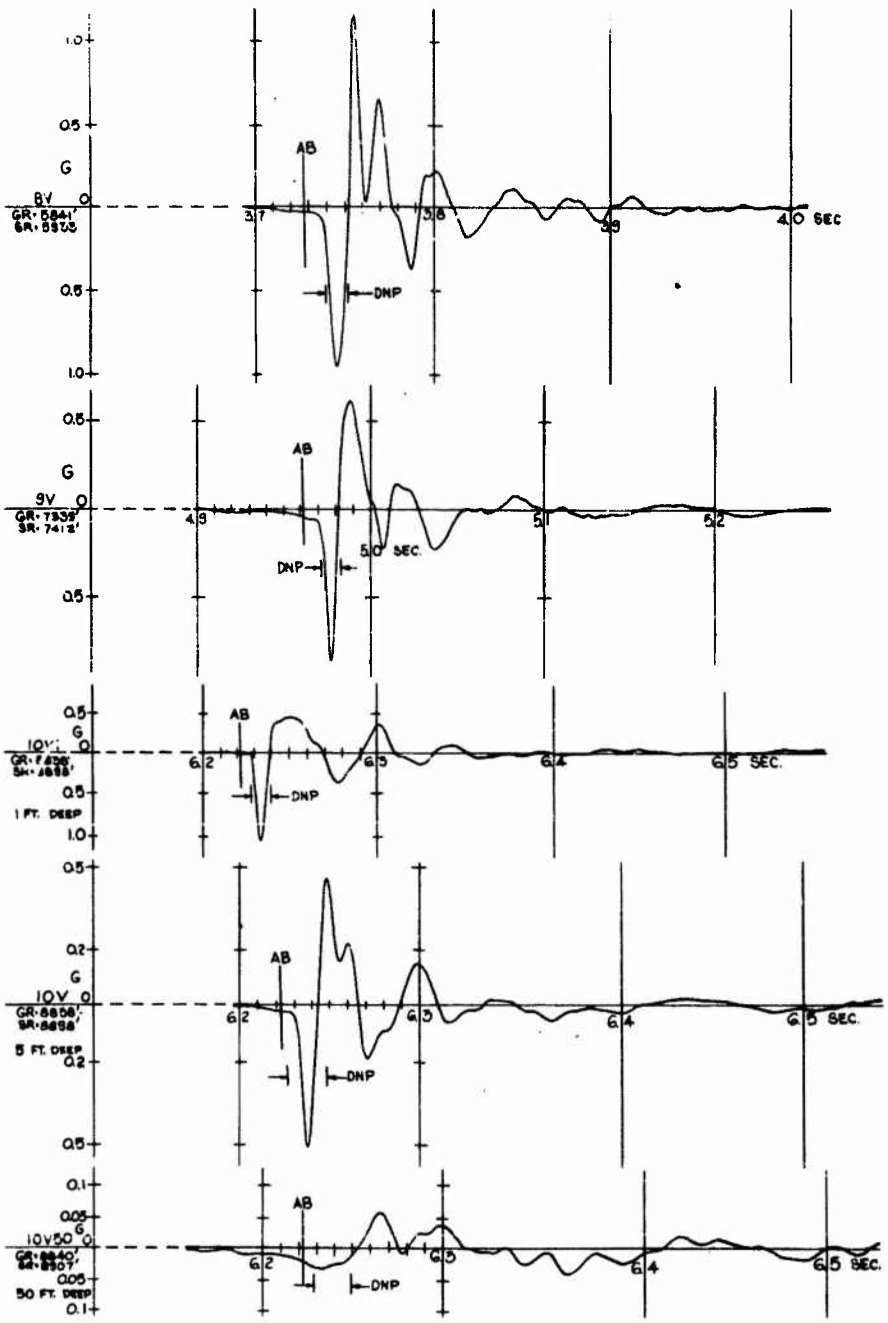


Fig. A.16 Shot 4, Gages 8V through 10V50

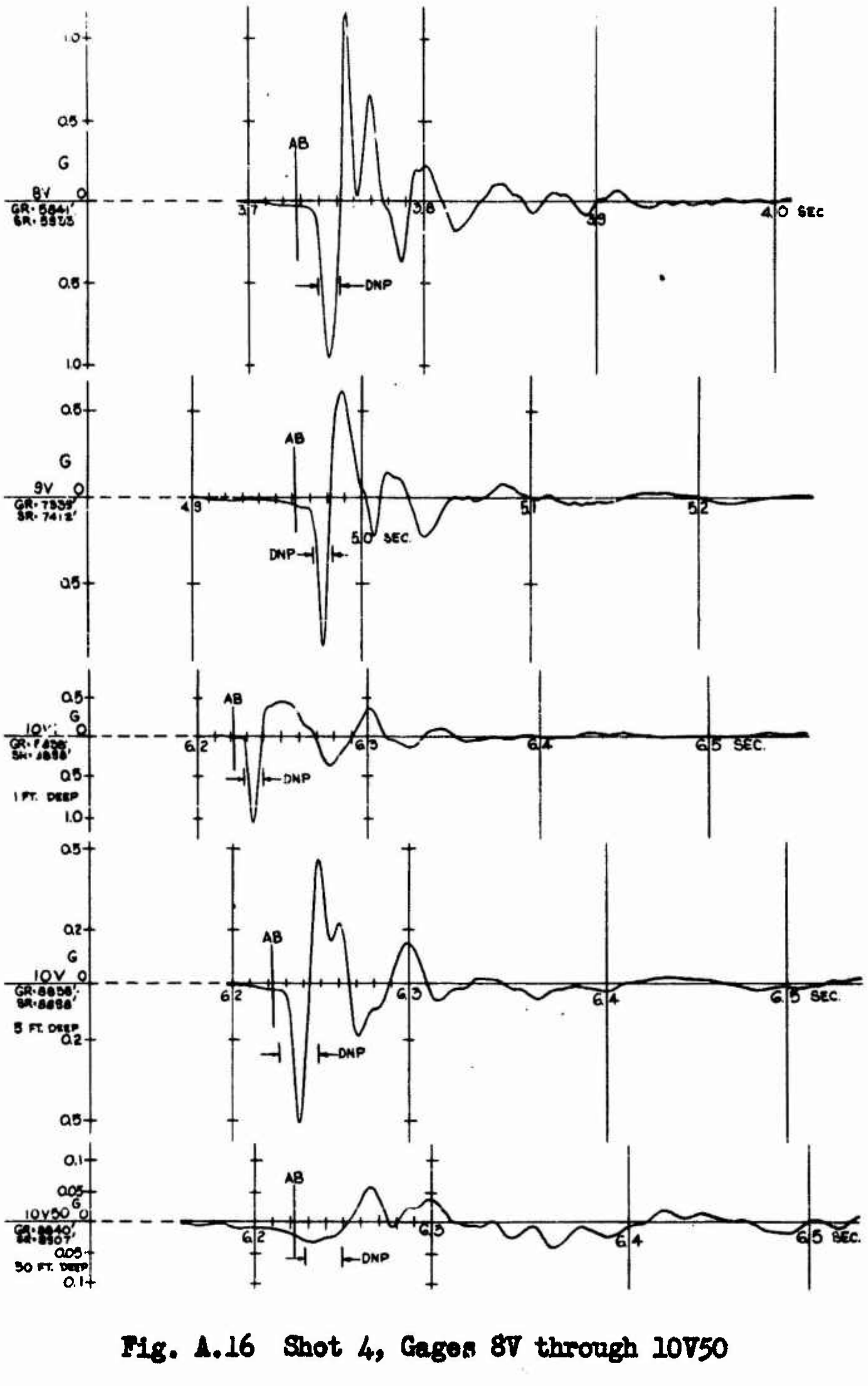


Fig. A.16 Shot 4, Gages 8V through 10V50